

2013-04-23

Characterization of Novel Materials as Platforms for Performing Microfluidic Gas Chromatography

Darko, Ernest

Darko, E. (2013). Characterization of Novel Materials as Platforms for Performing Microfluidic Gas Chromatography (Master's thesis, University of Calgary, Calgary, Canada). Retrieved from <https://prism.ucalgary.ca>. doi:10.11575/PRISM/25281

<http://hdl.handle.net/11023/616>

Downloaded from PRISM Repository, University of Calgary

UNIVERSITY OF CALGARY

Characterization of Novel Materials as Platforms for Performing Microfluidic Gas
Chromatography

by

Ernest Darko

A THESIS

SUBMITTED TO THE FACULTY OF GRADUATE STUDIES
IN PARTIAL FULFILMENT OF THE REQUIREMENTS FOR THE
DEGREE OF MASTER OF SCIENCE

DEPARTMENT OF CHEMISTRY

CALGARY, ALBERTA

APRIL, 2013

© Ernest Darko 2013

ABSTRACT

Analytical Gas Chromatography (GC) separation techniques are constantly being developed to reduce analysis time and cost as well as improve sensitivity and accuracy. One such development is the fabrication of miniaturized microfluidic columns for use in GC. There are vast reports of miniaturized columns fabricated in silicon and even other polymeric materials. While these devices show good separation efficiency, they lack physical robustness and the thermal stability demanded by GC. Alternatively, Low Temperature Co-fired Ceramics (LTCC) and titanium are novel materials that show promise for use in microfluidic GC column fabrication. They offer advantages such as low cost, ease of fabrication, and additionally, these materials are quite strong and can withstand the high temperatures required in GC. LTCC together with titanium metals have been studied and characterized as alternative platforms for microfluidic GC in this thesis. Both LTCC and titanium tiles produced good results that compared well with commercially available GC columns. For example, a 7.5m long channel within an 11 cm x 5.5 cm LTCC tile under optimum conditions generated theoretical plates for a dodecane test analyte of about 14327 compared to 4507 for a 7.5 m long commercial capillary column. Similarly, a 15m long channel within a 15 cm x 8 cm titanium tile produced 10377 plates for the same test analyte. Both of these tiles showed high resolving power, yielding benzene – toluene resolutions of about 14.07 and 8.29 respectively for LTCC and titanium. Peak capacity was also probed using temperature programming with a simple $nC_8 - nC_{20}$ alkane mixture. A cumulative peak capacity of about 53 was obtained for the LTCC tile while the titanium tile gave a value of 48. Polar analyte separations on both often produced peaks with a greater degree of tailing. Additionally, packed columns

fabricated on these materials were also investigated, and produced good separation efficiency with negligible flow restriction. For example, a 10 cm long channel within a 5.5 cm x 2.5 cm LTCC tile packed with 5 μ m C18 particles generated 2710 plates per meter. Likewise, a 10 cm long channel within a 9 cm x 5 cm titanium tile packed with 1.7 μ m C18 particles also produced 8430 plates per meter; a three fold increase. Neither displayed any adverse effects from operating the tiles up to 60 atm of carrier gas pressure. Results indicate that LTCC and titanium make excellent platforms for microfluidic GC. Further exploration of their properties in this area will be useful.

ACKNOWLEDGEMENTS

I would like to thank first and foremost Dr. Thurbide for providing me with an opportunity to be part of his research group and more importantly his knowledge, support and guidance throughout my years of study in the lab. I also would like to thank Waters Corporation for their support, none of these works would have been possible without the funding and resources provided to me by their outfit.

Again, my thanks go to the people, past and present in the Thurbide group. Their support is greatly appreciated and I am always indebted to them. Finally a special thanks to friends and family for their encouragement in my pursuit of the program

TABLE OF CONTENTS

APPROVAL PAGE	ii
ABSTRACT	iii
ACKNOWLEDGEMENTS	v
LIST OF TABLES	viii
LIST OF FIGURES	ix
LIST OF SYMBOLS, ABBREVIATIONS, ACRONYMS, AND INITIALISMS	xiv
1.1 INTRODUCTION	1
1.2 Gas Chromatography	1
1.3 Column Development	2
1.4 Types of Columns	3
1.5 Column Preparation	4
1.4.1 Surface Treatment of Capillary Columns	5
1.4.2 Stationary Phase Coating	7
1.4.3 Stationary Phase Immobilization	9
1.4.3.1 Crosslinking	9
1.4.3.2 Chemical Bonding	10
1.6 Evaluation of Column Efficiency	11
1.7 Fast Gas Chromatography	12
1.8 Need for Portability	15
1.9 On-Chip GC Columns	19
1.10 Statement of Purpose	22
CHAPTER TWO	24
2.0 EXPERIMENTAL	24
2.1 General Fabrication of LTCC Tiles	24
2.1.1 Texturing	24
2.1.2 Stacking of layers	25
2.1.3 Lamination	26
2.1.4 Co-firing	26
2.2 Titanium Chips	27
2.2.1 General Fabrication of Titanium Chips	27
2.4 Column Coating	33
2.5 Samples	34
2.6 High Pressure GC on Packed Columns	35
CHAPTER THREE	37
3.0 THE INVESTIGATION OF LTCC PLATFORMS IN GC	37
3.1 Design of GC Columns	37
3.2 Performance of Uncoated vs. Coated LTCC Tile	38
3.3 Thermal Stability of Column	40
3.4 Column Efficiency	43
3.5 Sample Capacity	47
3.6 Peak Splitting	48
2.7 Comparative Applications	52
3.8 Separation Number	55

3.9 Analyte Functional Groups	56
3.10 Deactivated LTCC Tile.....	58
3.11 Packed LTCC Columns	61
3.12 Packed LTCC Column Optimization.....	62
3.13 Packed LTCC Column Thermal Stability.....	65
CHAPTER FOUR.....	68
4.0 THE INVESTIGATION OF TITANIUM PLATFORMS IN GC.....	68
4.1 Uncoated and Coated Titanium Chips	68
4.2 Uncoated Titanium Chip.....	69
4.3 Column Efficiency	71
4.4 GC Applications	73
4.5 Polar Analytes on Titanium Tiles	75
4.6 Polar Analyte Comparison of Titanium vs. LTCC Tiles	79
4.7 Preliminary Trials with Deactivated Titanium Tile.....	81
4.8 Preliminary Trials with Titanium Packed Columns	82
4.9 General Comparison of LTCC and Titanium Platforms.....	85
CHAPTER FIVE	89
5.0 SUMMARY AND FUTURE WORKS	89
5.1 Conclusions.....	89
5.2 Future Work.....	90

LIST OF TABLES

Table 1. Representative properties of different column types for gas chromatography. Hmin = minimum plate height at the optimum mobile phase velocity (opt.) of a van Deemter curve	4
Table 2. Different columns investigated in this work.....	31
Table 3. Peak Asymmetry Values ^a between LTCC and Conventional Column	48
Table 4. Summary of column efficiency measures of the different columns investigated in this work for BTEX sample.....	86

LIST OF FIGURES

Figure 1: Schematic diagram of a Gas Chromatograph.....	2
Figure 2: Gas chromatograms of the basic test mixture on fused silica capillaries (A) deactivated with polyphenylmethylhydrosiloxane and (B) undeactivated ¹⁹	6
Figure 3: Fast GC chromatogram. Column, 120 cm x 0.065 mm I.D., coated with squalane (0.03 μ m thick); temperature 20 °C; carrier gas, hydrogen; flow – rate 121 cm/s. Compounds in their elution order; methane, n-heptane and n-octane ⁵¹	13
Figure 4: Conditions: 32 mm x 1.19 mm i.d. packed with 10 μ m particles of LiChrosorb Si-60, 100 °C, peaks – methane, ethane, propane and butane ⁵⁵	13
Figure 5: Effect of column diameter on analysis time. Column A = 10 m x 0.15 mm; B = 16 m x 0.25mm; C = 21 m x 0.32 mm. Columns have the same phase ratio (same capacity factor) and plate number ⁵³	14
Figure 6: A CO ₂ Laser Milling Procedure.	25
Figure 7: Illustration of the processes involved in the Fabrication of an LTCC tile. A) Texturing B) Stacking C) Lamination D) Co-firing ¹⁰⁴	28
Figure 8: Typical microstructure of a diffusion bonded joint ¹⁰⁵	28
Figure 9: Illustration of the processes involved in the Fabrication of a titanium chip	29
Figure 10: Schematic diagram of the GC Setup used.	29
Figure 11: A schematic of the LTCC tile used for GC. A dual spiral design is employed, where the center of each respectively acts as the inlet and outlet for the column.	32
Figure 12: Graphical representation of the coating technique	34
Figure 13: Schematic diagram of the High Pressure GC Setup used.	35
Figure 14: SEM image of LTCC coated tile cross-section near channel corner.	38
Figure 15: Chromatograms of n-alkane mixture separated in the LTCC tile without a stationary phase coated on the surface. Temperature program: 25 to 120°C at 10°C/min. Detector temperature: 220°C Analyte elution order:	

carbon disulfide (solvent), dodecane, tetradecane, and hexadecane. He flow rate: 0.29mL/min, Mass injected on column: 250 ng	39
Figure 16: Chromatograms of n-alkane mixture separated in the LTCC tile with a stationary phase coated on the surface. Temperature program: 120 to 180°C, at 10°C/min.	41
Figure 17: A chromatogram showing stationary phase bleeding from a 5 m x 100 µm i.d. fused silica column (A) without and (B) with dicumyl peroxide. Conditions: column temperature 50°C to 300°C at a programme rate of 40 °C/min.	42
Figure 18: Effect of flow rate on column efficiency for both the LTCC device (○) and a commercial Rtx-1 capillary GC column (●), 15 m x 100 µm i.d. and 20 m x 100 µm i.d., respectively. Column temperature: 180°C. Analyte solution: 1 µg/µL of dodecane in carbon disulfide.	44
Figure 19: SEM images of (A) plugged inlet and (B) the cleared inlet of the 15 m x 100 µm i.d. coated LTCC tile.	45
Figure 20: Effect of flow rate on column efficiency for both the LTCC device (○) and a commercial Rtx-1 capillary GC column (●), each 7.5 m x 100 µm i.d.. Column temperature: 130°C. Analyte solution: 1 µg/µL of dodecane in carbon disulfide.	46
Figure 21: Effect of sample size on chromatographic peak shape: (A) LTCC tile not overloaded, mass = 25 ng and (B) LTCC tile severely overloaded, mass = 1250 ng. Column temperature: 180°C. Detector temperature: 220°C. He flow rate: 0.25mL/min.	47
Figure 22: A chromatogram demonstrating peak splitting in an LTCC device with a defect. Test Analyte: tetradecane. Temperature Program: 35 to 100°C at 10°C/min. Detector temperature: 220°C. He flow rate: 0.25mL/min, Mass injected on column: 250 ng	49
Figure 23: Chromatograms demonstrating the effect of multiple coatings on peak splitting in an LTCC device with a defect. Test Analyte: dodecane, tetradecane and hexadecane in carbon disulfide (solvent). Temperature Program: (A) 50 to 100°C (B) 50 to 150°C, each at 10°C/min. Detector temperature: 220°C. Mass injected on column: 250 ng.....	50
Figure 24: An illustration of how peak splitting occurs within such a tile, where a portion of analyte (i) passes through the channel wall leaving the remainder (ii) behind.....	51
Figure 25: Chromatogram of a 1 µg/µL BTEX standard in carbon disulfide using the LTCC device (upper trace) and the commercial Rtx-1 capillary GC column (lower trace). Column temperature: 60°C. Detector	

temperature: 220°C. He flow rate: 0.30 mL/min, Mass injected on column: 250 ng Analyte elution order: Carbon disulfide (Solvent), benzene, toluene, ethylbenzene, m- and p-xylene (co-elution), and o-xylene.....	53
Figure 26: Chromatogram of a 40 mg/L C ₈ to C ₂₀ n-alkane standard using the LTCC device (upper trace) and the commercial Rtx-1 capillary GC column (lower trace). Column temperature program: 45 to 210°C at 5°C/min. Temperature is held at 180 °C for 10 min. Detector temperature: 220°C. He flow rate: 0.45mL/min. Solvent: dichloromethane.....	54
Figure 27: Graph showing approximate heating rates of the commercial column and the LTCC tile	56
Figure 28: Chromatogram of a mixture of organic compounds of varying functionalities using the LTCC device. Temperature program: 45 to 200°C at 10°C/min. Detector temperature: 220°C. He flow rate: 0.25mL/min. Analyte elution order: 1. 1,2-propanediol, 2. butylacetate, 3. phenol, 4. aniline, 5. octanol, 6. heptanoic acid, 7. decanal, 8. tetradecane, and 9. dicyclohexylamine. Solvent: dichloromethane	57
Figure 29: Chromatograms of (A) heptanoic acid and (B) 1,2- propanediol at different masses on an undeactivated LTCC tile. Temperature program: 45 to 220°C at 5°C/min. Detector temperature 220°C. He flow rate: 0.25 mL/min.....	59
Figure 30: Chromatogram of (A) heptanoic acid and (B) 1,2- propanediol, both 250 ng. Temperature program: 45 to 200°C at 5°C/min. Detector temperature 220°C. He flow rate: 0.95 mL/min.....	60
Figure 31: Chromatogram of a 1 µg/µL BTEX standard in carbon disulfide using the packed LTCC tile (10 cm x 300 µm, packed with 5 µm C18 particles). Column temperature: 25°C, CO ₂ Pressure: 120 atm. Analyte elution order: benzene, toluene, ethylbenzene, m-p and o-xylene (co-elution)....	62
Figure 32: Plate height as a function of atmospheric pressure on packed LTCC device (10 cm x 300 µm, packed with 5 µm C18 particles). Column temperature: 100°C. Analyte solution: 1 µg/µL of dodecane in carbon disulfide.....	63
Figure 33: Chromatogram of a 1 µg/µL BTEX standard in carbon disulfide using the packed LTCC tile (10 cm x 300 µm, packed with 5 µm C18 particles). Column temperature: 25°C, CO ₂ Pressure: 60 atm. Detector temperature: 220°C. Mass injected on column: 200 ng. Analyte elution order: benzene, toluene, ethylbenzene, m- p and o-xylene (co-elution)...	63
Figure 34: Chromatogram of n-alkane mixture on packed LTCC tile (10 cm x 300 µm, packed with 5 µm C18 particles). Temperature program: 80 to	

130°C at 5°C/min. Pressure: 60 atm. Detector temperature: 220°C. Mass injected on column: 200 ng. Analyte elution order: dodecane, tetradecane, hexadecane.....	64
Figure 35: An illustration of the thermal stability of the stationary phase in the packed LTCC column (10 cm x 300 µm, packed with 5 µm C18 particles). Capacity factor obtained over a period of 8 hrs with repeated injection of dodecane analyte every 30 minutes. Column temperature: 130°C.	66
Figure 36: Chromatograms of n-alkane mixture separated in the titanium tile without a stationary phase coated on the surface. Temperature programs: 45 to 200°C at 5°C/min, He flow rate: 0.55 mL/min. Detector temperature: 220°C. Mass injected on column: 250 ng. Analyte elution order: dodecane, tetradecane, and hexadecane after the solvent peak carbon disulfide.....	70
Figure 37: Chromatograms of n-alkane mixture separated in the titanium tile with a stationary phase coated on the surface. Temperature programs: 45 to 200°C at 5°C/min, He flow rate: 0.53 mL/min. Detector temperature: 220°C. Mass injected on column: 250 ng. Analyte elution order: dodecane, tetradecane, and hexadecane after the solvent peak carbon disulfide.....	71
Figure 38: Plate height as a function of flow rate on the titanium device (15 m x 100 µm). Column temperature: 120°C. Analyte solution: 1 µg/µL of dodecane in carbon disulfide.	72
Figure 39: Chromatogram of a 40 mg/L C ₈ to C ₂₀ n-alkane standard using the coated titanium device. Column temperature program: 45 to 210°C at 5°C/min, He flow rate: 0.53 mL/min. Detector temperature: 220°C.....	73
Figure 40: Chromatogram of a 1 µg/µL BTEX standard in carbon disulfide using the coated titanium tile (15 m x 100 µm). Column temperature: 60°C, helium flow rate: 0.53 mL/min. Analyte elution order after solvent peak: benzene, toluene, ethylbenzene, m- and p-xylene (co-elution), and o-xylene.....	74
Figure 41: Chromatogram of a mixture of organic compounds of varying functionalities using the coated titanium device. Temperature program: 45 to 200°C at 10°C/min. He flow rate: 0.3 mL/min. Detector temperature: 220°C. Analyte elution order: 1) 1,2-propanediol, 2) butylacetate, 3) phenol, 4) aniline, 5) octanol, 6) heptanoic acid, 7) decanal, 8) tetradecane, and 9) dicyclohexylamine. Solvent: dichloromethane.....	76
Figure 42: A chromatogram of decanal on coated titanium tile (15 m x 100 µm). Temperature program: 45 to 200°C at 5°C/min, He flow rate: 0.3 mL/min. Detector temperature: 220°C. Solvent: Dichloromethane.....	77

- Figure 43: A chromatogram of (A) octanol and (B) dicyclohexylamine on a coated titanium tile (15 m x 100 μ m). Temperature program: 45 to 200°C at 5°C/min, He flow rate: 0.3 mL/min. Detector temperature: 220°C. Solvent: dichloromethane. 78
- Figure 44: A chromatogram of (A) heptanoic acid and (B) 1,2-propanediol on a coated titanium (15 m x 100 μ m). Temperature program: 45 to 200°C at 5°C/min, He flow rate: 0.3 mL/min. Detector temperature: 220°C. Solvent: dichloromethane 79
- Figure 45: A chromatogram of (A) dicyclohexylamine and (B) heptanoic acid on coated titanium and LTCC tiles (15 m x 100 μ m each). Temperature program: 45 to 200°C at 5°C/min, He flow rate: 0.3 mL/min and 0.25 mL/min for titanium and LTCC tile respectively. Detector temperature: 220°C. Solvent: dichloromethane. 80
- Figure 46: Chromatogram of a mixture of organic compounds of varying functionalities using the deactivated titanium device (15 m x 100 μ m). Temperature program: 45 to 200°C at 10°C/min, He flow rate 0.42 mL/min. Detector temperature: 220°C. Solvent: dichloromethane. Analyte elution order: 1) 1,2-propanediol, 2) butylacetate, 3) phenol, 4) aniline, 5) octanol, 6) heptanoic acid, 7) decanal, 8) tetradecane, and 9) dicyclohexylamine. 82
- Figure 47:** Chromatogram of a 1 μ g/ μ L BTEX standard in carbon disulfide using a 10 cm x 300 μ m titanium tile packed with 1.7 μ m C18 particles. Column temperature: 60°C, CO₂ Pressure: 60 atm. Detector temperature: 220°C. Mass injected on column: 200 ng. Analyte elution order: benzene, toluene, then ethylbenzene, m-, p-, and o-xylene co-elution. 83
- Figure 48: Chromatogram of a 1 μ g/ μ L BTEX standard in carbon disulfide using a 10 cm x 300 μ m titanium tile packed with 1.7 μ m C18 particles. Column temperature: 25°C, CO₂ Pressure: 60 atm. Detector temperature: 220°C. Mass injected on column: 200 ng. Analyte elution order: benzene, toluene, then ethylbenzene, m-, p- and o-xylene co-elution. 84

LIST OF SYMBOLS, ABBREVIATIONS, ACRONYMS, AND INITIALISMS

BTEX	Benzene, Toluene, ethyl benzene, and xylenes
°C	Degrees Celcius
cm	Centimeter
ECD	Electron Capture Detector
FID	Flame Ionization Detector
GC	Gas Chromatography
HPLC	High Performance Liquid Chromatography
I.D.	Internal Diameter
LC	Liquid Chromatography
L	Liters
LTCC	Low Temperature Co-fired Ceramic
μFID	micro Flame Ionization Detector
μGC	micro Gas Chromatography
μg	micrograms
μL	microliters
mL	mililiters
m	meter
μm	micrometer
ms	milliseconds
min	minutes
ng	nanograms

TCD	Thermal Conductivity Detector
SEM	Scanning Electron Microscope
SGC	Solvating Gas Chromatography
MEMS	Micro Electro-Mechanical Systems

CHAPTER ONE

1.1 INTRODUCTION

1.2 Gas Chromatography

Gas chromatography (GC) is among a wide range of techniques used in analytical chemistry. The technique was initially developed in 1952 by James *et al.*¹ and has since been used for a number of analytical applications. Its popularity stems from the ease of use, reliability, and affordability towards analyzing semi-volatile and volatile mixtures. GC has been applied in solving many problems in various fields. The technique has found usage in monitoring chemical processes, monitoring the environment², oil exploration, and purification of compounds³. The technique was also successfully used to separate and determine the many components in petroleum⁴. It has also played an important role in chemical warfare agent detection and in quality control of food products⁵, and for that matter has helped to improve the quality of life on the whole.

GC is a separation process which employs a column where analytes partition between a stationary phase and a carrier gas phase as they move through the column. A general schematic diagram of a GC instrument is shown in figure 1. The column is composed of a stationary phase that can either be a solid, or a liquid adhered to a solid support (e.g. column wall, or particles). The mobile phase is the carrier gas, and is usually nitrogen, helium or hydrogen introduced to the column through a pressure regulator from a cylinder of compressed gas. Separation is achieved when components of a mixture have different partition coefficients between the stationary phase and the mobile phase. As a result, these components are eluted at different times. A detector is used to register

the composition of the gas stream as it emerges from the column carrying the separated components and a data system is used to record and display the resulting chromatogram.

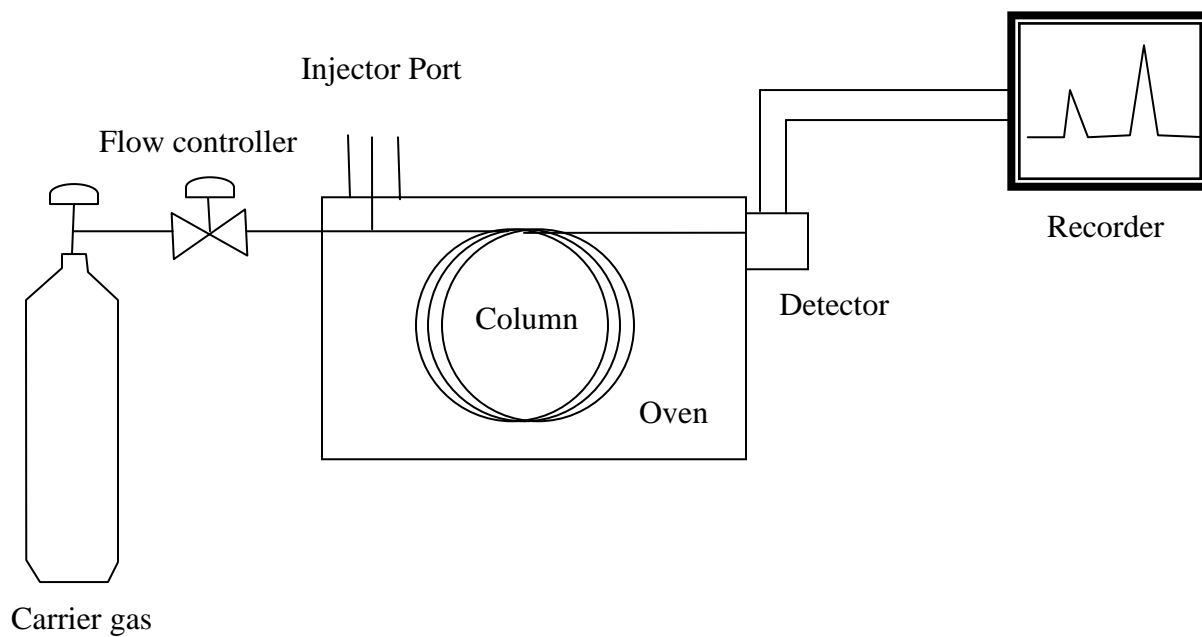


Figure 1: Schematic diagram of a Gas Chromatograph

1.3 Column Development

Among the basic components of a GC instrument, the column is the central piece for successful analytical separations. Prior to the invention of chromatography, target analytes were separated from the rest of the matrix through distillation, liquid extraction and also crystallization. However, Tswett⁶, in 1906 introduced chromatography when he described the separation of a plant pigment. The different components of the pigment mixture were resolved on a calcium carbonate column. Thus, the column is a critical part of the GC instrument and separation largely depends upon it.

1.4 Types of Columns

GC is generally classified into two categories based on the type of column: packed or open tubular also known as capillary⁷⁻⁹. Early GC was carried out on packed columns which consisted of either a metal or glass tube, ~1-5 m long and 1-5 mm internal diameter (i.d.) filled with particles. The particles are either uncoated inorganic adsorbents or a liquid phase coated onto a solid support. Packed columns can either be classified as classical or micropacked based on their internal diameter. Classical packed columns have internal diameters greater than 1 mm (as noted above) and are packed with particles ranging from 100 to 250 μm in diameter. Micropacked columns, on the other hand, have diameters less than 1 mm but often a similar packing density to classical packed columns ($d_p/d_c < 0.3$) where d_p is the average particle diameter and d_c the column diameter. Packed columns are particularly disadvantageous when it comes to increasing their length and efficiency because their high gas flow resistance makes this difficult.

Capillary columns were suggested by Martin¹⁰ and later realised in 1957 by Golay^{11,12}, and help remove this restriction. Unlike packed columns, capillary columns have the stationary liquid phase coated on the internal surface of the column. Capillary columns thus provide much less restriction to the flow of carrier gas, thereby reducing the pressure drop. This low gas flow resistance associated with capillary columns in turn permits the use of longer columns without needing extremely high pressures at the column inlet. Overall, these characteristics mean more theoretical plates are possible for capillary columns. A disadvantage to this, though, is that capillary columns also tend to have less sample capacity due to their lower surface area. Less sample capacity can be

compensated using a sample splitter, which allows less mass to be injected onto the column while the rest of the sample goes to waste.

There are three types of open tubular capillary columns, namely wall coated open tubular (WCOT), porous-layer open tubular (PLOT), and support coated open tubular (SCOT). WCOT is a column in which liquid stationary phase is coated on the inner wall of the column (as mentioned above). SCOT columns on the other hand are prepared by coating the stationary phase onto a porous support material attached to the inner column wall^{13,14}. PLOT columns are similar to SCOT columns; however, here the uncoated porous material is deposited on the inner column walls and used for separation directly.

Table 1 summarizes some features of a number of GC column types for comparison.

<i>Column Type</i>	<i>Phase ratio</i>	<i>Hmin (mm)</i>	<i>Uopt (cm/s)</i>
Classical packed	4-200	0.5-2	5-15
Micropacked	50-200	0.02-1	5-10
SCOT	20-300	0.5-1	10-100
WCOT	15-500	0.03-0.8	10-100

Table 1. Representative properties of different column types for gas chromatography.

Hmin = minimum plate height at the optimum mobile phase velocity (opt.) of a van Deemter curve

1.5 Column Preparation

GC columns (packed or capillary) are capable of producing high efficiencies. One of the primary concerns for generating very efficient columns is column preparation. The

general practice used with packed columns is to fill tubing with stationary phase particles and continuously and tightly pack them in place with the assistance of vibration. While this might seem straightforward, great care is taken to achieve a uniform particle bed. On the other hand, the steps to coating a capillary column are quite unique. For example, steps leading to a finished capillary column are comprised of surface treatment, stationary phase coating and stationary phase immobilization. These steps have to be carefully performed for optimal results. To help illustrate the process, these steps are detailed below for a capillary column, which will be the main column type explored in this thesis and the primary focus of discussion going forward.

1.4.1 Surface Treatment of Capillary Columns

Prior to coating the surface of a column with a stationary phase, surface pre-treatment is sometimes carried out. This entails an acid wash where typically the column is filled with 10 % w/w hydrochloric acid and capped at both ends. The column is then heated to 100 °C for an hour followed by a distilled water rinse to get rid of the acid. The main objective for this step is to remove any traces of heavy metal ions that can cause unwanted adsorption effects. Acid leaching treatments restore the high surface energy of the column and provide a more stable, uniform surface to achieve maximum surface deactivation prior to coating.

Deactivation has an important function in shielding any residual active sites on the surface which can negatively impact separation and peak shapes, and it creates a surface that is highly inert. The general practice involves filling the column with a solution of deactivation agent contained in a suitable solvent. The column is heated to the

boiling point of the solvent with both ends of the column sealed for an hour. Deactivation reagents such as non-polar silazanes, cyclic and polymeric siloxanes and their mixtures have successfully been used¹⁵⁻¹⁷. For example, Schutjes et al.¹⁸ used a 1: 1: 2 (v/v) mixture of hexamethyldisilazane (HMDS), diphenyltetramethyldisilazane, and pentane to successfully deactivate a 50 μm i.d column. Markides et al.¹⁹ were able to show (see figure 2) the effect of deactivation on a capillary column. Efficiency and surface inertness towards basic compounds were investigated each on an untreated and a deactivated capillary column. One of their findings was that the untreated capillary column was missing some peaks believed to be strongly retained on the surface shown in figure 2B. The deactivated capillary column yielded a less active surface which allowed analytes to elute from the column without being irreversibly bound.

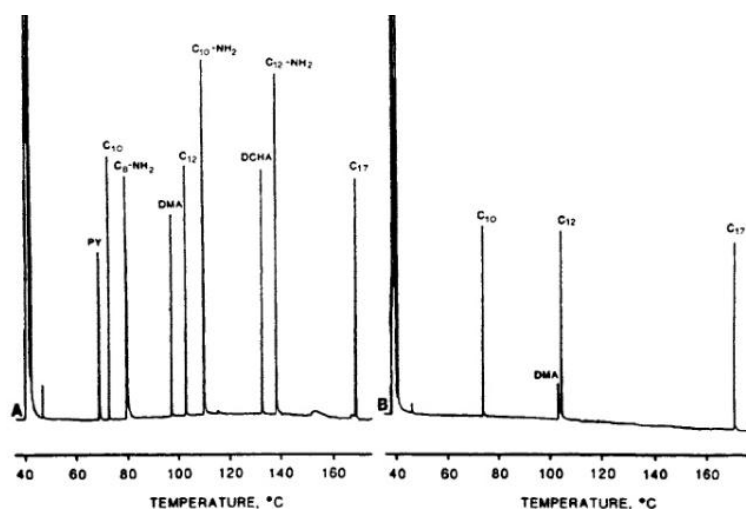


Figure 2: Gas chromatograms of the basic test mixture on fused silica capillaries (A) deactivated with polyphenylmethylhydrosiloxane and (B) undeactivated¹⁹

The production of high efficiency columns requires that the stationary phase be deposited as a thin homogeneous film on the column surface. This process is dependant upon the ability to get the surface completely wet with the stationary phase. The importance of column wettability was echoed by Farre-Rius et al²⁰ in 1962. The Zisman²¹ concept was adopted in their study to determine the critical surface energies for various tubing materials. Several studies have since been carried out to determine the degree of glass surface wetting by stationary phases²²⁻²⁵. Column wettability in general can be enhanced by either roughening the interior surface of the tubing or by chemical modification of the surface. Roughening of the interior surface of columns is achieved by etching the inside surface or by depositing microcrystalline structures on the surface²⁶. Roughening enhances the wettability of the surface by increasing the surface area over which interfacial forces can act and dissipate the cohesion energy of the drop. According to Ogden et al,²⁶ chemical modification is at present the most satisfactory way for enhancing the wettability of a surface and can also be used for surface deactivation. A frequently used technique is silylation, where active surface hydroxyl groups are replaced with silyl ether groups containing similar or identical functional groups to those of the stationary phase. Silylating reagents other than silyl ether, such as disilazanes, disiloxanes and chlorosilanes^{27,28} have also been used.

1.4.2 Stationary Phase Coating

The goal of coating a capillary column is to uniformly deposit a thin stationary phase film usually 0.1 to 8 μm thick on the inner walls of the column. The surface may or may not be deactivated. There have been several methods proposed for coating columns.

Among these, static and dynamic coating are the two most frequently employed methods used by column manufacturers.

1.4.2.1 Static Coating

The static coating method was first proposed by Bouche and Verzele²⁹. In static coating mode, the column is initially filled completely with a solution of known concentration often (0.02 – 4.0 % V/V) of the stationary phase in a volatile solvent, for example, pentane, dichloromethane, or freon. The solvent is removed when one end of the column is sealed and the other end is attached to a vacuum source. A uniform film is deposited on the column wall as the solvent evaporates when the process is carried out at a constant temperature. This coating method yields efficient columns with predictable film thicknesses.

1.4.2.2 Dynamic Coating

For dynamic coating, a solution containing the stationary phase is passed through the column at constant velocity. The coating is generally done by filling about 10 % of the column length with the stationary phase. The column is connected to a gas supply where pressure is applied to the front of the column causing the plug to travel through the column. The gas flow is continued for an hour to evaporate residual solvent. This method is the simpler of the two; however it does not yield the higher column efficiency. According to Parker and Marshall²⁴, the principal cause of low column efficiency for dynamically coated columns is the formation of small plugs of solution left behind the main plug during the coating process. A modification of the dynamic coating process was suggested by Schomburg et al.,^{30,31} to help improve the success of dynamic coating. The process was dubbed mercury plug dynamic coating. In this method a mercury plug is

used to interpose between the coating solution plug and the driving gas. Due to mercury's high surface tension, the plug is able to wipe most of the coating solution off the surface of the column's wall as it moves through. After coating, the column is subjected to a heat treatment to immobilize the film.

1.4.3 Stationary Phase Immobilization

Current practice in capillary column production has been enriched by immobilization techniques where the stationary phase film is immobilized on the inner wall of the fused silica tubing. The immobilization of the stationary phase is often achieved either by surface bonding or cross-linking. This approach allows the stationary phase to be adhered strongly to the column and by doing so the film is stabilized on the surface, and can withstand relatively more elevated temperatures. Thus, less column bleed and higher operating temperatures are possible with these phases. Another benefit of film immobilization is that stationary phase dissolution is not realized when large volumes of solvents are injected. More so, a column with an immobilized phase can be backflushed to remove contaminants without destroying the stationary phase. One of the pioneers in this area of research, Madani et al., provided a detailed description of capillary columns coated with polysiloxane and immobilized through hydrolysis of dimethyl and diphenyl chlorosilanes³².

1.4.3.1 Crosslinking

Crosslinking is the process of chemically joining two or more molecules by a covalent bond often using crosslinking agents. Crosslinking reagents (or crosslinkers) on

the other hand, are molecules that contain two or more reactive ends capable of chemically attaching to specific functional groups. Various crosslinking approaches have been explored in GC, including using chemical additives such as organic peroxides^{33,34} and azo compounds³⁵⁻³⁷. Gamma radiation has also been explored to this effect³⁸⁻⁴⁰. Peroxides are one of the most commonly employed free radical crosslinking agents, although their usage can alter the activity of columns by generating polar decomposition products that remain in the immobilized film of the stationary phase. Another disadvantage of organic peroxides is that they may undergo oxidation leading to increased polarity and decreased thermal stability of the column. Recent studies have shown that the use of azo compounds^{35,36} such as azo-tert-butane and azo-tert-octane, can produce good columns and do not affect the polarity or activity of the column³⁷. In all, crosslinking helps promote efficient and lasting column stability.

1.4.3.2 Chemical Bonding

Chemical bonding is a technique where a chemical bond is formed between the fused silica tubing and the stationary phase. In this process, a capillary is coated in the conventional modes using a hydroxy-terminated polysiloxane and subjected to a temperature program to elevated temperatures. During this stage, a condensation reaction occurs between the surface silanol (i.e. – SiOH) groups of the fused silica and those of the bonded stationary phase to produce water and an –Si-O-Si bond. Investigation into this technique was first reported by McMurray and Lipsky⁴¹ where they looked into hydroxyl-terminated polymethylsilicones. This process was further used by Blum et al.^{42,43} where they employed hydroxyl-terminated phases to produce inert, high-

temperature stationary phases of varying polarities. Evaluation of the performance of these hydroxyl-terminated phases has also been reported by Schmid et al.⁴⁴ and Welsch et. al.⁴⁵ Interestingly, both coating and active site deactivation can be achieved in this technique in a single step process leading to the formation of Si-O-Si bonds. This kind of bond is more thermally stable than the Si-C-C-Si bond achieved via crosslinking.

1.6 Evaluation of Column Efficiency

Research is continuously being carried out to improve GC separations and the efficiency of the system. One measure of column efficiency is the number of theoretical plates (N), which is expressed as follows;

$$N = 5.545 \left(\frac{t_R}{W_{1/2}} \right)^2$$

Where $W_{1/2}$ is the width at half maximum of the analyte peak and t_R is the retention time. N can also be expressed in terms of length (L), and theoretical plate height (H) as follows;

$$N = \frac{L}{H}$$

Column Efficiency is dependent on column dimensions (length, and diameter) as well as stationary phase film thickness. Normally, increasing column length enhances column efficiency by generating a larger number of theoretical plates⁴⁶. Additionally, reducing the column internal diameter results in higher efficiency per unit length as well as a reduced minimum plate height^{47,48}. In terms of stationary phase film thickness, column efficiency generally increases with the use of thin film stationary phase since mass

transfer is quick between the mobile and stationary phase. In addition to the three variables discussed (length, diameter, and film thickness), column efficiency can also be influenced by the type of carrier gas, type of stationary phase, and the chemical properties of the analyte being injected.

1.7 Fast Gas Chromatography

High efficiency is not necessarily the main goal for all analytical problems⁴⁹. There is always the growing need to develop separation strategies with emphasis on fast separation times. Fast GC has a lot of benefits to offer in this regard. Fast GC provides an increased signal to noise ratio, increased precision and lower limit of detection under certain conditions. Studies have shown that fast GC can be achieved in many different ways. The option to select often depends on the application under study. Equipment design plays an important role in this area. There have been several reports on the use of short capillary columns in the quest to achieve fast GC. Desty *et al.*⁵⁰ demonstrated the separation of a 15 component mixture using a short capillary column of 1.2 m in 2 sec. Very rapid chromatograms with analysis times of 2 sec or less have also been shown or reported in the literature by others⁵¹⁻⁵⁴. Figure 3 shows an example of a fast GC separation carried out in less than 2 seconds on a short capillary column. The authors were able to separate three alkane analytes within 2 seconds.

Figure 4 is also a chromatogram for even faster GC analysis demonstrated by Jonker *et al.*⁵⁵, where the time of analysis for the separation of four analytes, (methane, ethane, propane and butane) was 0.15 seconds. This was carried out on a 32 mm x 1.19

mm column packed with 10 μm LiChrosorb Si-60 particles. The temperature for the separation was 100 $^{\circ}\text{C}$.

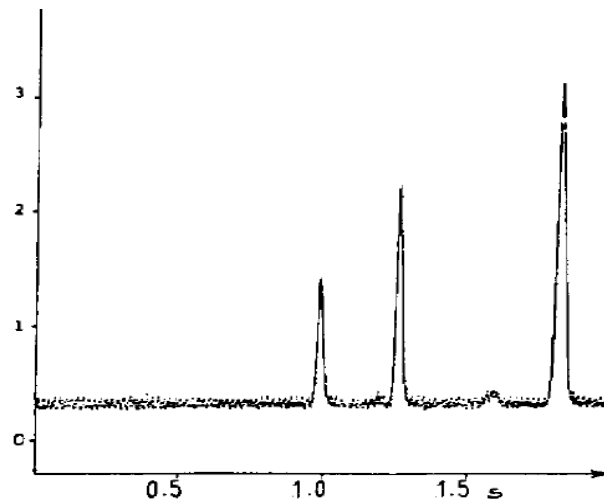


Figure 3: Fast GC chromatogram. Column, 120 cm x 0.065 mm I.D., coated with squalane (0.03 μm thick); temperature 20 $^{\circ}\text{C}$; carrier gas, hydrogen; flow – rate 121 cm/s. Compounds in their elution order; methane, n-heptane and n-octane⁵¹.

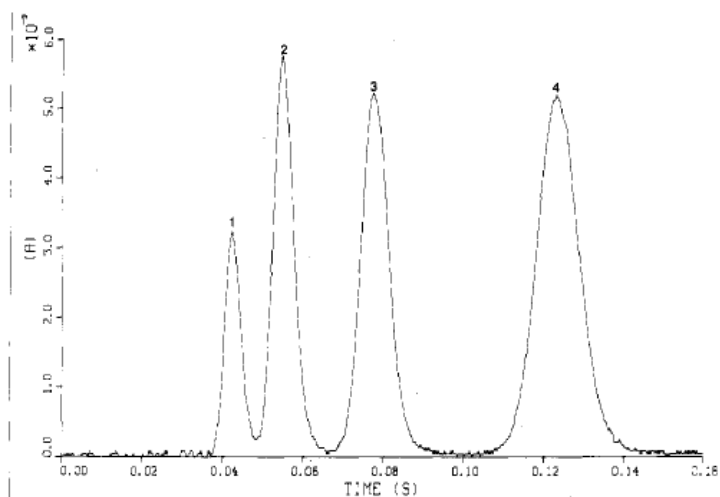


Figure 4: Conditions: 32 mm x 1.19 mm i.d. packed with 10 μm particles of LiChrosorb Si-60, 100 $^{\circ}\text{C}$, peaks – methane, ethane, propane and butane⁵⁵.

Aside from short columns, small diameter columns have also been used to reduce analysis time in GC⁵⁶. Generally, carrier gas velocity can increase with minimal efficiency loss as the column inner diameter decreases, so that a short analysis time can be obtained.

Figure 5 shows the influence of column diameter on Fast GC. Three columns A, B, and C having different column diameters displayed different times of separation. Though the columns have the same phase ratio and plate number, the column with the smallest diameter gave the faster separation.

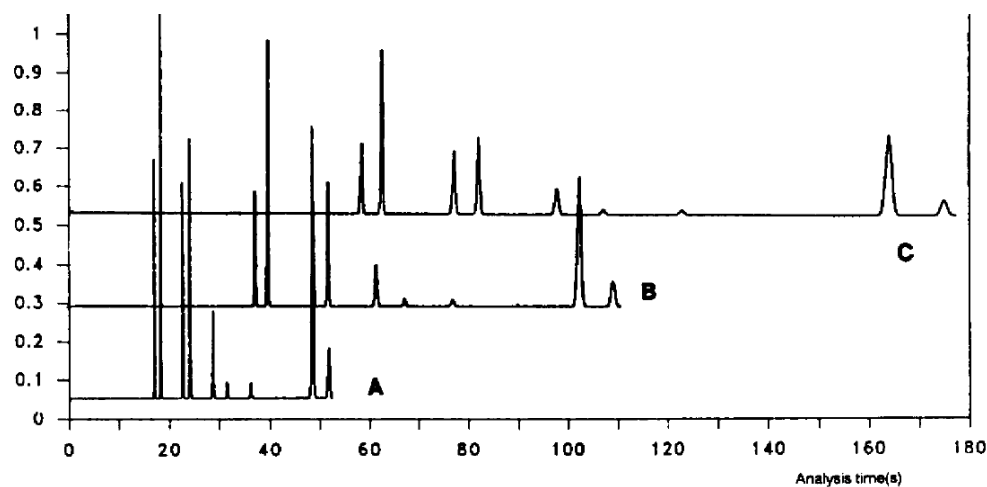


Figure 5: Effect of column diameter on analysis time. Column A = 10 m x 0.15 mm; B = 16 m x 0.25mm; C = 21 m x 0.32 mm. Columns have the same phase ratio (same capacity factor) and plate number⁵³.

Extremely fast analysis has thus been greatly exploited, especially with fused silica capillary columns. Still, although fast separation can be achieved on shorter

columns, the resolving power of these columns is greatly reduced. This can be compensated somewhat by the proper selection of column dimensions and uniform coating of stationary phase, but the application of fast GC needs to be appropriate at the outset of the particular analysis.

1.8 Need for Portability

An on-going area of interest in GC is instrumentation development. Recent development of analytical chromatographic systems not only allow for a more efficient and fast analysis in the lab but also enables the possibility for such instruments to be used for field analysis as well. While conventional GC systems are very sophisticated analytical tools, they remain relatively bulky and power intensive which usually make them inconvenient for field analysis. Another area of concern is that such devices can generally consume large amounts of sample in a given analysis. These concerns have been addressed through miniaturization over the last several years.

There is currently emerging interest in downsizing most chromatography systems through miniaturization. Terry et al in the 1970s reported the first miniaturized GC at Stanford University⁵⁷. Various versions of miniaturization have been increasingly reported. Many of these devices either have one or two system components (e.g. column and/or detectors) scaled down, or the entire system. For example, a portable, high speed GC system using micromachined valves and a sample loop on a silicon chip is commercially available⁵⁸. The above device produced by Terry and coworkers was fabricated on a silicon wafer using photolithography and chemical-etching techniques⁵⁷.

The device included a 1.5 m long column and thermal conductivity detector that was internally mounted on the silicon wafer. Devices where all subcomponents of the GC system such as injector, column, and detector are formed on a single planar fabrication allows for less usage of connections and better structural geometry that is much easier to heat.

Advances in the manufacturing processes of portable instruments, which include silicon micromachining techniques⁵⁹, have produced practical injectors and detectors suitable for use with microbore columns. The following sections describe some of the primary components of portable GC devices in more depth.

1.8 Portable GC Devices

1.8.1 Injectors on Portable Devices

For most capillary sample introduction systems that are commercially available, there continues to be a limitation in terms of band broadening. According to Korytar et al.,⁶⁰ in order to avoid peak broadening, the injection system has to satisfy a certain input band width. Korytar reiterates that any extra-column contribution to band broadening will undermine the efficiency of a system. Split injectors seem to be the simplest way to go around this problem. It allows a narrow initial band width to be achieved. However, there are some drawbacks to this technique. For example, poor limits of detection are often associated with splitting techniques, since they limit the amount of sample introduced onto a column, while most of the sample is split to vent. Split injectors also require relatively low volume injections, which negatively impact the minimum detectable amount for either a mass sensitive or a concentration sensitive detector, since the amount

on column can be far too low for many practical applications. Splitless injection has also been extensively studied^{5,61,62}. It generally requires a liner with a small inner diameter to obtain acceptable splitless time at the low flow of the narrow bore column. Introduction of volumes up to 1 μl without any peak distortion was observed for columns with inner diameters of 100 μm ⁶¹. Other alternatives for portable devices have been explored, including on-column injection, which is one of the most suitable injection modes for GC applications in the field. On-column injection mode offers the possibility of injecting larger sample volumes and allows for narrow input bands. Van Es et al.,⁶³ used an on-column cold-trap reinjection system to obtain very narrow input bands of 1.1 ms. With on-column injection the liquid sample is introduced directly onto the column without an intermediate vaporisation step^{64,65}. Nonetheless, there are limitations with this technique as well. Analysis of real-life samples might lead to challenges considering the tolerance of a GC system to co-injected matrix components in the sample⁶⁶.

A revolutionary approach was described by Lee et al.⁶⁷ where they used miniaturised mechanical switching valves for injection. A typical switching time is around 1.5 ms and is controlled by a microprocessor. The extra-column broadening contribution is usually very low. Portable high speed GC systems using these micromachined valves and sample loops on a silicon chip are commercially available. The inlet system is optimized for use with short narrow-bore columns⁶⁸. Silicon micromachining technology permits the integration of low-dead volume (4 nl) micro valves and sample loops.

1.8.2 Detectors on Portable Devices

Detectors are generally classified into two types, universal and selective. These could additionally be either mass or concentration sensitive. For column efficiency to be preserved, the peak broadening caused by a given detector must be small, and also the sampling frequency of the detector must be high enough to provide some 15 – 20 data points across the peak for a true and accurate representation of the peak shape⁶⁹. The data sampling rate for most instruments currently falls between 0.5 and 500 Hz, with an electrometer-amplifier time constant of about 5 ms being common⁷⁰. When it comes to portability, universal detectors such as the flame ionization detector (FID) and the thermal conductivity detector (TCD) have been explored⁷¹. That is not to suggest that selective detectors have not been used in this regard also. For example, a micro electron capture detector (μ ECD) was used in the trace analysis of selective chemical congeners in food⁵. An FID often uses three kinds of gas (a carrier gas, hydrogen and air) which all have to be controlled with accurate flow rates. More so, appropriate polarization voltages and weak current amplifiers must be furnished, which bring unavoidable complexity to develop a practical portable instrument. However, a lot of successes have been realized in this area of research. Thurbide et al.^{72,73} introduced a micro-FID using counter-flowing streams of gas with quartz and stainless steel tubes. Zimmermann et al.⁷⁴ then reported a sandwiched-constructed version of this counter flowing FID using a micro electro mechanical systems (MEMS) technique. Sensitivity and applicability continue to be a source of investigation for these micro detectors, and researchers have demonstrated that they can be useful for a wide range of samples.

1.8.3 Columns on Portable Devices

Nowadays, there are practically no technical limitations to the manufacturing of columns for portable devices. An approach that is often employed is to have the dimensions of these conventional columns etched onto miniaturized platforms using MEMS technology. The various platforms or substrates that are currently being explored for use in this area of technology are detailed below.

1.9 On-Chip GC Columns

Many revolutionary advances have occurred in column technology during the past 15 years. Presently, almost all open tubular columns are prepared from sodalime, borosilicate, or fused-silica. Fused silica has become the most widely used since its introduction in 1979⁷⁵ and this stems from the fact that its surface is relatively inert and also flexible to use. It has remarkable properties that can facilitate the formation of a smooth surface with chemically stable, precisely machined channels and sub-micron surface features^{76,77}. In this way, analytical tasks such as capillary electrophoretic separations on a microfluidic chip have been demonstrated to be readily achievable^{78,79}. However, there are certain disadvantages to performing micro gas chromatography (μ GC) on silicon substrates. For example, when dissimilar materials such as borosilicate are used as a cover plate for the channels, the seal that is formed between the two can cause thermal gradients to develop along the column that can erode separation efficiency, and even leak upon temperature changes due to the thermal coefficient mismatch that exists between the two materials⁸⁰. μ GC devices fabricated on silicon chips also often need relatively specialized manufacturing facilities that require expensive lithography

and machining tools as well as high quality clean-rooms. While silicon has been the most widely used substrate to date for microfabricated GC columns⁸¹⁻⁸⁶, other materials are now being explored in this regard.^{58,87,88}

For example, other microfluidic applications performed at or near room temperature have also been achieved using polymeric substrates^{79,89,90}. Examples include polydimethylsiloxane (PDMS), polycarbonate, polyethyleneterephthalate (PET), and poly ether-ether ketone (PEEK)^{91,92}. Malainou et. al.⁹³ showed in a study that polymeric materials can function both as a structural platform and as a stationary phase. The advantage of using the structural material as a stationary phase reduces the need for homogeneous deposition of the stationary phase film on the column. However, these materials are not resistant to the high temperatures often required in GC. Therefore, considering the thermal difficulties that can be encountered with silicon or polymeric substrates, different materials that could be used for μ GC separations would be useful to explore. Further, development of columns with greater inertness to GC conditions via either new construction materials or better surface deactivation techniques would also be important to the area.

One material that is gaining greater prominence recently is Low Temperature Co-fired Ceramics (LTCC). Studies have helped to characterize the chemical, structural and mechanical properties of LTCC. LTCC tape in the so called ‘green unfired state’ is mainly comprised of 45% filler (mainly Al_2O_3), 40% glass and 15% organic components (solvent, plasticizers and binder)⁹⁴. LTCC has enjoyed a great deal of success over the years in the electronics industry as a reliable material for high-volume, low-cost

fabrication of multi-layer printed circuit boards⁹⁵. In recent years, LTCC has also been explored as a new substrate for microfluidic analytical tools⁹⁵⁻⁹⁷.

In this technology, channels are created in un-fired pliable “green” tapes that are subsequently layered together and baked to form a monolithic, channeled structure. The sturdy mechanical properties of such structures have been extensively tested⁹⁸, and LTCC devices of this nature are known to be stable up to exceptionally high temperatures and pressures⁹⁶. Other benefits to using LTCC materials include being readily constructed in three dimensions, incorporating embedded supporting metal and electronic components, allowing for rapid low-cost fabrication without the need for a special clean room, and not requiring sealing elements due to their monolithic design⁹⁵⁻⁹⁷.

In light of these favorable properties, LTCC substrates have been increasingly used in many analytical applications, including examples of microfluidic separations by capillary electrophoresis⁹⁹ and high performance liquid chromatography^{95-97,100}. However, analogous μ GC separations on LTCC platforms have not been explored to any depth. For example, Briscoe et. al. successfully described the detailed design and construction of a μ GC-LTCC device¹⁰¹. Unfortunately, however, no data was provided to show how the device actually performs. Later, Dziurdzia et. al. reported the design and union of a LTCC channel with an on-board FID within a single functional device⁸⁸. However, while it produced good quality analytical signals for injected hydrocarbon analytes, the channel was not coated and therefore did not possess any separation capacity to act as or be evaluated as a GC device.

1.10 Statement of Purpose

This work will focus on the design, fabrication and characterization of some new substrates, LTCC and titanium tiles, for use as platforms for μ GC separations. The analytical separation properties of these new substrates (LTCC and titanium tiles) coated with a stationary phase are investigated. Other substrates such as silicon, polymers, and carbon nanotubes have all made strides in instrumentation development. Nonetheless, these substrates present difficulties when used in fabricating miniaturized devices for μ GC separations. LTCC shows a lot of promise in this area of miniaturization of GC systems. Considering its potential, it would be useful to know if such a substrate can successfully be used for analytical separations and how those separations compare to conventional modes of operation. Such information would promote a better understanding of the potential of LTCC in μ GC, and facilitate the development of this area. The first part of this work will centre on capillary LTCC tiles. Emphasis will also be on bare and deactivated forms of these tiles. Separation capability of these tiles in the absence of a stationary phase will first be tested at the start of characterization. Characterization will include probing column efficiency, (e.g. theoretical plate numbers and a Van deemter plots). Thermal stability of the LTCC tile will also be assessed and finally, peak shapes resulting from the injection of various analytes (polar and non-polar) will be looked into as well. These variables will help explain the performance of the LTCC tile and broaden knowledge regarding its application.

Another interesting substrate used as a column material that will be optimised and characterized in this work will be titanium tiles (bare and deactivated). This is the first time such a substrate is being used in GC. This substrate can be fabricated to form a

monolith structure as in LTCC. Similar work will be done to showcase their potential for use as μ GC columns. In order to better evaluate the performance of these tiles, the results will be directly compared with experiments using a similarly coated length of fused silica tubing and a comparable commercial capillary GC column.

Finally, short packed columns with very small particle sizes will be explored in a high pressure GC mode. This is another route to achieving fast GC separation where high pressure and short columns are employed. This will be achieved using short packed columns fabricated on ceramic and titanium metal. Normally columns packed with very small particles tend to provide very efficient separations. This will be studied to see if they can be useful in fast GC or if any high pressure drops due to the size of the particles within the column may interfere with this approach. All of these efforts will greatly expand the current understanding of these unique column materials (LTCC and titanium) in the promotion of better portable and/or fast GC devices. In particular, if they can operate successfully at such higher pressures it would be useful to know for future optimization.

CHAPTER TWO

2.0 EXPERIMENTAL

2.1 General Fabrication of LTCC Tiles

LTCC tiles are made from ceramic tapes also known as ‘green’ tapes because they are machined in the ‘green unfired stage’. The tapes are glass-ceramic composite materials¹⁰¹, produced in flat tapes with a thickness in the range of 100-400 μm . These composite materials include inorganic particles of glass, ceramic, or mixture thereof dispersed in a polymer binder, and may also include additives such as plasticizers¹⁰². The composition of the tapes can be formulated in different ways to meet particular applications. The processing of the green ceramic tapes takes place in four different steps. These are texturing, stacking, lamination and co-firing which will be discussed in further detail in the following sections

2.1.1 Texturing

Vias, channels and cavities are very important parts of fluidic microsystems. Patterning ceramic tapes can be achieved in several different ways. For instance, vias and channels can be formed by punching, jet vapour etching, and photolithographic patterning¹⁰². Patterning may also be achieved by embossing the surface of the green-sheet where an embossing plate with a negative image of the desired structure is pressed against the green-sheet¹⁰². Laser micromachining¹⁰³ shown in figure 6 can be used as well. Laser equipment allows computer controlled x-y movement of the workpiece in order to machine complex shapes. Material processing by laser is preferred because it

provides a non-contact, low heat input, precise method for the formation of small holes with low taper and smooth wall structure.

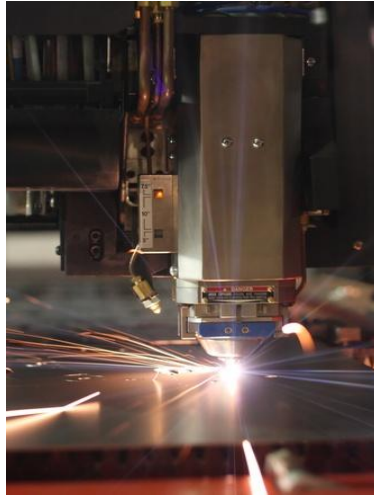


Figure 6: A CO₂ Laser Milling Procedure.

Three layers are generally required to fabricate a channel: a top layer to make media interconnection, a middle layer for the channel and a bottom layer to serve as the chip's base.

2.1.2 Stacking of layers

Following the texturing is a technique called stacking. Here, the LTCC green-sheet layers are stacked into one module in their respective order. To accomplish that, room temperature adhesives are applied to either surface of the green-sheets. Room temperature adhesives are preferred as they do not undergo chemical change or react chemically with components of the substrate. The room temperature adhesives are applied to the green-sheets with conventional coating procedures where spin coating and

spraying are the preferred methods. A sprayer is used in the latter for the spraying and often a higher dilution level of the adhesive is preferred. Spin coating on the other hand, involves placing an excess amount of a solution on the substrate which is then rotated at high speed in order to spread the fluid by centrifugal force. Rotation is continued, until the desired thickness of the film is achieved. After coating, the room temperature adhesive is allowed to dry and the tapes are stacked together afterwards to form a structure.

2.1.3 Lamination

Typically, the stacking process alone is sufficient to bind the green-sheet layers together with room temperature adhesives. However, in order to effect a more secure binding of the layers, lamination is used. There are two techniques that are used in practice by industry; these include uniaxial pressing and isostatic pressing. Uniaxial pressing occurs when the stacked green-sheet layers are pressed between two parallel heated plates. One drawback to this technique is that deformation of the etched channel or cavity can occur due to the high operating pressure on the edges. The alternative method, isostatic lamination, uses water heated to 80 °C as a medium to uniformly distribute the force of the lamination with a recommended pressure of 300 psi. This process minimizes the de-lamination and has more uniform shrinkage.

2.1.4 Co-firing

The firing of the stacked layers in a furnace finally follows the lamination procedure. Co-firing can be achieved in two different ways: constrained and

unconstrained sintering. The constrained process uses two additional tape layers to co-laminate the unfired LTCC tapes. These two additional layers constrain the shrinking of the LTCC tapes during the firing process. The constraining tapes do not shrink or sinter themselves, but maintain a uniform high friction contact to the surface of the LTCC. This allows shrinking to reduce greatly.

Depending on the composition of the green-sheets, a specific temperature-time program is needed for the firing process. Typically, the oven is heated to 450 °C with a gradient of about 2 - 5 °C per minute. During this stage the organic solvents are removed. The temperature is then further raised and held at 880 °C for 15 minutes to complete the sintering. A controlled cooling of the furnace to room temperature is performed in the last phase of the firing process. Figure 7 presents a graphical representation of the entire fabrication processes; texturing, stacking, lamination and co-firing.

2.2 Titanium Chips

2.2.1 General Fabrication of Titanium Chips

Other substrates were also investigated in this study. Unlike the ceramic, titanium chips are assembled differently. A process called diffusion bonding is used in which two prepared surfaces are joined at elevated temperature and under applied pressure. Diffusion bonding is a method of joining metallic or non-metallic materials. This bonding technique is based on the atomic diffusion of elements at the joining interface as seen in figure 8. One advantage of this technique is that, certain dissimilar materials can be welded together since bonding is driven by diffusion of atoms.

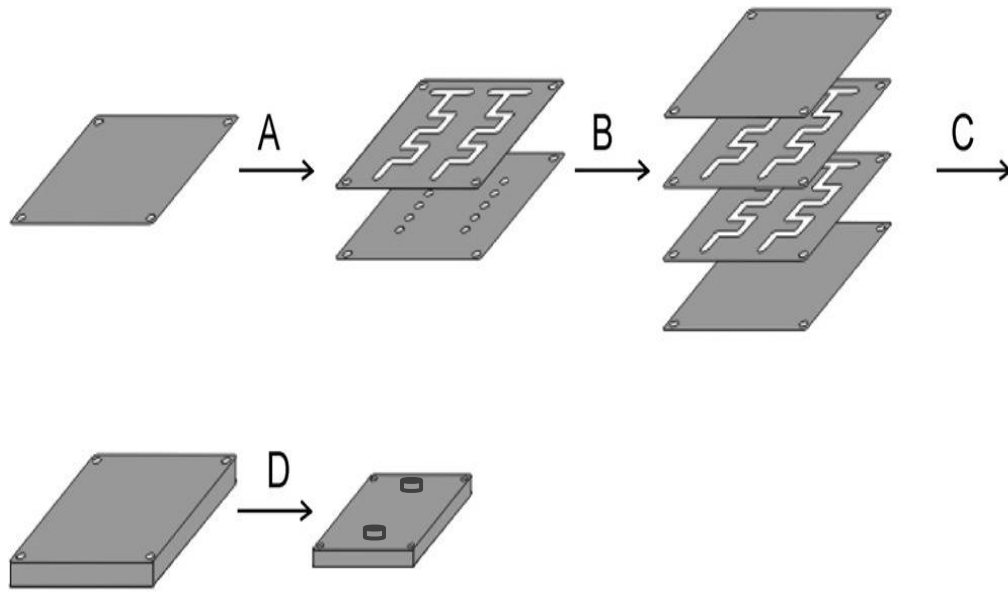


Figure 7: Illustration of the processes involved in the Fabrication of an LTCC tile. A) Texturing B) Stacking C) Lamination D) Co-firing¹⁰⁴

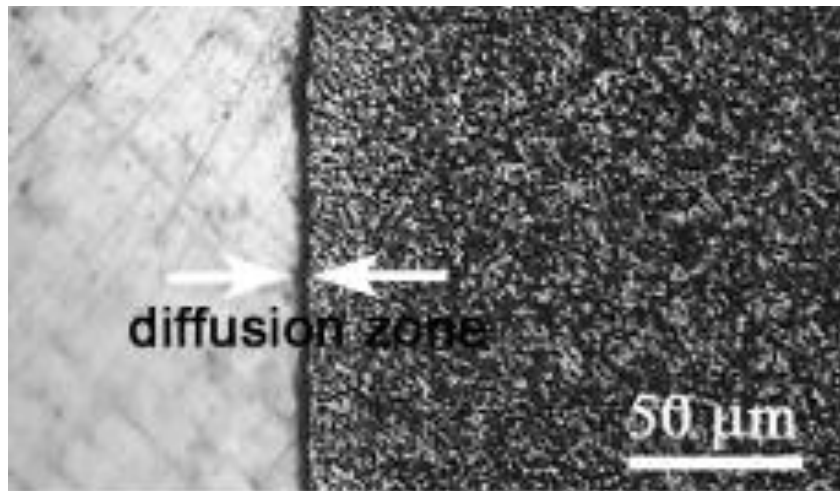


Figure 8: Typical microstructure of a diffusion bonded joint¹⁰⁵.

Figure 9, depicts the process of fabricating these titanium chips. The processes include, texturing, stacking and bonding.

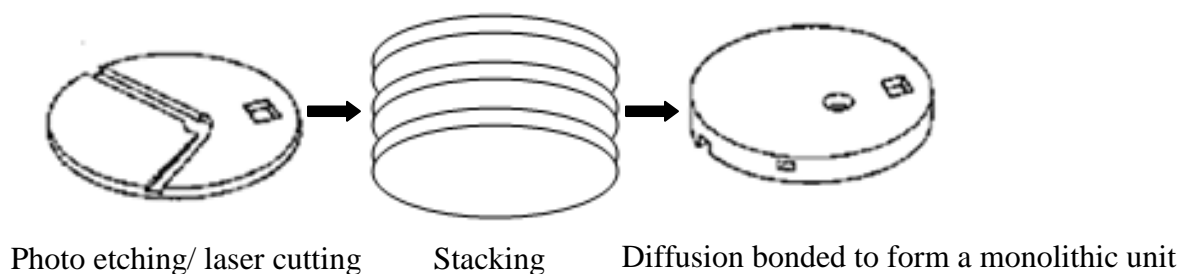


Figure 9: Illustration of the processes involved in the Fabrication of a titanium chip

2.3 Instrumentation and Supplies

In order to probe separation characteristics, the various columns examined were individually mounted inside a commercial GC-FID instrument (Shimadzu model GC-9A) that was used as a common platform from which to perform injections, control temperature, and detect analytes. A schematic of the experimental setup used is shown in figure 10.

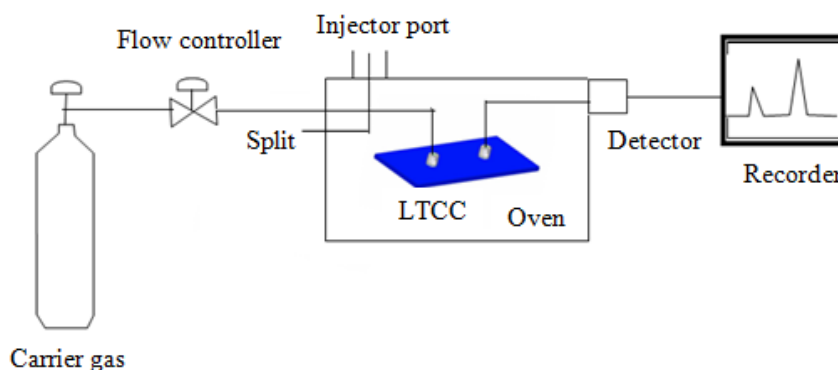


Figure 10: Schematic diagram of the GC Setup used.

Eight columns were examined in these experiments; six of which were open capillary and the remaining two were packed columns. The first was a coated LTCC chip with square channel (100 μm x 15 m; Waters Corporation, Milford, MA, USA). This chip had a dual spiral design as shown in figure 11, where the center of each spiral contained a via that connected to the column inlet or outlet by way of a 50 cm length of 100 μm i.d. uncoated fused silica capillary tubing (Polymicro, Phoenix, AZ, USA). The second column was a coated LTCC chip with square channels (100 μm x 7.5 m; Waters Corporation, Milford, MA, USA). The third is a coated length of deactivated fused silica capillary tubing (100 μm x 5 m; Polymicro). The fourth is a coated titanium chip with square channels (100 μm x 15 m; Waters Corporation, Milford, MA, USA) which also has a dual spiral design. The fifth and sixth columns examined were a commercial Rtx-1 capillary GC column (100 μm x 20 m, and 100 μm x 7.5 m; 0.4 μm film thickness; dimethyl polysiloxane stationary phase; Restek, Bellefonte, PA, USA). The last two are packed ceramic and titanium columns (Waters Corporation, Milford, MA, USA). The Ceramic and titanium tile columns are both 10 cm long x 300 μm and are packed with 5 μm and 1.7 μm C18 particles respectively (Waters Corporation, Milford, MA, USA). Table 2 summarizes the various types and properties of the GC columns studied in this work.

Table 2. Different columns investigated in this work

<i>Column Type</i>	<i>Column Dimension</i>		<i>Stationary Phase</i>
	<i>Length</i> <i>(m)</i>	<i>Diameter</i> <i>(μm)</i>	
LTCC Chip	15	100 s	OV-101
LTCC Chip	7.5	100 s	OV-101
Fused Silica Tubing	5	100	OV-101
Titanium Chip	15	100 s	OV-101
Rtx-1 Capillary Column	20	100	100% dimethyl polysiloxane
Rtx-1 Capillary Column	7.5	100	100% dimethyl polysiloxane
Ceramic Packed Column	0.1	100 s	3 μm C ₁₈ particles
Titanium Packed Column	0.1	100 s	1.7 μm C ₁₈ particles

s = denotes a square channel

High purity helium (99.999 %; Praxair, Calgary, Canada) was used as the carrier gas. An injection split ratio of 40:1 was employed in the separations. High purity hydrogen (99.99%; Praxair) and medical - grade air (Praxair) were used to support the detector flame at respective flow rates of 35 and 350 mL/min. An injector/detector temperature of 220 °C was maintained during the experiments.

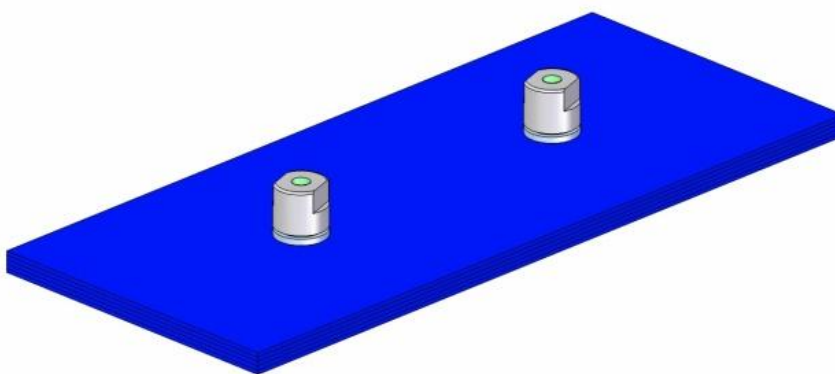
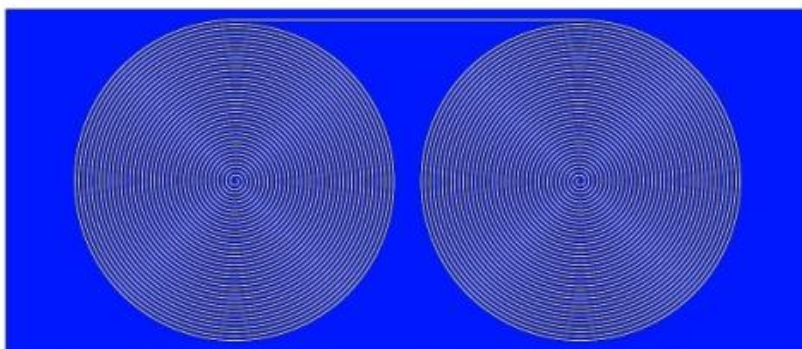


Figure 11: A schematic of the LTCC tile used for GC. A dual spiral design is employed, where the center of each respectively acts as the inlet and outlet for the column.

2.4 Column Coating

LTCC chips were coated with a non-polar film of polydimethyl siloxane stationary phase (OV-101) using a dynamic coating method adapted from earlier μ GC work involving silicon substrates with square channels¹⁰⁶. The coating procedure is shown in figure 12. Briefly, the LTCC column channel was first filled with the stationary phase solution (5% w/w OV-101 in hexane) using nitrogen (Praxair) pressure. A cross-linking agent of 1% w/w dicumyl peroxide was also present in this solution. Next, the nitrogen pressure was dynamically adjusted such that the coating solution was displaced from the LTCC chip at a steady rate of about 0.5 cm/s. Once the coating solution had completely exited the channel, the remaining deposited layer of stationary phase was further dried under a flow of nitrogen gas for 1 hr at ambient temperature. After this, the tile was connected to the inlet only using a fresh piece of fused silica and the column was set to 80 °C, and then immediately raised at 5 °C/min to 160 °C for 1 hour, and then again raised at this same rate to 200 °C and left for another hour in order to crosslink the stationary phase. After this, the column outlet was connected to the detector using a fresh piece of fused silica and separations were initiated. Using this method a stationary phase thickness of around 0.5 μ m was normally achieved and the crosslinking was effective enough to prevent stationary phase bleed up to temperatures of about 250 °C. Similar results were also achieved when using this same method to coat the fused silica capillary tubing column.

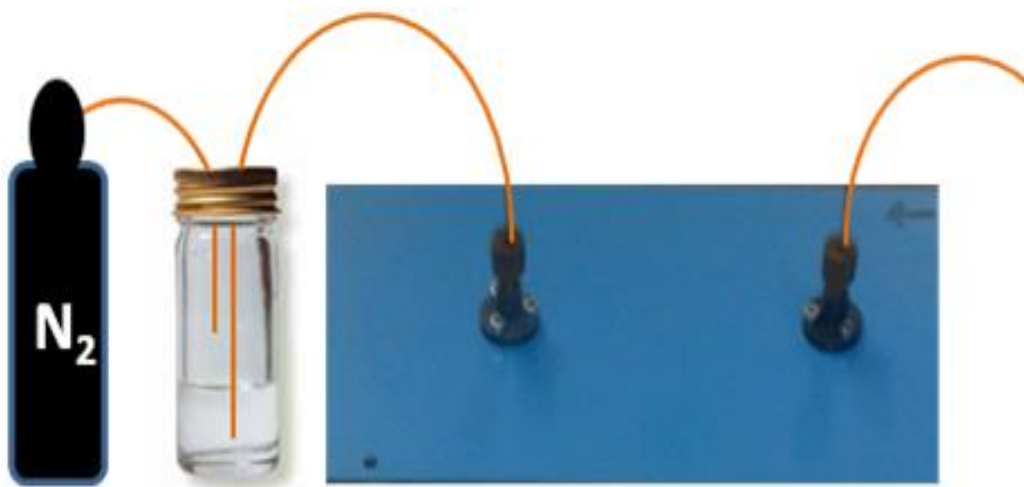


Figure 12: Graphical representation of the coating technique

2.5 Samples

Commercial samples examined in this study included an analytical grade n-alkane (C_8 - C_{20}) standard solution (40 mg/L each in hexane; Sigma-Aldrich, Oakville, ON, Canada) and a Grob test mixture (Grob test mix 35000; Restek) containing individual components within a concentration range of 280 to 530 $\mu\text{g/mL}$. Additionally, a BTEX sample containing 1 $\mu\text{g}/\mu\text{L}$ each of benzene, toluene, ethylbenzene, meta-xylene, para-xylene, and ortho-xylene (99%; Sigma-Aldrich) was prepared in carbon disulfide (99.9%; Sigma-Aldrich). Dodecane, tetradecane, and hexadecane (99%; Sigma-Aldrich) standards were also prepared at 1 $\mu\text{g}/\mu\text{L}$ in carbon disulfide.

2.6 High Pressure GC on Packed Columns

A schematic of the experimental setup is shown in figure 13.

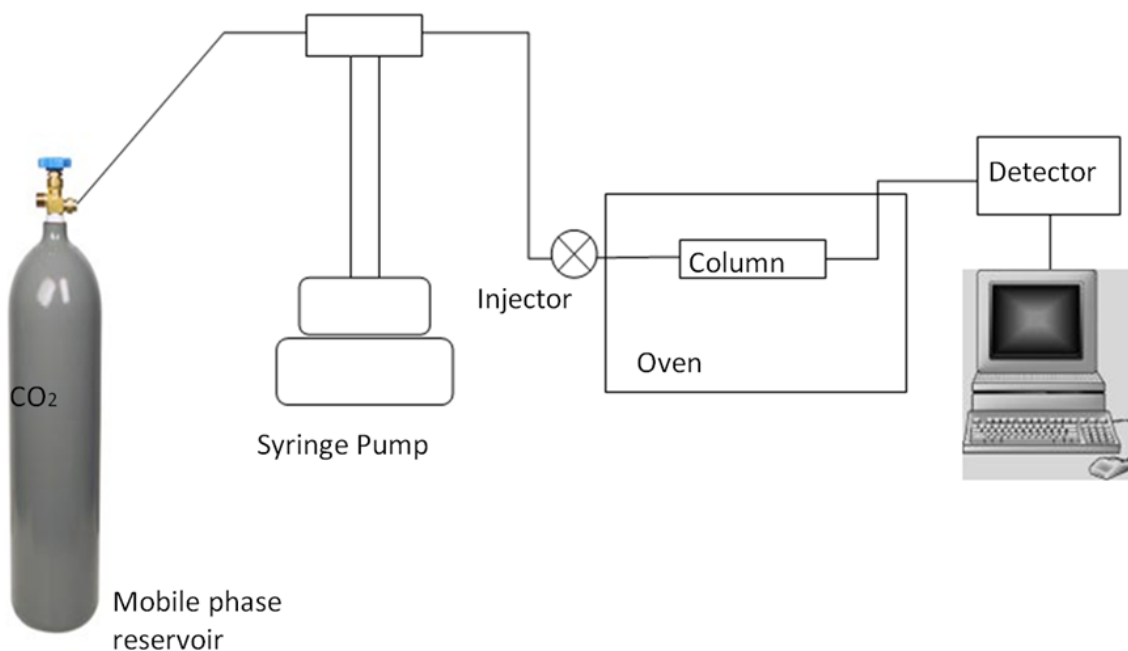


Figure 13: Schematic diagram of the High Pressure GC Setup used.

Here, high purity carbon dioxide (99.99%, Praxair, Calgary, Canada) was used as the mobile phase. An ISCO syringe pump was also occasionally employed in the separations (Teledyne ISCO, Lincoln, USA). High purity hydrogen and air (99.99%; Praxair) were used to support the detector flame at respective flow rates of 35 and 350 mL/min. The packed columns were examined by mounting each inside a commercial GC-FID instrument (Shimadzu model GC-9A) using a 30 cm and 50 cm length of 100 μ m i.d. uncoated fused silica capillary tubing (Polymicro, Phoenix, AZ, USA) to connect the injector to the column inlet and the column outlet to the detector respectively. An

injector/detector temperature of 220 °C was maintained during the experiments. All other variations are described in the text.

CHAPTER THREE

3.0 THE INVESTIGATION OF LTCC PLATFORMS IN GC

3.1 Design of GC Columns

Since the introduction of Chromatography, most separations have always been carried out in columns with circular cross-sections made of a variety of materials which include glass, plastic, and metals¹⁰⁷. The circular cross-section of these columns is often favoured because of the ease of accessing tubes of this nature, their simple machining and threading. Lately, columns with different types of cross-section such as square and rectangular, have also been explored¹⁰⁸. Square channel columns for chromatography emerged with the advent of microfluidic separation devices. The typical methods of fabricating these devices (laser ablation, etching, and embossing) are not well suited to the fabrication of channels with circular profile. As a result, microfluidic channels with a non-circular profile such as semicircular, rectangular and trapezoidal are most common. Theoretical calculations comparing open rectangular to circular formats predict a better separation performance in GC for the former, even though its use in pressure driven LC separations continues to be a source of concern^{109,110}. For example, a finding made by Giddings et al.¹⁰⁸, showed that fluid drag at the edges and corners is often associated with non-circular columns in LC, and as such, can negatively impact the column efficiency through zone distortion and tailing. This situation appears to be no different with our LTCC Tile.

A Scanning Electron Microscope (SEM) image shown in figure 14 revealed a thicker phase at the corners of the LTCC chip after it was coated, which is indicative of fluid drag in these zones. Nonetheless, Rozing et al. in an experiment comparing the

separations between circular capillaries with those obtained in microfluidic chips demonstrated that better performance was still achievable with the latter¹¹¹. The performance of the LTCC chips as coated was thus tested and will be discussed below.

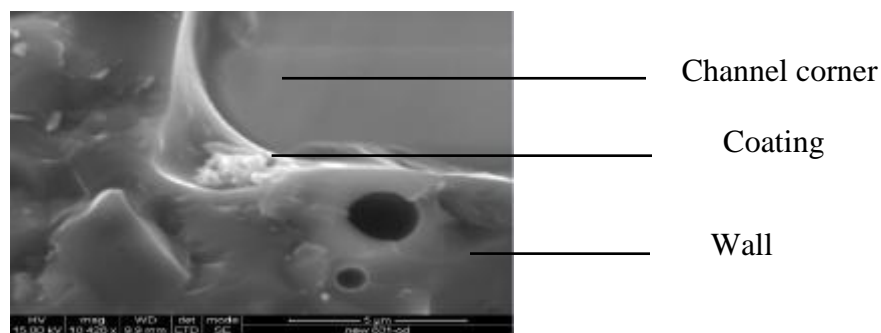


Figure 14: SEM image of LTCC coated tile cross-section near channel corner.

3.2 Performance of Uncoated vs. Coated LTCC Tile

Initially, the retention properties of the LTCC device in the absence of a coated stationary phase were examined. This was done not only to determine any potential separation capacity that the bare LTCC material may have, but also to better ascertain the influence that it may have on peak shape. A mixture of n-alkanes was analyzed on the uncoated LTCC device and the results are shown in figure 15. The tile did appear to separate the mixture of analytes, even though the peak shapes were rather poor. This is contrary to experiments on other bare LTCC devices that did not separate individual components.⁸⁸ The peaks observed on the bare LTCC tile in our case were broad and tailing which can be attributed to the adsorptive interactions at the gas-solid interface. This suggests that this gas-solid mode of interaction on the bare tile surface could

potentially be developed and optimized to produce useful separations in future experiments.

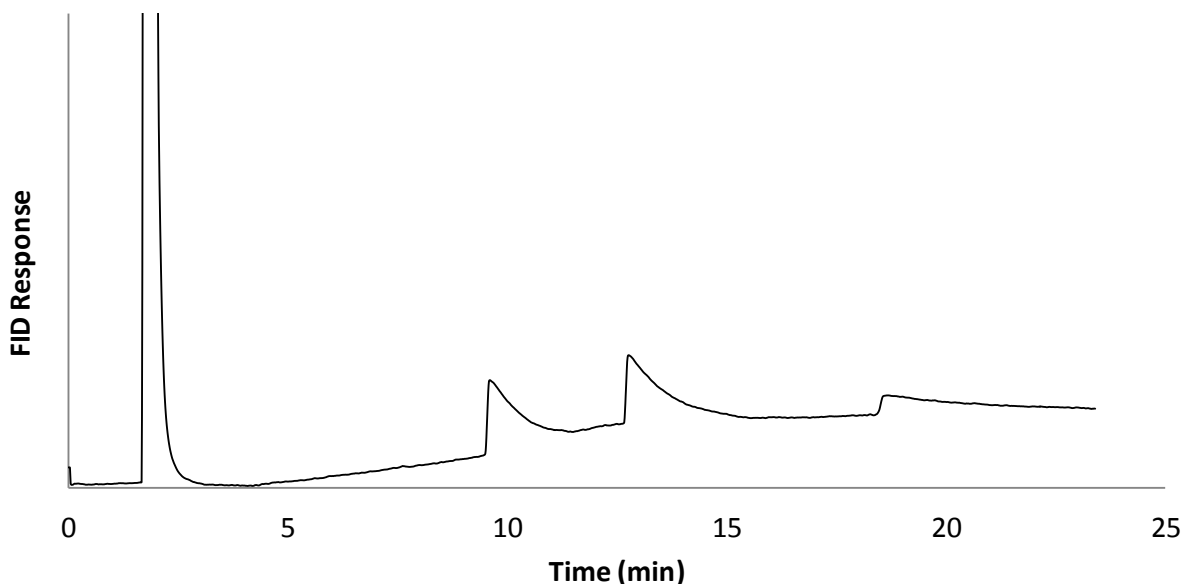


Figure 15: Chromatograms of n-alkane mixture separated in the LTCC tile without a stationary phase coated on the surface. Temperature program: 25 to 120°C at 10°C/min. Detector temperature: 220°C Analyte elution order: carbon disulfide (solvent), dodecane, tetradecane, and hexadecane. He flow rate: 0.29mL/min, Mass injected on column: 250 ng

For example, LTCC tiles are rich in alumina and studies have shown the use of aluminium oxide (alumina) columns for separations of light hydrocarbons^{112,113}. As such, the separation capabilities shown by the bare tile during the preliminary studies are reasonable. Future experiments aimed at increasing the porosity of the channels in these devices could perhaps result in better separation efficiency. However, this was not undertaken in this study. Next, a stationary phase was applied to the column in an attempt to improve the separation efficiency and enhance the peak shapes observed on the bare LTCC tile.

Generally, it is desirable to have a stationary phase with a wide temperature operating range covering as far as possible the full temperature range of GC, -60 °C to 400 °C. One stationary phase with a wide temperature range is OV-101, a type of polysiloxane (methyl silicone) GC liquid phase. This has a working temperature range from 0 – 350 °C. In addition to this property, OV-101 liquid phase has low vapour pressure and good film forming properties. More so, it tends to be soluble in some common volatile organic solvents making it easier to work with. The bare tile was coated with this stationary phase, and figure 14 above shows an image of the typical coated channel under microscopic magnification. The application of the stationary phase on the bare LTCC tile influenced the separation positively. Figure 16 shows a separation of the same analyte mixture from figure 15 after coating the bare LTCC tile with OV-101 stationary phase. The results display a dramatic improvement in the appearance of the separation. In particular, relatively narrow symmetrical peaks are produced for each of the three analytes, demonstrating that coated LTCC tiles can function as reasonable platforms for GC separations.

3.3 Thermal Stability of Column

Further studies looked into the thermal stability of the column. This test was carried out to predict the maximum allowable operating temperature for this column coated with OV-101 liquid phase. Normally, a crosslinking reagent is added to low to medium viscosity polysiloxane oils to improve their thermal stability. Dicumyl peroxide was chosen in this study to increase the thermal stability of the liquid phase. The test was

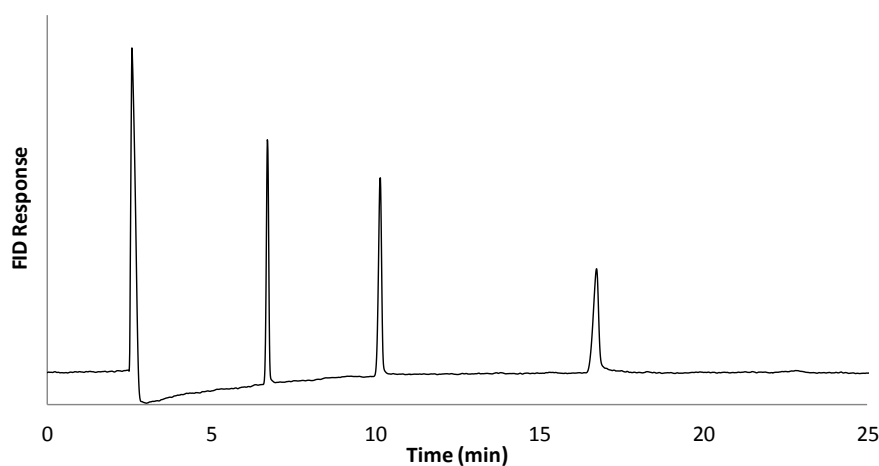


Figure 16: Chromatograms of n-alkane mixture separated in the LTCC tile with a stationary phase coated on the surface. Temperature program: 120 to 180 °C, at 10 °C/min. Analyte elution order: carbon disulfide (solvent), dodecane, tetradecane, and hexadecane. Detector temperature: 220 °C. He flow rate: 0.25 mL/min, Mass injected on column: 250 ng

first carried out with a 5 m x 100 μ m i.d. fused silica column in the absence of a crosslinking reagent using a temperature gradient. With BTEX analytes present (coincidentally), the analysis was allowed to run from 50 °C to 300 °C at a programming rate of 40 °C/min. The stationary phase began to bleed from the surface of the fused silica when the temperature reached 170 °C. This can be seen by the sudden rise or offset of the baseline in figure 17A. However, with the addition of a crosslinking agent (dicumyl peroxide) to the stationary phase, the column did not show any sign of bleeding until the temperature reached 290 °C, at which time, the stationary phase began to bleed from the surface of the fused silica under the same conditions. This latter test was carried out with no analyte present. By comparison, the dicumyl peroxide was able to improve the thermal stability of the column by about 100 °C. This can be seen in figure 17B. Hence, all

separations carried out on the LTCC tile were done with respect to this upper temperature limit, and care was taken to operate well below it.

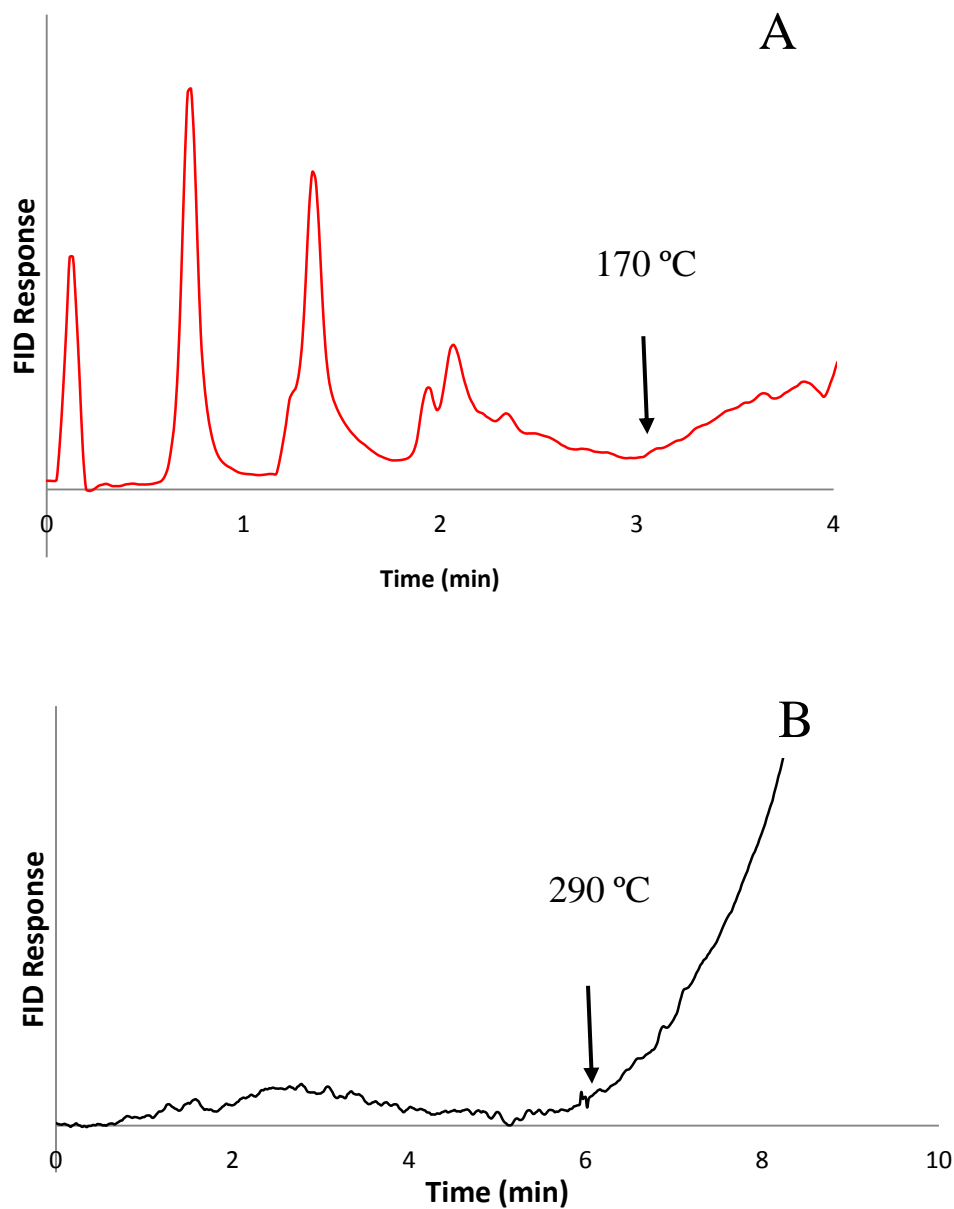


Figure 17: A chromatogram showing stationary phase bleeding from a 5 m x 100 μm i.d. fused silica column (A) without and (B) with dicumyl peroxide. Conditions: column temperature 50°C to 300°C at a programme rate of 40 °C/min.

3.4 Column Efficiency

The assessment of column quality is of paramount importance. Column quality includes efficiency which can be measured by parameters such as plate number (N) and plate height (H). Plate number and height are normally measured from isothermal chromatograms for inert substances such as hydrocarbons and both values depend on the operating conditions and the properties of the analyte. Figure 18 presents a plot of plates per meter as a function of column flow rate for a dodecane test analyte separated on the LTCC tile and a commercial capillary GC column. The LTCC tile is 15 m x 100 μm i.d. whereas the commercial capillary GC column is 20 m x 100 μm i.d. As seen in figure 18, the trace for the commercial column follows the anticipated trend and yields a maximum plate per meter at a flow rate of around 0.25-0.30 mL/min. Comparatively, the LTCC tile produces similar results of increasing plates per meter up to a column flow rate of about 0.25 mL/min. However, further increases in flow rate were unattainable with the LTCC tile. Methods to overcome this were examined by increasing carrier gas pressure and altering the split flow ratio, but were not able to further raise the gas flow through the tile. Some reasons first pondered to account for the flow restriction were the double-coil design of the LTCC channel and its relatively intense radius of curvature compared to that of a conventional capillary column coil. To investigate this, a 15 m x 100 μm i.d. length of fused silica capillary tubing was coated by the exact same method and did not exhibit any flow restrictions suggesting that the design of the LTCC tile might be the cause.

Given the observed flow constraints of the LTCC tile, it appeared that higher efficiency would be possible at higher flow rates. Nonetheless, at its current optimum

value in Figure 18, the LTCC tile produced about 560 plates/m for dodecane while the commercial capillary GC column yielded around 780 plates/m for the same analyte. This approximate difference factor of 1.4 is quite reasonable considering that the LTCC tile design and coating procedure used here were only initial prototypes adopted for preliminary testing.

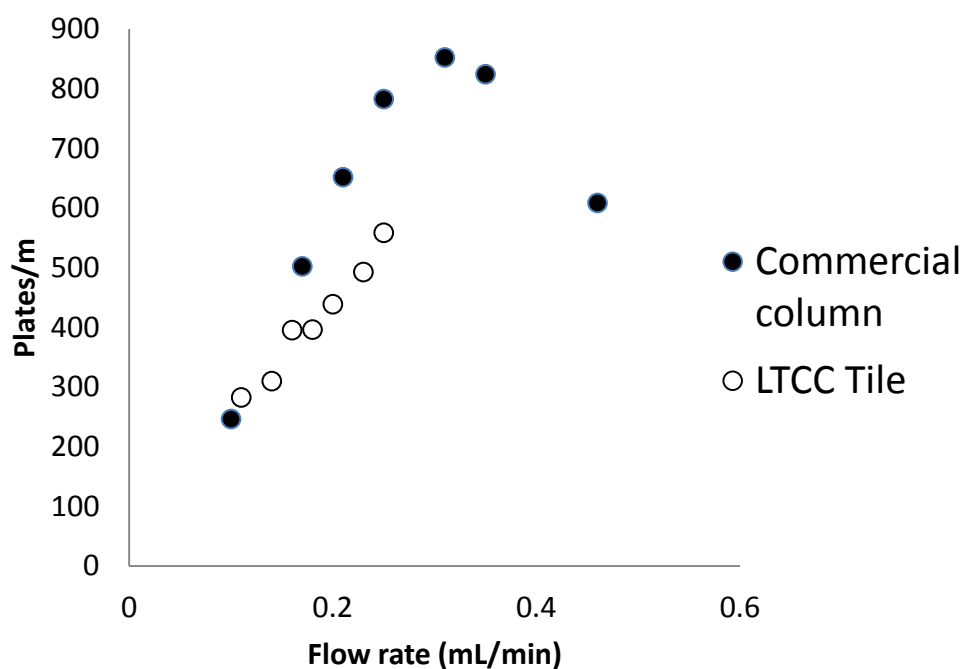


Figure 18: Effect of flow rate on column efficiency for both the LTCC device (○) and a commercial Rtx-1 capillary GC column (●), 15 m x 100 μm i.d. and 20 m x 100 μm i.d., respectively. Column temperature: 180°C. Analyte solution: 1 $\mu\text{g}/\mu\text{L}$ of dodecane in carbon disulfide.

The LTCC tile suffering from flow restriction was sent to the manufacturer to further examine, and the cause of this difficulty was uncovered. Their investigation showed that pieces of broken fused silica tubing had plugged both the inlet and outlet of the tile vias. This material was being used to connect both the injector and the detector to the column in the GC oven. Figure 19A shows the plugged inlet of the LTCC tile and figure 19B shows after being cleared. Once the silica was cleared from the inlet and outlet of the column, an increased gas flow rate to about 1 mL/min was achieved, compared to the maximum 0.25 mL/min generated previously. Unfortunately, a Van Deemter plot could not be carried out after being fixed because the LTCC tile was accidentally destroyed during packaging and shipping.

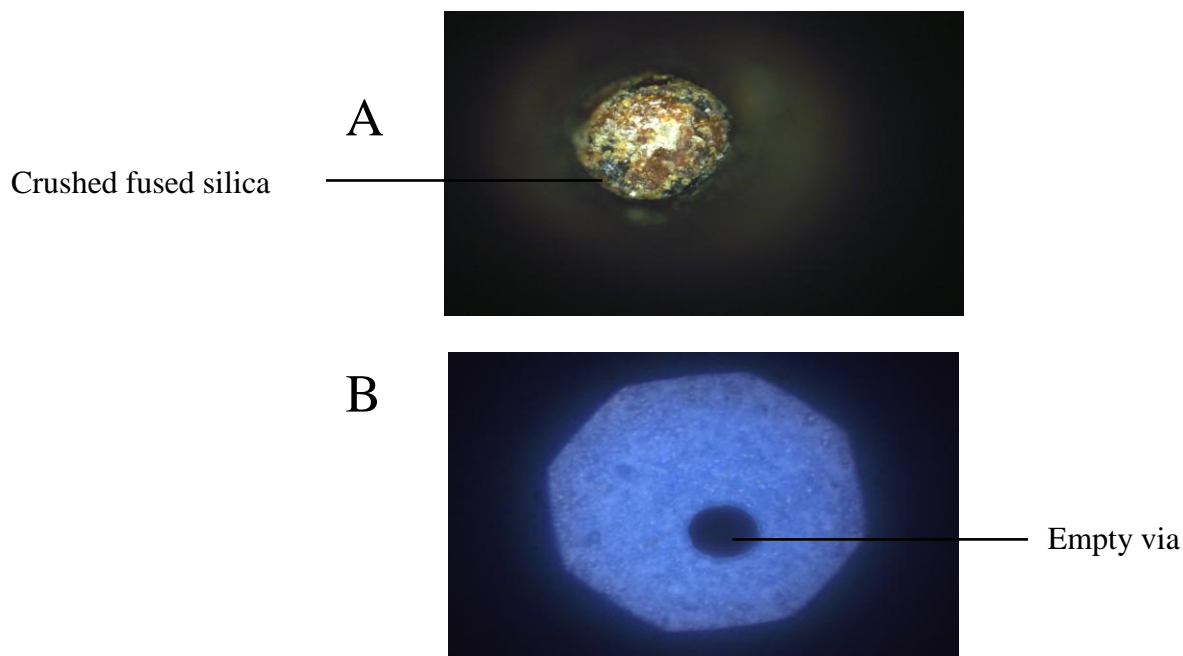


Figure 19: SEM images of (A) plugged inlet and (B) the cleared inlet of the 15 m x 100 μm i.d. coated LTCC tile.

Subsequent experiments utilized a new 7.5 m x 100 μm i.d. LTCC tile to replace the broken one. 15 m lengths were unavailable. For further comparison to the tile a similar dimension and length of the commercial capillary column was used. Figure 20 presents a formal Van Deemter plot where plate height was plotted as a function of flow rate for a dodecane analyte. It can be seen that both the LTCC tile and the commercial capillary column again followed a similar trend, recording a minimum plate height at the same flow rate, 0.31 mL/min. The LTCC tile produced about 14300 plates for dodecane while the commercial capillary column yielded about 4500 plates. This difference of a factor of three is encouraging and demonstrates that LTCC tiles can perform on par with commercial capillary columns in GC.

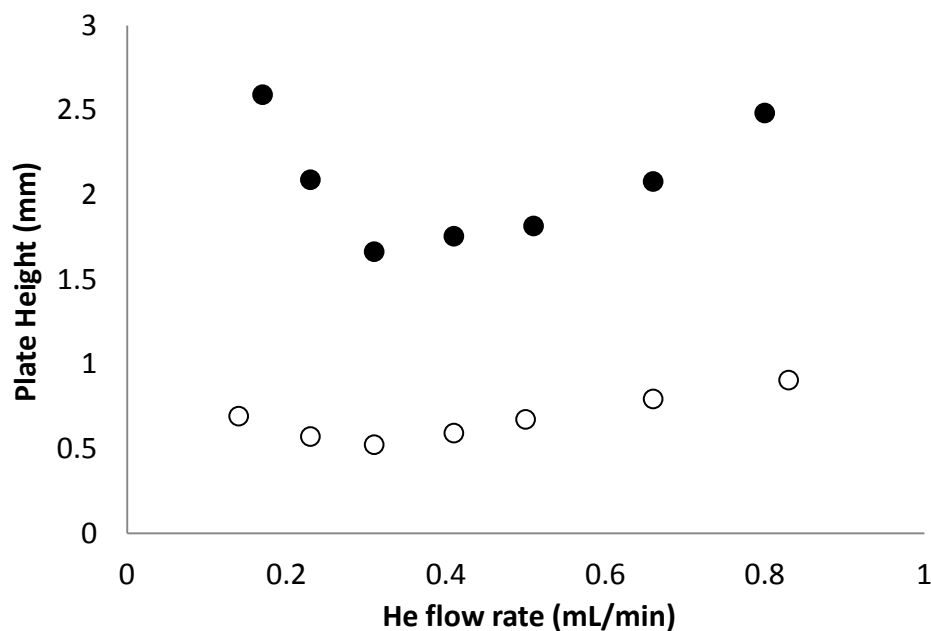


Figure 20: Effect of flow rate on column efficiency for both the LTCC device (○) and a commercial Rtx-1 capillary GC column (●), each 7.5 m x 100 μm i.d.. Column temperature: 130°C. Analyte solution: 1 $\mu\text{g}/\mu\text{L}$ of dodecane in carbon disulfide.

3.5 Sample Capacity

The sample capacity of the tile was probed to determine how analyte mass loading would impact peak shape. It is expected that when a higher mass of sample is introduced onto a column for its given diameter and stationary phase thickness, the column will be overloaded, leading to peak fronting and also causing the peak maximum to shift to a longer time. Figure 21 displays this concept of sample capacity for peak shapes of a test analyte injected onto the LTCC tile. Using a dodecane test solute, analyte masses from 1 to 50 μg were injected onto the LTCC tile and the commercial column and their peak asymmetry was measured at 10% of the total peak height. As shown in table 3, similar values for peak asymmetry are obtained for both columns and the onset of peak fronting appears to occur in each for injected masses beyond about 1 μg . Considering the 40:1 split ratio employed, this translates into an on column mass of about 25 ng, which is reasonable for a narrow bore GC column. Therefore, no major difference was noted between the LTCC tile and the conventional capillary column with regard to sample capacity.

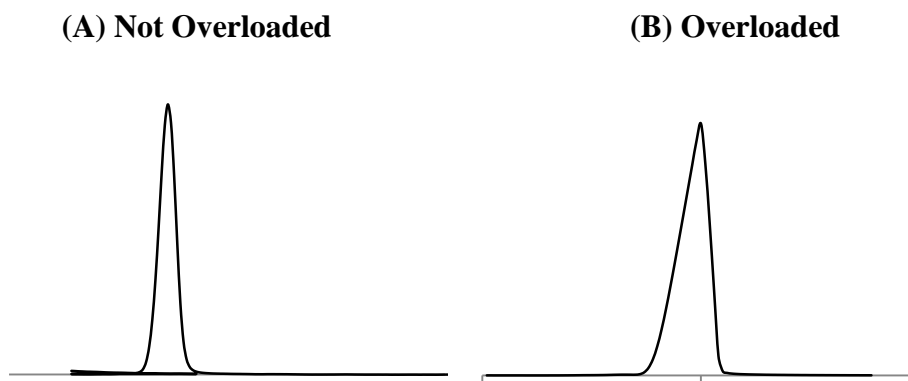


Figure 21: Effect of sample size on chromatographic peak shape: (A) LTCC tile not overloaded, mass = 25 ng and (B) LTCC tile severely overloaded, mass = 1250 ng. Column temperature: 180°C. Detector temperature: 220°C. He flow rate: 0.25mL/min.

Table 3. Peak Asymmetry Values^a between LTCC and Conventional Column

		Peak Asymmetry	
Injected Mass (μg)	Mass On Column ^b (ng)	LTCC Tile	Conventional Column ^c
1	25	1.00	1.00
5	125	0.85	0.88
10	250	0.81	0.78
20	500	0.71	0.64
50	1250	0.36	0.46

- a. Measured for dodecane in carbon disulfide at 180°C, at 10% of full peak height
- b. Factoring the 40:1 split injection ratio
- c. Restek Rtx-1 capillary GC column

3.6 Peak Splitting

One observation that was occasionally made in the early stages of this investigation with some LTCC tiles was peak splitting into two or more sections. Figure 22 shows a typical result of this nature for a tetradecane test analyte. As can be seen, the peak observed is rather broad and exhibits about 3 different maxima instead of a singular

sharp profile for the injected analyte. Initially, it was postulated that this may have been a result of a flawed coating procedure. In response, multiple additional coatings of the LTCC tile (normally 4 to 5) were attempted. Results are shown in figure 23 where dodecane, tetradecane and hexadecane were injected after the second through to the fifth coatings were performed. While it was found that this approach did eliminate the peak splitting observed, the resulting peaks were considerably broadened from the various extra layers of stationary phase that were applied. Eventually, while examining the coating on the LTCC tile, it was discovered that a channel defect had occurred within the device, while assembling it.

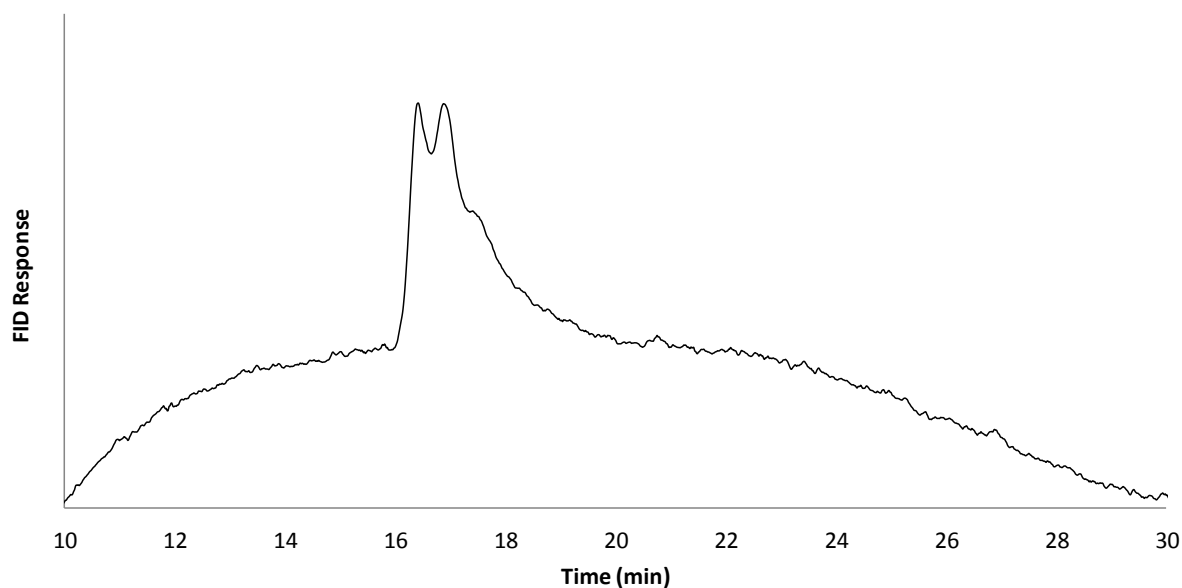


Figure 22: A chromatogram demonstrating peak splitting in an LTCC device with a defect.

Test Analyte: tetradecane. Temperature Program: 35 to 100°C at 10°C/min. Detector temperature: 220°C. He flow rate: 0.25mL/min, Mass injected on column: 250 ng

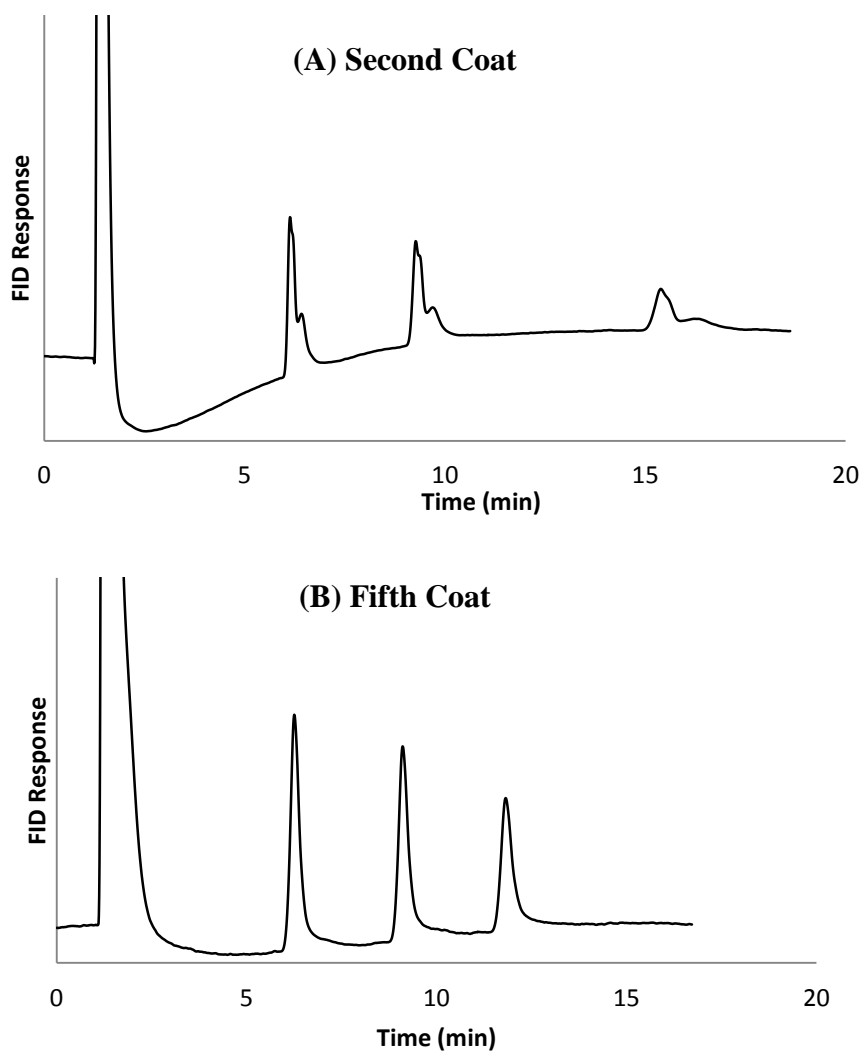


Figure 23: Chromatograms demonstrating the effect of multiple coatings on peak splitting in an LTCC device with a defect. Test Analyte: dodecane, tetradecane and hexadecane in carbon disulfide (solvent). Temperature Program: (A) 50 to 100°C (B) 50 to 150°C, each at 10°C/min. Detector temperature: 220°C. Mass injected on column: 250 ng

Such problems occur in an LTCC tile as a result of various issues. For example, small distortions and warping within the layers that make up LTCC tiles are known to

occur occasionally and have been well characterized¹¹⁴. In this case, a portion of the channel wall was destroyed while applying the covering layer of the LTCC tile, effectively leaving a hole in the channel wall sufficient to allow passage of an analyte through the channel wall between two spirals of a column. This process is illustrated in Figure 24. As a result, an analyte can partition into portions that either cross through the channel wall or remain in the existing channel. For those that cross through, they have effectively skipped ahead of the chromatographic band, arriving at the detector earlier and causing the appearance of peak splitting. Therefore, as was observed, for tiles with several wall defects, a peak with multiple split features would be expected. Fortunately, such problems can be easily avoided by optimizing the manufacturing process and scanning the assembled LTCC device by acoustic microscopy prior to coating with stationary phase. Once these measures were put into place, we did not observe any further defects or peak splitting.

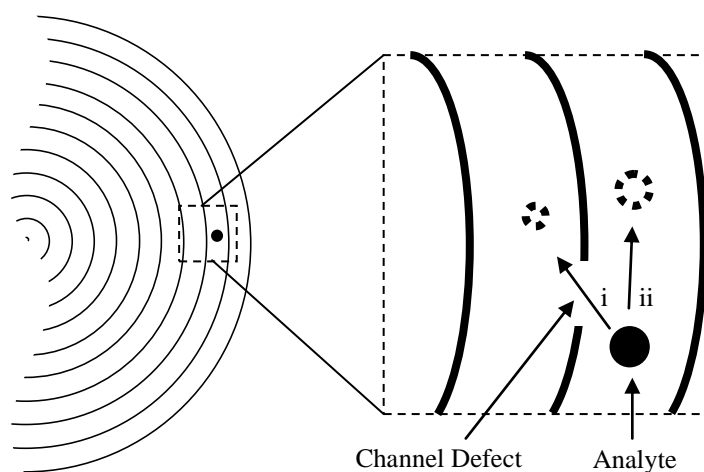


Figure 24: An illustration of how peak splitting occurs within such a tile, where a portion of analyte (i) passes through the channel wall leaving the remainder (ii) behind.

2.7 Comparative Applications

Some routine GC applications were carried out on the LTCC tile and the commercial capillary column (each 7.5 m x 100 μ m i.d.) in order to get a practical perspective on the relative analytical GC performance of the ceramic device. Figure 25 displays an isothermal separation of a BTEX standard using each system. For the LTCC tile (upper trace), it can be seen that all of the sample components separated well, with the exception of the overlapping meta- and para-Xylene isomers, which commonly co-elute. For the commercial capillary column (lower trace) under the same conditions, a similar separation was also achieved with this sample, where again all components were resolved except the same Xylene isomers. However, the sample components are less retained and resolved by comparison.

Figure 26 shows chromatograms for a C₈ to C₂₀ n-alkane standard using each system. As can be observed, for the LTCC tile (upper trace) and the commercial capillary GC column (lower trace), similar profiles are once more observed for each. For example, both yield the same detector baseline offset around 40 minutes into the temperature program, and each separates all of the alkanes in the mixture. Also consistent with the above, the LTCC column generally retains the analytes more compared to the commercial column. Nonetheless, the chromatograms in Figure 26 reflect overall good performance for both.

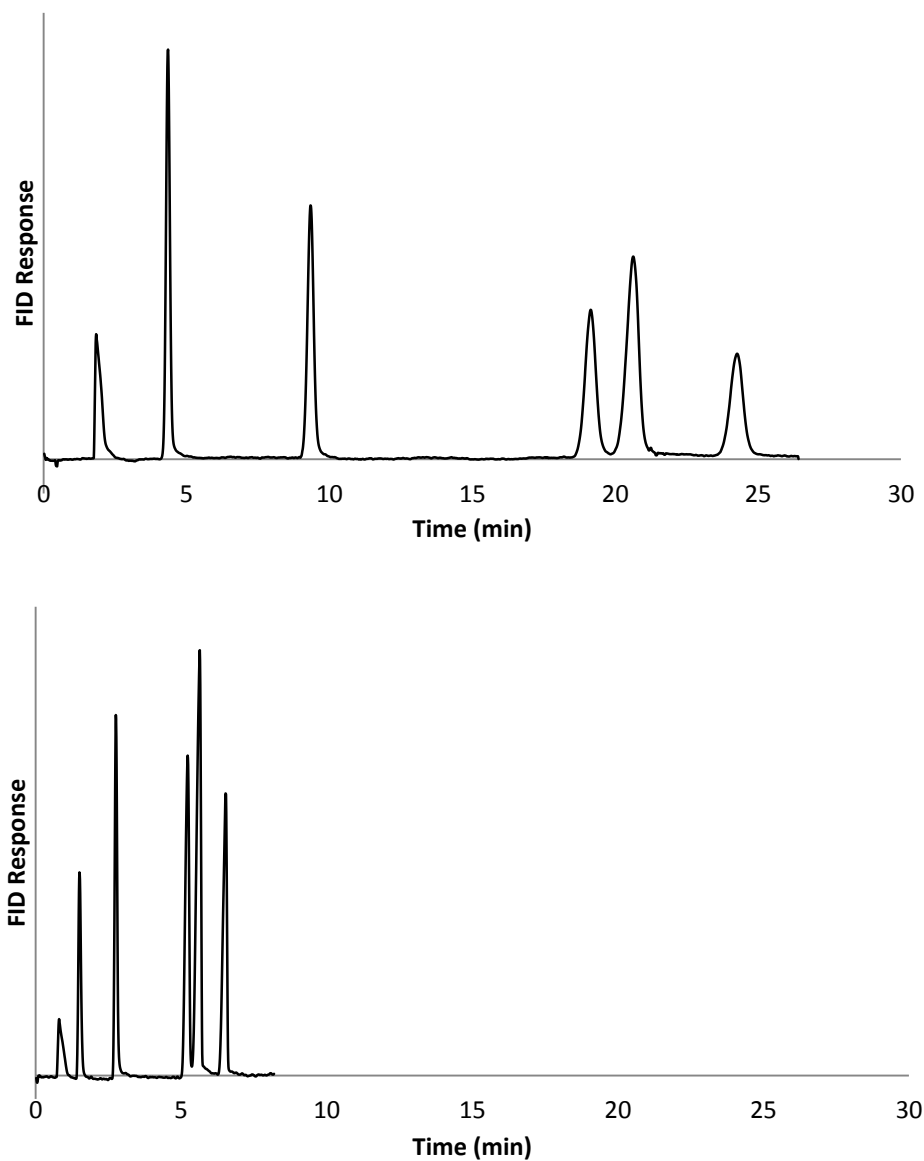


Figure 25: Chromatogram of a 1 $\mu\text{g}/\mu\text{L}$ BTEX standard in carbon disulfide using the LTCC device (upper trace) and the commercial Rtx-1 capillary GC column (lower trace). Column temperature: 60°C. Detector temperature: 220°C. He flow rate: 0.30 mL/min, Mass injected on column: 250 ng Analyte elution order: Carbon disulfide (Solvent), benzene, toluene, ethylbenzene, m- and p-xylene (co-elution), and o-xylene.

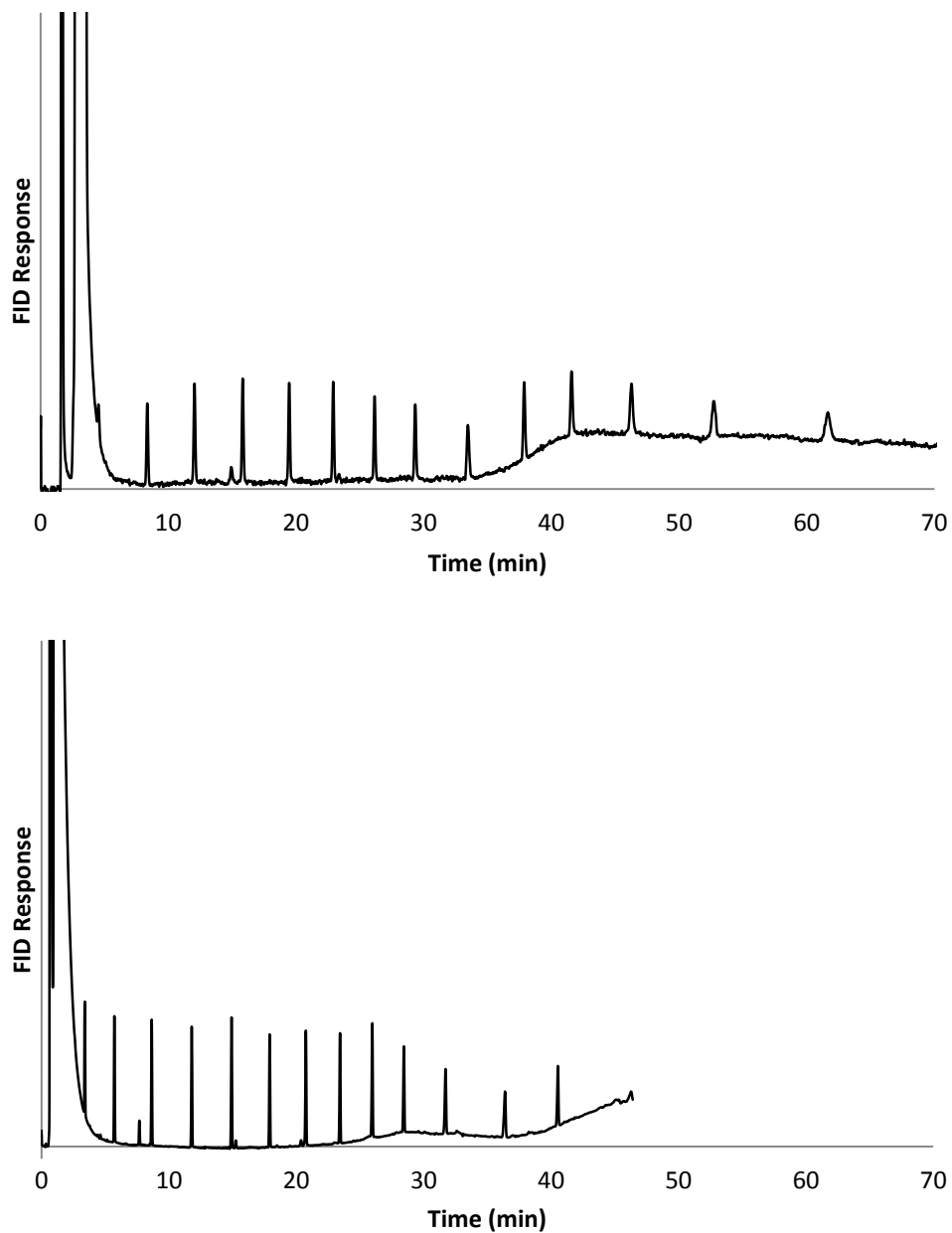


Figure 26: Chromatogram of a 40 mg/L C₈ to C₂₀ n-alkane standard using the LTCC device (upper trace) and the commercial Rtx-1 capillary GC column (lower trace). Column temperature program: 45 to 210°C at 5°C/min. Temperature is held at 180 °C for 10 min. Detector temperature: 220°C. He flow rate: 0.45mL/min. Solvent: dichloromethane.

3.8 Separation Number

In addition to absolute resolution, this is another parameter that is often used to describe the resolving power of a column or column efficiency and is most frequently used with temperature programming in GC. Separation number is the number of possible peaks that appear between two n-alkane peaks with consecutive carbon numbers. It is expressed as

$$SN = \frac{t_{R2} - t_{R1}}{(W_{1/2})_1 + (W_{1/2})_2} - 1$$

Where $W_{1/2}$ is the width at half maximum of the analyte peak and t_R is the retention time.

The LTCC tile produced a cumulative separation number of about 53 peaks between C_{10} to C_{15} alkanes at a programming rate of $5^\circ\text{C}/\text{min}$. This is a reasonable value for narrow bore columns and is also consistent with those obtained from other silicon-based GC tiles¹¹⁵.

The influence of LTCC on temperature programming (if any) was also investigated. Figure 27 shows a plot of device temperature as a function of time. This was done by monitoring flow within the tile and capillary also as a function of temperature, which gave a rough measure of their relative heating rates. As can be seen, there was a temperature lag between the LTCC tile and the commercial column, which could be due to the thermal mass of the LTCC tile being larger than the commercial column. This implies that the LTCC tile compared to the commercial column takes a little longer to heat under the same conditions. Nonetheless, this can be offset by using a larger rate for the LTCC tile. For example, $8^\circ\text{C}/\text{min}$ provided an equivalent profile for the tile to the

5°C/min trial of the column. Overall then, good quality GC separations can be obtained using the LTCC tile isothermally or through temperature programs.

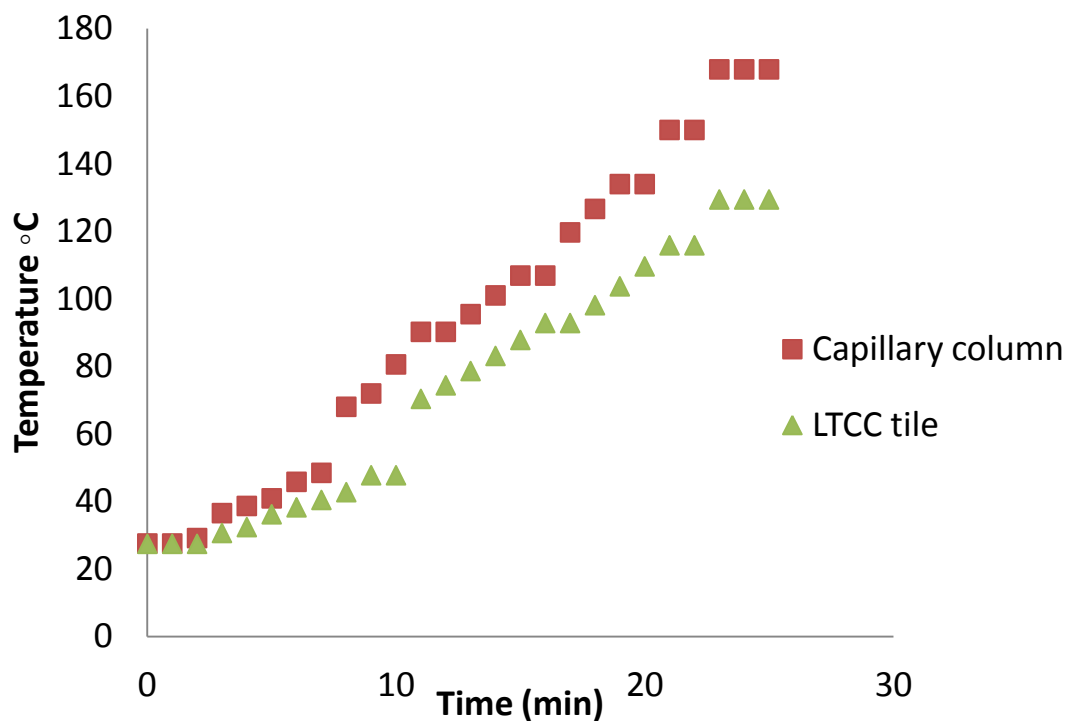


Figure 27: Graph showing approximate heating rates of the commercial column and the LTCC tile

3.9 Analyte Functional Groups

In order to better gauge the ability of the LTCC tile (15 m x 100 μ m i.d.) to separate more polar analytes, a Grobs mixture containing solutes of several different organic functionalities (e.g. amines, alcohols, carboxylic acids) was examined. While 8 of the 12 compounds eluted from the LTCC tile with reasonably symmetrical peak shape, it was found that several of them eluted in clusters of peaks that made it difficult to

determine their retention time and/or peak shape. As such, this did not allow for a clear indication of how the various analytes interact with or elute from the ceramic device. Therefore, separate standards representing the same functional groups from this mixture were prepared and examined individually.

In general it was observed that aldehydes, esters, and mono-substituted alcohols elute from the LTCC device with relatively decent peak shapes. In contrast to this, di-substituted alcohols, carboxylic acids, and amines typically eluted with broad tailing peak shapes. Figure 28 illustrates this for a separation of the above prepared mixture on the LTCC tile.

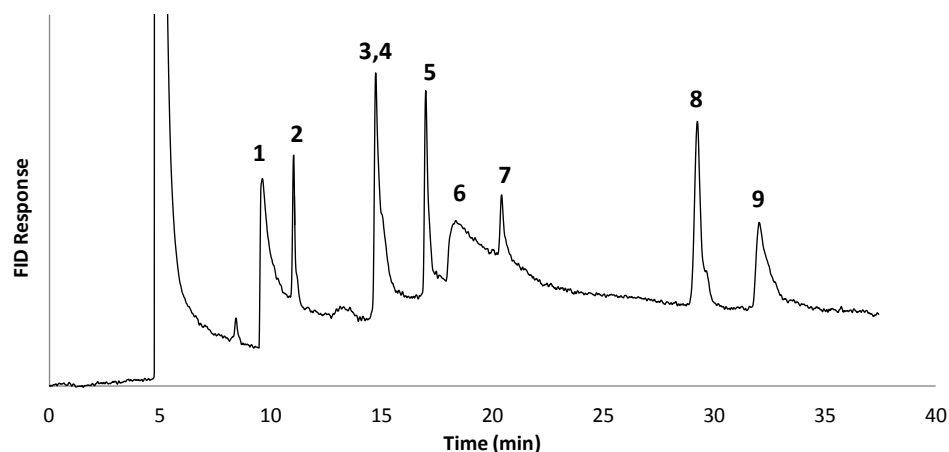


Figure 28: Chromatogram of a mixture of organic compounds of varying functionalities using the LTCC device. Temperature program: 45 to 200°C at 10°C/min. Detector temperature: 220°C. He flow rate: 0.25mL/min. Analyte elution order: 1. 1,2-propanediol, 2. butylacetate, 3. phenol, 4. aniline, 5. octanol, 6. heptanoic acid, 7. decanal, 8. tetradecane, and 9. dicyclohexylamine. Solvent: dichloromethane

It is likely that the peak shapes observed are a direct consequence of the coating procedure used with the ceramic tile. For instance, the stationary phase was simply deposited and crosslinked onto the ceramic channel surface. However, this still potentially leaves most of the ceramic substrate (e.g. alumina content) available for interaction with analyte functional groups as solutes traverse the stationary phase. In this way it is further interesting to note that when the length of coated fused silica capillary tubing (mentioned earlier) was used to separate the above polar analytes, the resultant peak shapes were also broad and tailing. Conversely, the peak shapes for these solutes on the commercial capillary GC column were much improved with relatively less tailing overall. This latter observation can be attributed to the extensive surface deactivation and stationary phase bonding that a typical commercial capillary column embodies relative to the prototype LTCC device used for testing in these initial studies.

3.10 Deactivated LTCC Tile

Treatment of the column through deactivation is an established technique often used to overcome tailing associated with polar analytes. The technique has been used over the years and continues to be useful in eliminating the presence of active sites on the surface of a column. Deactivation allows for the analysis of compounds at lower concentrations, and also reduces tailing which in turn minimizes retention time shifts. To explore this with the LTCC tile, a 7.5 m x 100 μm i.d. deactivated tile was used. The surface of the LTCC tile was deactivated with a priority deactivation reagent supplied by Waters Corporation.

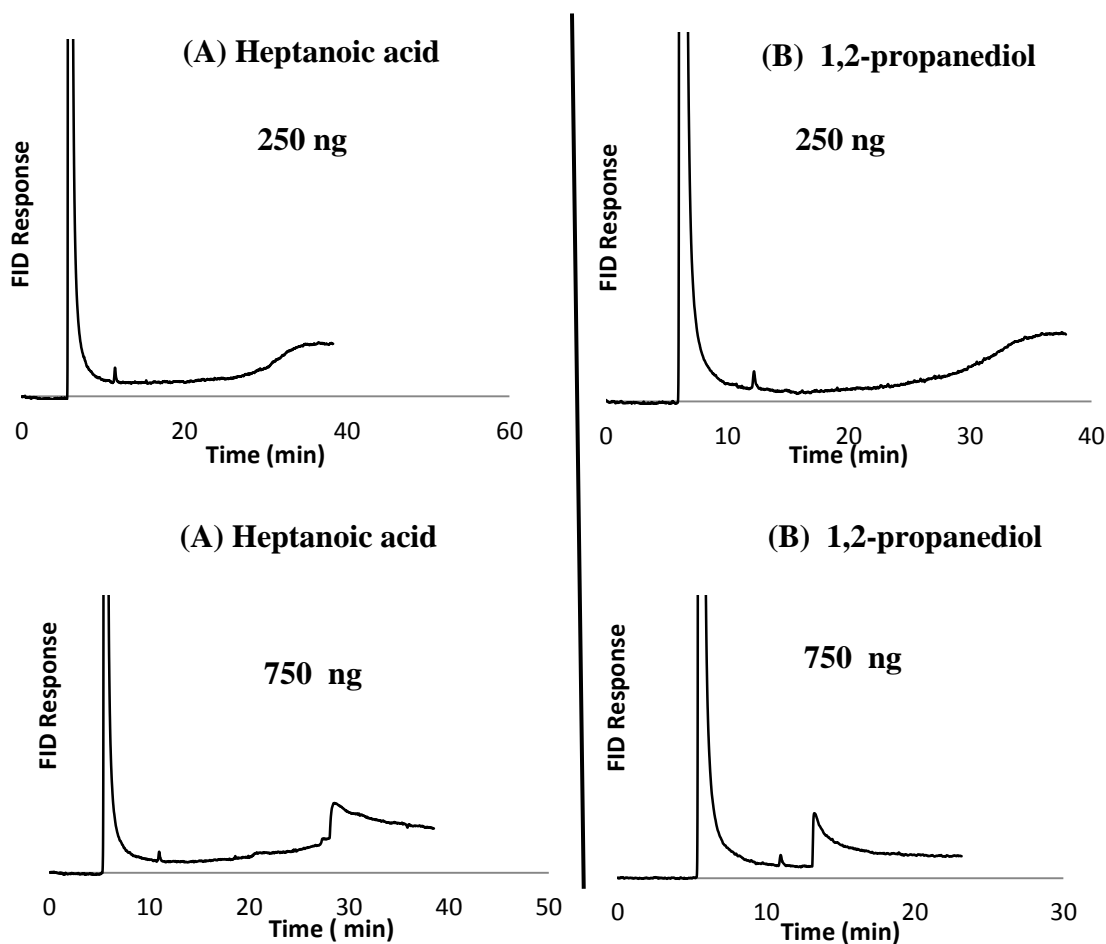


Figure 29: Chromatograms of (A) heptanoic acid and (B) 1,2- propanediol at different masses on an undeactivated LTCC tile. Temperature program: 45 to 220°C at 5°C/min. Detector temperature 220°C. He flow rate: 0.25 mL/min.

The deactivated LTCC tile was then mounted in the GC mainframe the same way as was the nondeactivated LTCC tile. Once again an FID detector was employed. Among the analytes of interest to test were bases, acids and diols, as they gave very poor shapes in the previous experiments with the nondeactivated LTCC tile. Specifically, in those trials, tailing was observed with most of the analytes, as seen from the examples in figure

29. In addition, lower analyte concentrations for the acids were difficult to analyze because they were strongly retained on the column.

Figure 30 presents similar chromatograms of heptanoic acid and 1,2-propanediol on the deactivated LTCC tile. It can be inferred from the chromatograms that the diol and the acid, which were previously unobservable at the level of 250 ng, can now be seen at that concentration. In addition, an improved peak shape for both was observed, as each had a narrower base width. Therefore, deactivating the LTCC tile surface appropriately can improve the tailing peaks observed. More work is needed to completely eliminate the tailing though.

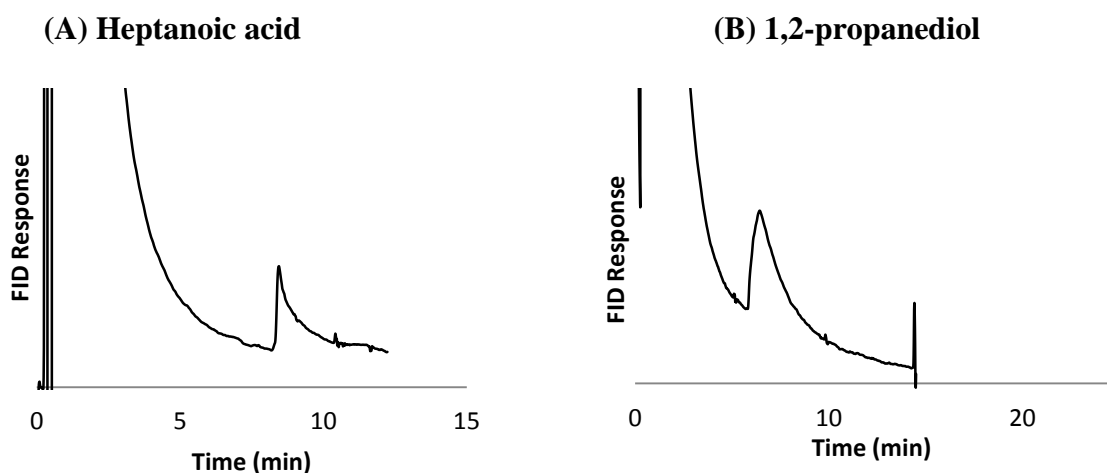


Figure 30: Chromatogram of (A) heptanoic acid and (B) 1,2- propanediol, both 250 ng. Temperature program: 45 to 200°C at 5°C/min. Detector temperature 220°C. He flow rate: 0.95 mL/min.

3.11 Packed LTCC Columns

While fused silica capillary columns have emerged as the column of choice for most GC applications, packed columns still continue to contribute in niche applications. For example, they are commonly used for gas analysis, preparative separations, and in separations where high resolution is not required. These columns are packed with particles of various materials and sizes to effect separations. For example, particle sizes of 30 to 200 μm have shown good sample capacities. The large particle size and broad size distribution however, result in poor efficiency and long separation times. Conversely, microparticles with narrow size range and average particle diameters less than 10 μm can provide faster separations and an increase of up to an order of magnitude in column efficiency and sample capacity.

Packed columns have been applied extensively in liquid chromatography (LC)^{116,117}. Milton Lee¹¹⁸ also showed packed columns can be employed in solvating gas chromatography (SGC). This is where the carrier is liquid at the inlet and expands to a gas as it approaches the outlet. SGC has the potential to provide fast separations where simple mixtures whose retention factor and selectivity is of importance can be separated in short analysis times. SGC also can provide high solvating power for large and polar compounds as well using various mobile phases. High pressures are often used in these kinds of GC applications. Therefore it was of interest to briefly see how the LTCC tiles behave under such high pressure separations as well.

Figure 31 presents a preliminary high pressure separation of a BTEX sample on a packed LTCC tile containing 5 μm C18 particles. The result was a partial separation using CO_2 as the mobile phase at a column inlet pressure of 120 atm. As can be seen,

resolution for many of the analytes was poor. Nonetheless, separation of the first two components was achieved in less than two minutes. Most importantly, no adverse pressure effects were noted on the LTCC tile and it continued to operate at this elevated pressure without difficulty.

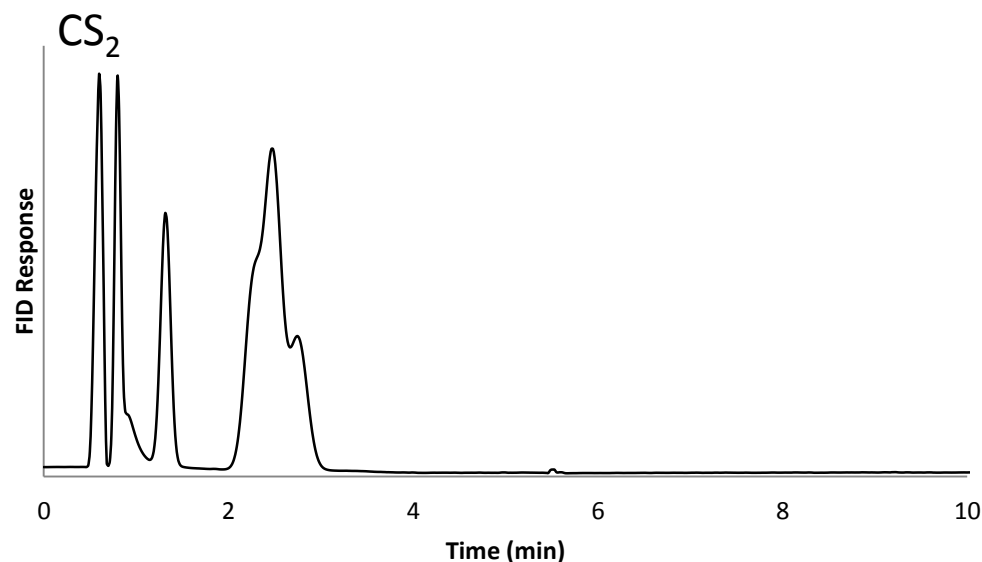


Figure 31: Chromatogram of a 1 $\mu\text{g}/\mu\text{L}$ BTEX standard in carbon disulfide using the packed LTCC tile (10 cm x 300 μm , packed with 5 μm C18 particles). Column temperature: 25°C, CO_2 Pressure: 120 atm. Analyte elution order: benzene, toluene, ethylbenzene, m-p and o-xylene (co-elution).

3.12 Packed LTCC Column Optimization

In an experiment to determine the optimum operating conditions for the packed LTCC column, it was observed that the highest efficiency was obtained when the pressure was lower. This is represented by figure 32, where the optimum pressure condition for the column was found to be 60 atm, which produced a plate number of

around 1400 for dodecane. Interestingly, fast separations were still obtained at this lower atmospheric pressure with the LTCC packed column as shown in figure 33.

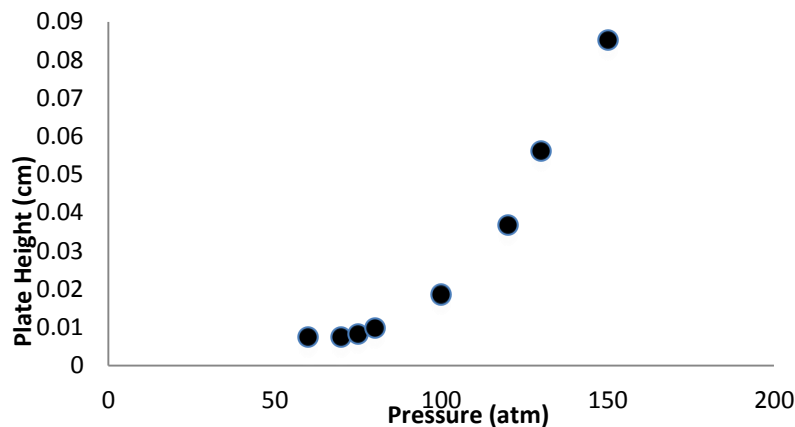


Figure 32: Plate height as a function of atmospheric pressure on packed LTCC device (10 cm x 300 μm , packed with 5 μm C18 particles). Column temperature: 100°C. Analyte solution: 1 $\mu\text{g}/\mu\text{L}$ of dodecane in carbon disulfide.

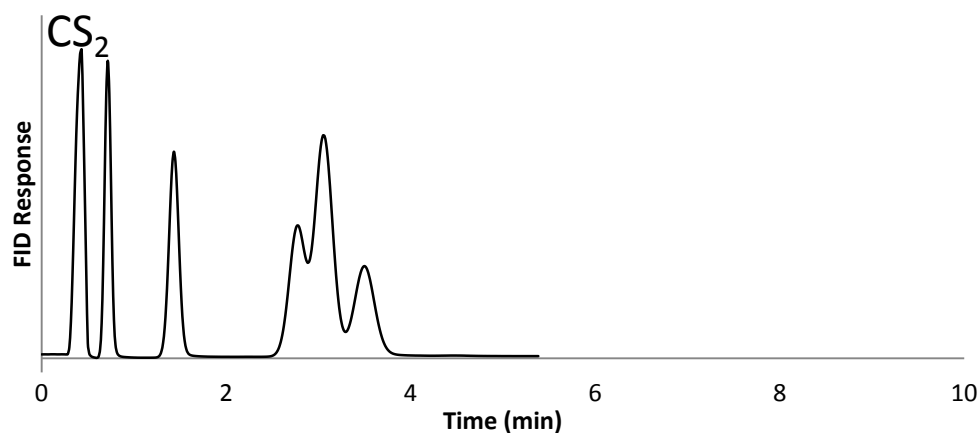


Figure 33: Chromatogram of a 1 $\mu\text{g}/\mu\text{L}$ BTEX standard in carbon disulfide using the packed LTCC tile (10 cm x 300 μm , packed with 5 μm C18 particles). Column temperature: 25°C, CO₂ Pressure: 60 atm. Detector temperature: 220°C. Mass injected on column: 200 ng. Analyte elution order: benzene, toluene, ethylbenzene, m- p and o-xylene (co-elution).

Figure 33 is a chromatogram of BTEX using CO₂ as a mobile phase at a column inlet pressure of 60 atm, where the pressure was direct from the CO₂ gas cylinder without the use of a pump. There were not any significant differences in terms of the speed of separation between the result obtained at 60 atm and that obtained before at 120 atm. However, resolution was improved at 60 atm. One other advantage of this outcome is that the use of a pressure pump to generate high pressures for such separations can be avoided, as CO₂ tank pressure is sufficient for the separation.

Figure 34 shows a temperature programmed separation of three alkane analytes (dodecane, tetradecane and hexadecane) in carbon disulfide.

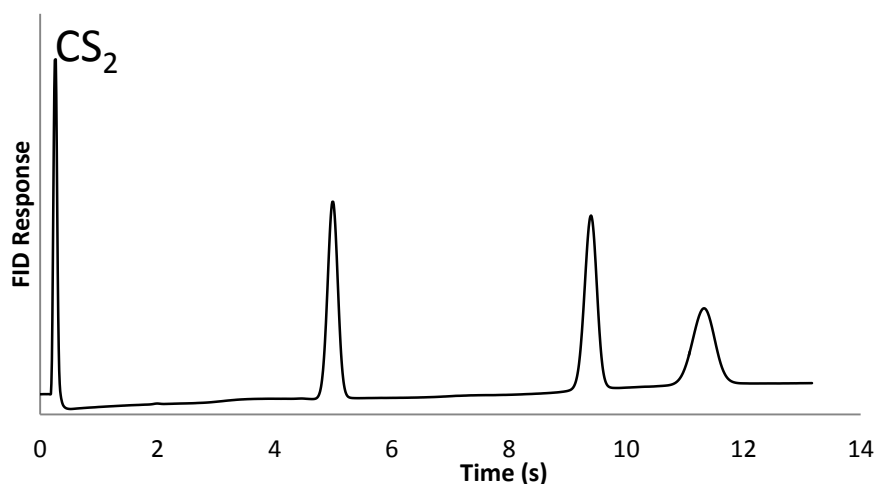


Figure 34: Chromatogram of n-alkane mixture on packed LTCC tile (10 cm x 300 μ m, packed with 5 μ m C18 particles). Temperature program: 80 to 130°C at 5°C/min. Pressure: 60 atm. Detector temperature: 220°C. Mass injected on column: 200 ng. Analyte elution order: dodecane, tetradecane, hexadecane.

This was obtained at an atmospheric pressure of 60 atm direct from the CO₂ cylinder as mentioned above. Again, a fairly decent separation and analyte peak shape was obtained,

and no operating difficulties were noted from using a 60 atm CO₂ input directly from the tank to the system, without a pump being used.

3.13 Packed LTCC Column Thermal Stability

Next, the highest operating temperature at which the packed LTCC column could operate was studied. Figure 35 presents the capacity factor of a test analyte as a function of time. Repeated injections were made isothermally at 130 °C using the packed LTCC column. A straight line would have been seen with a stationary phase not undergoing changes; however the column did show some deterioration of the stationary phase with time. This was minimal but significant enough to establish the upper limit of the column operation at 130°C. This is not large compared to conventional GC, but presents a window where more volatile analytes may be separable with this phase. No erosion of stationary phase was noted as a function of pressure.

In all, the LTCC tiles have shown potential and applicability to be used as platforms for GC separations. The results to date illustrate the need to further explore the LTCC tiles to improve separation performance, such as polar analyte behaviour. Nonetheless, relatively good separation efficiency and sample capacity were obtained on the LTCC tiles and it was on par with the commercial columns.

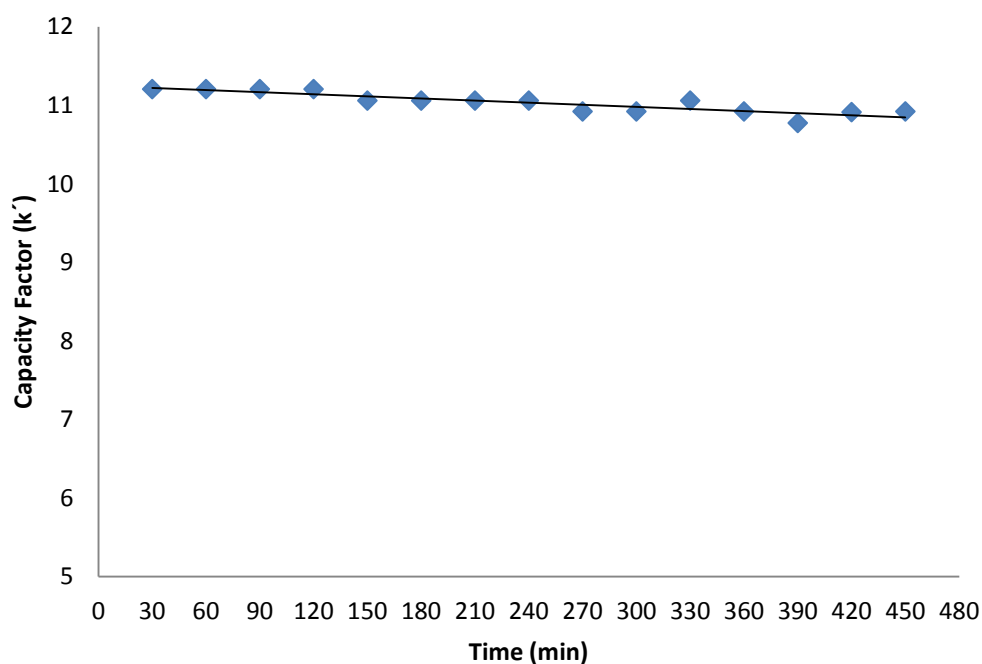


Figure 35: An illustration of the thermal stability of the stationary phase in the packed LTCC column (10 cm x 300 μm , packed with 5 μm C18 particles). Capacity factor obtained over a period of 8 hrs with repeated injection of dodecane analyte every 30 minutes. Column temperature: 130°C.

The LTCC packed columns have been shown to be an interesting platform as well. Though a lot is yet to be exploited with these types of packed columns, their ability to operate under higher pressure conditions without back pressure effects was encouraging. More so, an upper temperature limit of 130°C demonstrated by the packed LTCC tiles showed that separation of more volatile analytes (e.g. up to about C₁₆) can be achieved. Similar to the capillary LTCC tiles, the packed LTCC tiles had a high

efficiency and relatively decent resolution between adjacent peaks at lower pressure (60 atm). Preliminary tests showed that a pressure pump was not necessary to achieve analyte separation and this can be seen as an advantage in terms of cost in the study. Further studies of these types of columns will continue to give an in-depth knowledge and information on how to maximise their separation potential.

CHAPTER FOUR

4.0 THE INVESTIGATION OF TITANIUM PLATFORMS IN GC

4.1 Uncoated and Coated Titanium Chips

The surface chemistry of a substrate is important to help establish/explain its chromatographic properties. Typically many substrates often may contain surface hydroxyl groups and/or metal oxides. The metal oxides have a wide variety of surface structures including acidic and basic, which may influence their chemical properties. This illustrates that substrates of varying chemical composition can have different chromatographic behaviours.

For example, the surface chemistry of silica has been extensively studied and shown to consist of silanol groups and metal oxides¹¹⁹. These silanol groups act as the centers of molecular interaction with adsorbates capable of forming a hydrogen bond or in other words, can undergo donor-acceptor interactions. Removal of the hydroxyl groups from the surface of silica leads to a decrease in adsorption, and the surface acquires hydrophobic properties¹¹⁹. The surface chemistry of ceramic and titanium metal whose metal oxides are predominantly aluminium and titanium oxides respectively may be somewhat different compared to a fused silica substrate. Our work comparing ceramic tiles to conventional fused silica columns have shown the former to produce very decent separations for most analytes. However, results of polar analyte separations on LTCC substrates need to be further improved. Here, it will be interesting to now explore titanium substrates for their separating properties, with the aim of also exploring their behaviour with polar analytes.

Titanium is an interesting material and has become indispensable for most chemical, and biomedical industries since its introduction¹²⁰. This interest stems from its unique mechanical properties, high strength-to-weight ratio, and resistance to corrosion. This resistance to a vast range of chemical environments and conditions is provided by the surface oxide film (TiO_2). Besides, titanium metal is also known for its ability to withstand higher temperatures and exhibits good strength. Titanium metal is relatively easy and inexpensive to produce and can be assembled through diffusion bonding to form a monolithic unit. These and many more properties have recently encouraged its usage in manufacturing micro-components in MEMS devices¹²¹. To help explore its separation potential, a similar experimental setup and protocol to the LTCC tiles/experiments was again implemented here.

4.2 Uncoated Titanium Chip

The titanium tile to be studied had a 15m long and 100 μm I.D. channel. Similar to the LTCC tile, the retention properties of the titanium device alone were examined in the preliminary studies, in the absence of a coated stationary phase. This was necessary to give an insight to any potential separation capacity that the bare titanium material may have, and to see if it would impart any influence on analyte peak shapes. A mixture of n-alkanes was analyzed on the uncoated bare titanium device and the results are shown in figure 36. As seen, the bare titanium device produced broad tailing peaks for each of the analytes, but did separate them. This agrees well with similar experiments on the bare LTCC tiles which had peak shapes equally as poor. Thus, as anticipated, the need for a stationary phase on the titanium tile in order to improve separations was clear.

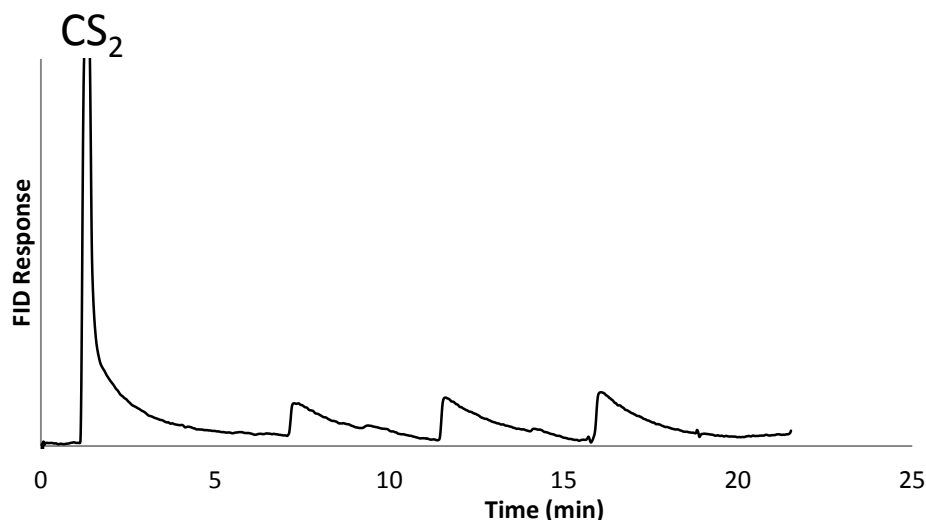


Figure 36: Chromatograms of n-alkane mixture separated in the titanium tile without a stationary phase coated on the surface. Temperature programs: 45 to 200°C at 5°C/min, He flow rate: 0.55 mL/min. Detector temperature: 220°C. Mass injected on column: 250 ng. Analyte elution order: dodecane, tetradecane, and hexadecane after the solvent peak carbon disulfide.

A similar separation using OV-101 as a stationary phase to coat the column is presented in Figure 37. The coating method employed was the same as that presented earlier in the LTCC experiments. The results showed a much improved separation compared to that obtained on the bare titanium. Relatively narrow and well-defined peaks were produced for each of the three analytes separated. The enhanced separation demonstrated that the coated titanium tiles can apparently function as reasonable platforms for performing GC separations, similar to LTCC tiles. Coated titanium tiles were therefore used for the remainder of this study

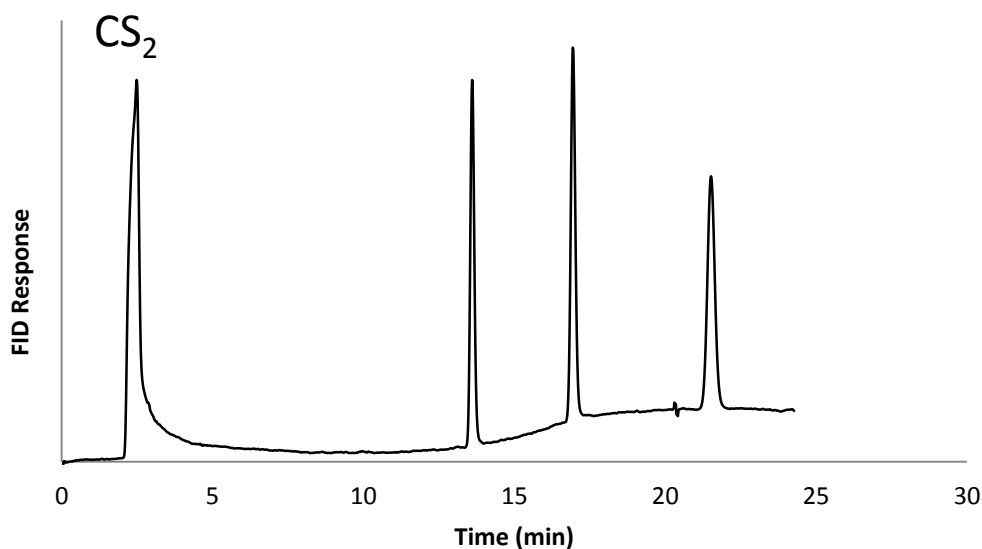


Figure 37: Chromatograms of n-alkane mixture separated in the titanium tile with a stationary phase coated on the surface. Temperature programs: 45 to 200°C at 5°C/min, He flow rate: 0.53 mL/min. Detector temperature: 220°C. Mass injected on column: 250 ng. Analyte elution order: dodecane, tetradecane, and hexadecane after the solvent peak carbon disulfide.

4.3 Column Efficiency

The efficiency of the titanium tile was also studied and is represented in Figure 38 by a Van Deemter plot showing plate height as a function of flow rate. (In general, separation becomes better as the number of plates increases. Thus the plate number provides information about the separation power of a column). Minimum plate height on the titanium tile was registered at a flow rate of 0.30 mL/min corresponding to total plates

of about 10,380. This was obtained for a dodecane test analyte isothermally at 120°C. This corresponds to about 692 plate/m for this 15 m titanium tile, which was less than the 1910 plate/m value obtained on the LTCC tiles. In contrast to this, though, the profile of the titanium tile Van Deemter curve is much flatter at higher flow rates than is that of the LTCC tile, making for faster separations. One possible reason for these differences could be the porosity of the LTCC material relative to the titanium tile. For example, this may provide more surface area for stationary phase application; however it could be applied less evenly over the length of the channel. More experiments are needed to confirm this. Nonetheless, it is the first time titanium metal has been used as a microfluidic platform for GC separations and the results obtained look promising for further characterization of the titanium.

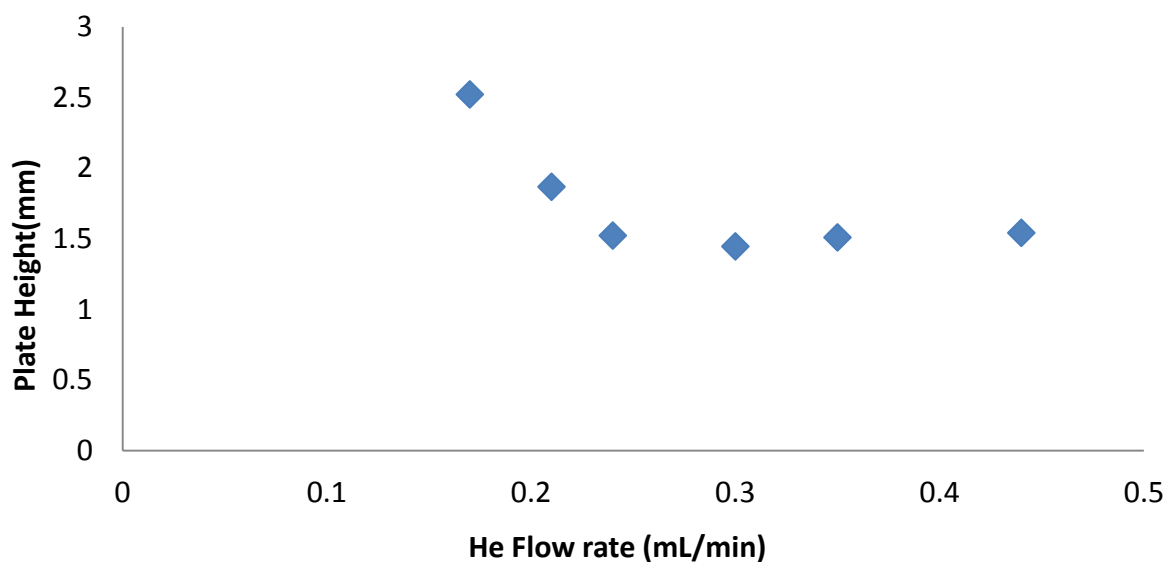


Figure 38: Plate height as a function of flow rate on the titanium device (15 m x 100 μm). Column temperature: 120°C. Analyte solution: 1 $\mu\text{g}/\mu\text{L}$ of dodecane in carbon disulfide.

4.4 GC Applications

In order to further gauge the titanium tile performance, temperature programming and isothermal separations of polar and non-polar analytes were performed using the coated titanium tile (15 m x 100 μ m i.d). Temperature programming is often used to reduce analysis time through utilizing the sample volatility range. Figure 39 shows a temperature programmed chromatogram for a mixture of normal alkanes from n-C₈ through n-C₂₀. The initial column temperature was 45 °C at a programming rate of 10 °C/min through to 210 °C. Relatively symmetrical peaks were obtained for this mixture on the titanium tile. The chromatogram on the titanium tile was also similar to that obtained on the coated LTCC tile, having similar peak shapes and resolution between the analytes.

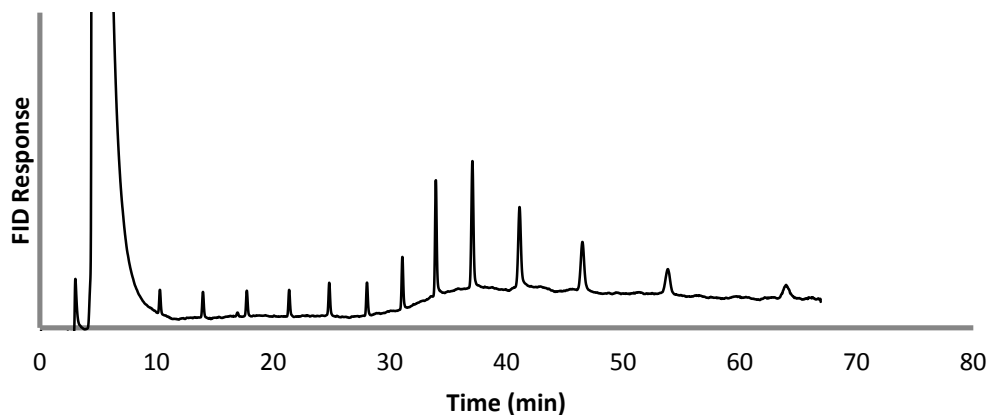


Figure 39: Chromatogram of a 40 mg/L C₈ to C₂₀ n-alkane standard using the coated titanium device. Column temperature program: 45 to 210°C at 5°C/min, He flow rate: 0.53 mL/min. Detector temperature: 220°C.

In the separation of complex mixtures the total number of observed peaks is very important. Systems that separate mixtures into the largest number of observable peaks are often desirable. The cumulative peak capacity obtained for figure 39 above is about 48 for C_{10} to C_{15} alkanes, which is similar to the LTCC tiles (i.e peak capacity of 53) and indicates a decent resolving power for this column. In all, similar to LTCC tiles, there were no difficulties associated with hydrocarbon separations on titanium tiles either.

Aside from the aliphatic compounds, separation of aromatic compounds was also carried out on the titanium tile. BTEX analytes in carbon disulfide solvent were separated on the coated titanium tile as shown in figure 40.

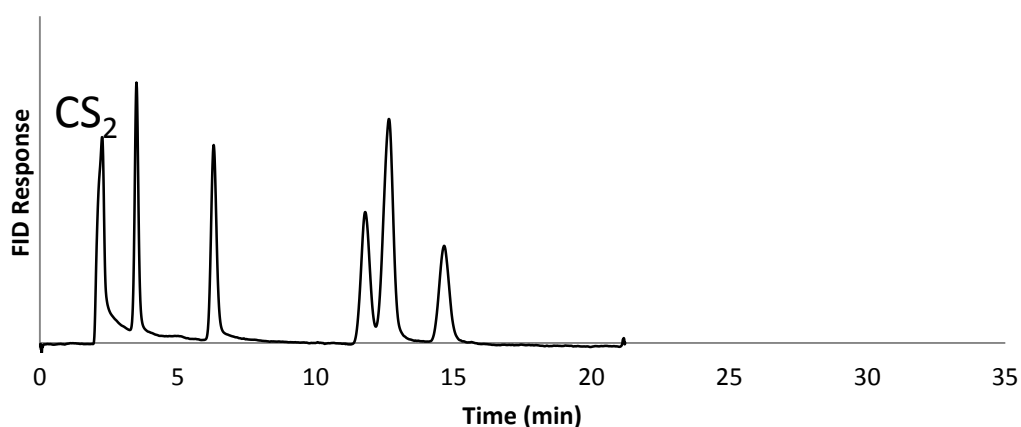


Figure 40: Chromatogram of a 1 $\mu\text{g}/\mu\text{L}$ BTEX standard in carbon disulfide using the coated titanium tile (15 m x 100 μm). Column temperature: 60°C, helium flow rate: 0.53 mL/min. Analyte elution order after solvent peak: benzene, toluene, ethylbenzene, m- and p-xylene (co-elution), and o-xylene.

Again, a similar performance to the LTCC tile with respect to this separation was observed. For instance, resolution of the main components and overlapping of the meta - and para-Xylene isomers was again found. Since hydrocarbon separations on titanium and LTCC tiles generally compared well, this prompted investigations of analytes with several functional groups on the titanium tile, which had posed challenges earlier with LTCC tiles.

4.5 Polar Analytes on Titanium Tiles

As mentioned earlier, the impact of substrate on peak shapes is best exposed by using a Grob's test mixture. Using different individual analyte classes such as bases, acids, ketones, esters and simple hydrocarbons, the information obtained could better our understanding of the relative surface activity of these columns compared to LTCC tiles. Specifically, it helps to ascertain if the coated surface will still have a strong interaction with the analytes or not. Figure 41 shows a chromatogram of a laboratory made Grob's test mixture of 9 components on the titanium tile.

In general, most of the peak shapes were relatively decent. However, some of the 9 components were less discernable (e.g. propanediol and phenol) while another (decanal) was seen to be either strongly retained on the titanium tile or coeluting with the acid analyte. Thus a closer examination was performed.

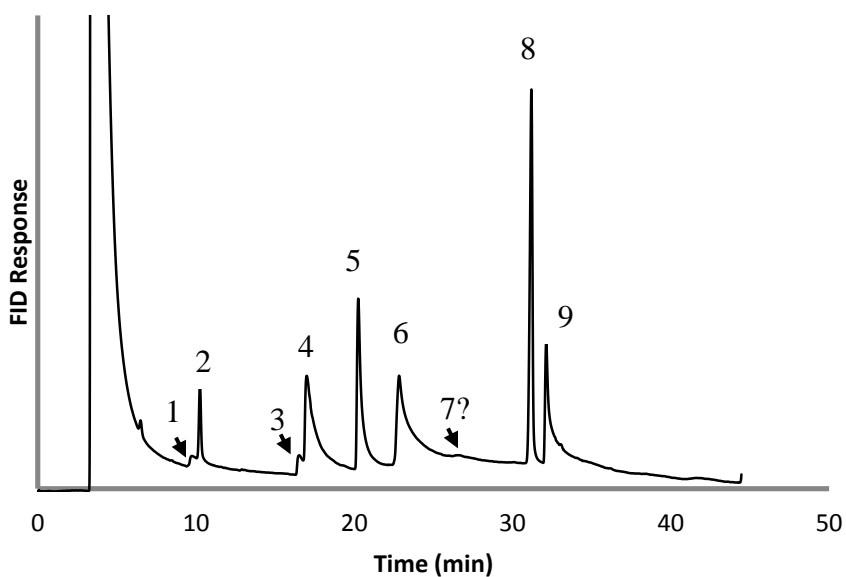


Figure 41: Chromatogram of a mixture of organic compounds of varying functionalities using the coated titanium device. Temperature program: 45 to 200°C at 10°C/min. He flow rate: 0.3 mL/min. Detector temperature: 220°C. Analyte elution order: 1) 1,2-propanediol, 2) butylacetate, 3) phenol, 4) aniline, 5) octanol, 6) heptanoic acid, 7) decanal, 8) tetradecane, and 9) dicyclohexylamine. Solvent: dichloromethane.

To help explain the missing decanal peak, a similar standard was made in dichloromethane solvent and separated on the titanium tile under the same conditions as that observed in figure 41 above. The decanal peak appeared with excellent shape at about 25 minutes in figure 42, which shows that it was actually coeluting with the acid in the chromatogram of the Grob's mixture.

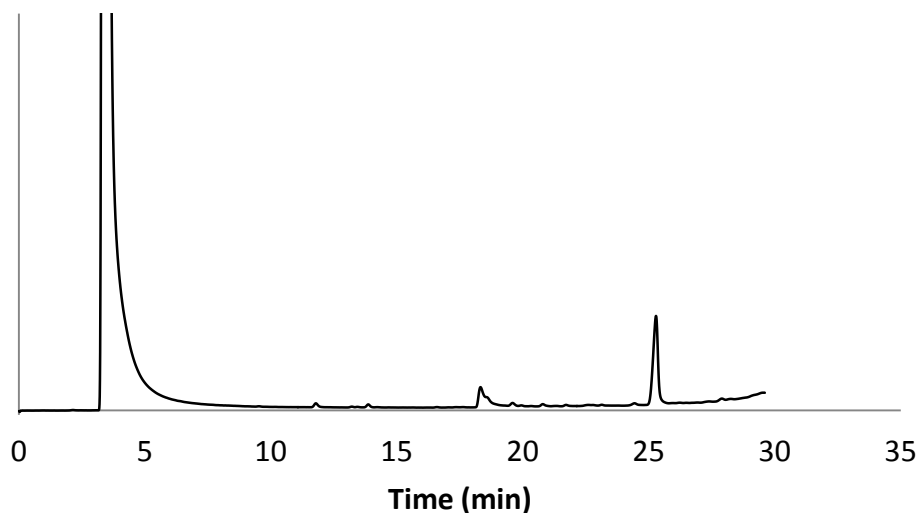


Figure 42: A chromatogram of decanal on coated titanium tile (15 m x 100 μ m). Temperature program: 45 to 200°C at 5°C/min, He flow rate: 0.3 mL/min. Detector temperature: 220°C. Solvent: Dichloromethane.

Many of the other co-eluted peaks made it difficult to determine their retention time and/or peak shapes. As a result, this did not allow for a clear indication of how the various analytes interact with the titanium tile. Therefore, separate standards representing many of the same functional groups from this mixture, were prepared and examined individually. Overall, esters, mono-substituted alcohols, and amines generally eluted from the titanium tile with relatively decent peak shapes. As an example, the chromatograms of an alcohol and amine are shown in figure 43.

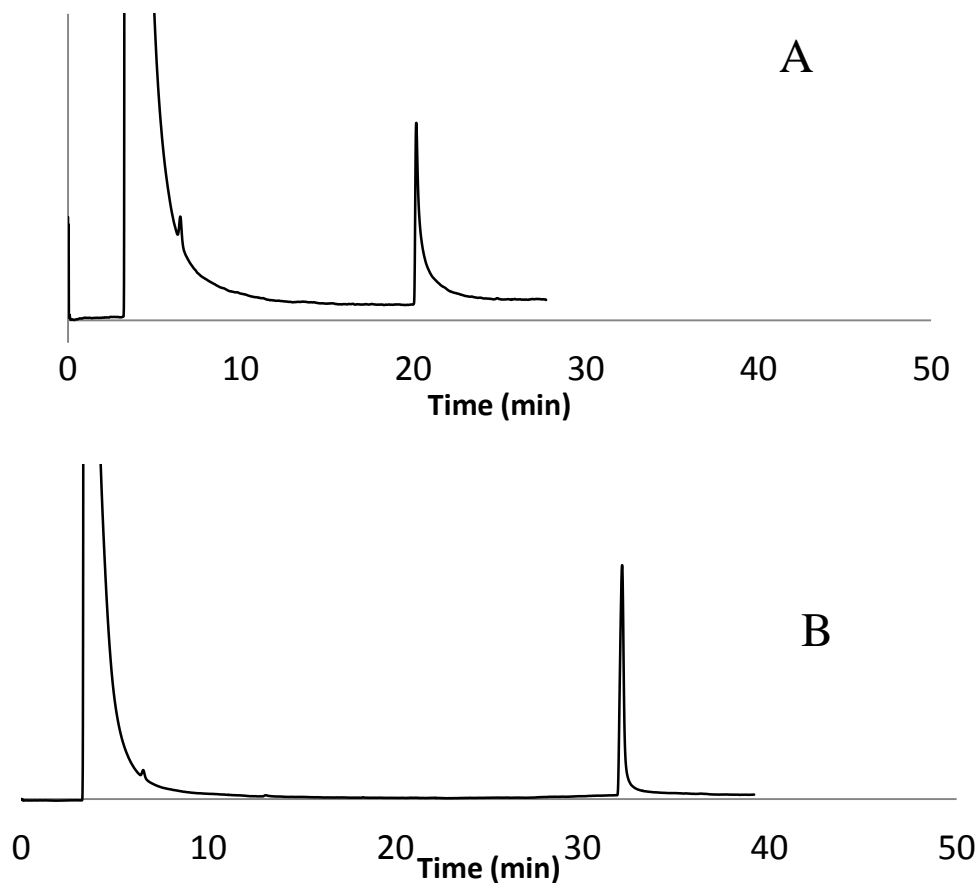


Figure 43: A chromatogram of (A) octanol and (B) dicyclohexylamine on a coated titanium tile (15 m x 100 μ m). Temperature program: 45 to 200°C at 5°C/min, He flow rate: 0.3 mL/min. Detector temperature: 220°C. Solvent: dichloromethane.

In contrast to this, di-substituted alcohols, and carboxylic acids eluted with broad tailing peak shapes which is demonstrated in figure 44. While similar results were found for the LTCC tiles, the width of tailing for the majority of these peaks on the titanium tile was relatively less (about 3 – 5 minutes wide vs. 5 – 8 min wide).

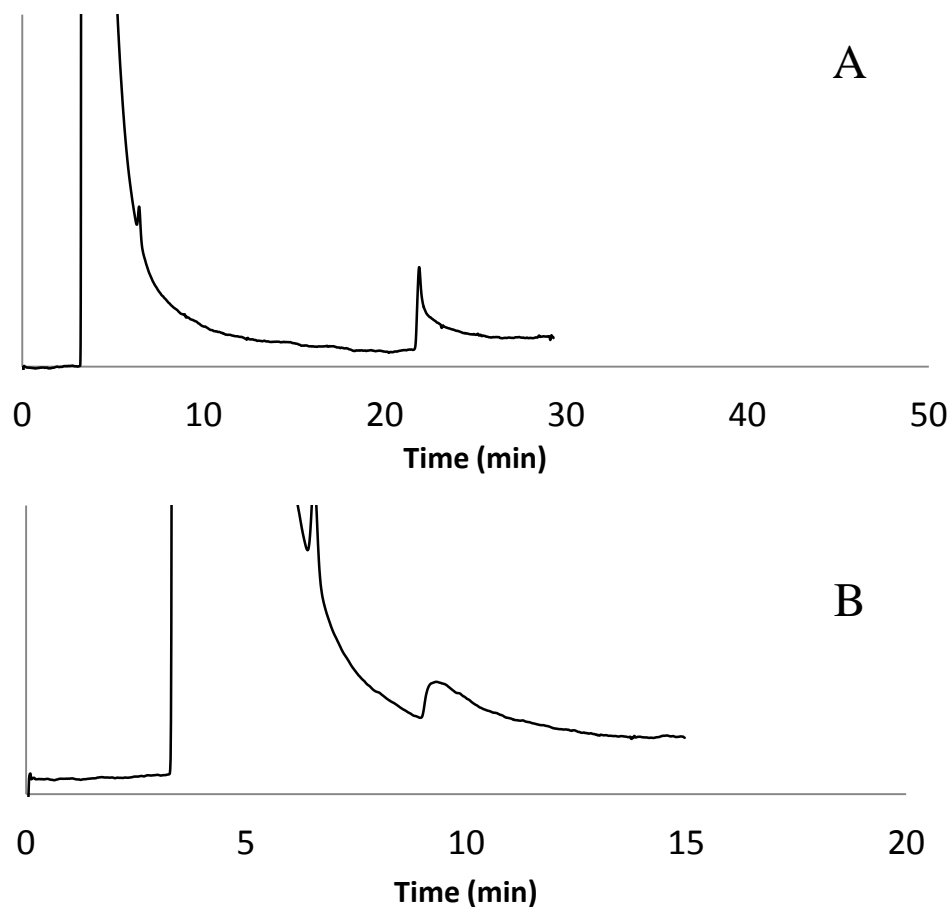


Figure 44: A chromatogram of (A) heptanoic acid and (B) 1,2-propanediol on a coated titanium (15 m x 100 μ m). Temperature program: 45 to 200°C at 5°C/min, He flow rate: 0.3 mL/min. Detector temperature: 220°C. Solvent: dichloromethane

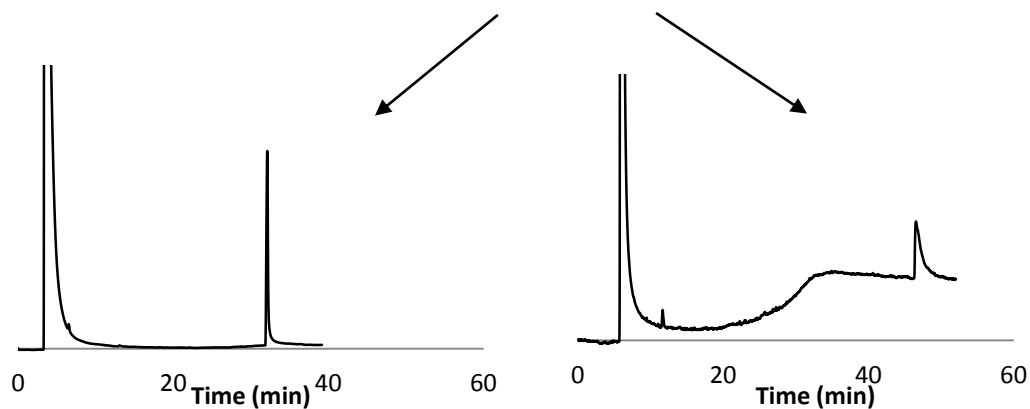
4.6 Polar Analyte Comparison of Titanium vs. LTCC Tiles

In order to determine the influence of substrate choice on separation, a side by side comparison was drawn for both titanium and LTCC tiles. The most striking differences found, are presented in figure 45 showing peak shapes of two such polar analytes on coated titanium and LTCC tiles.

Titanium Tile

LTCC Tile

(A) Dicyclohexylamine



(B) Heptanoic acid

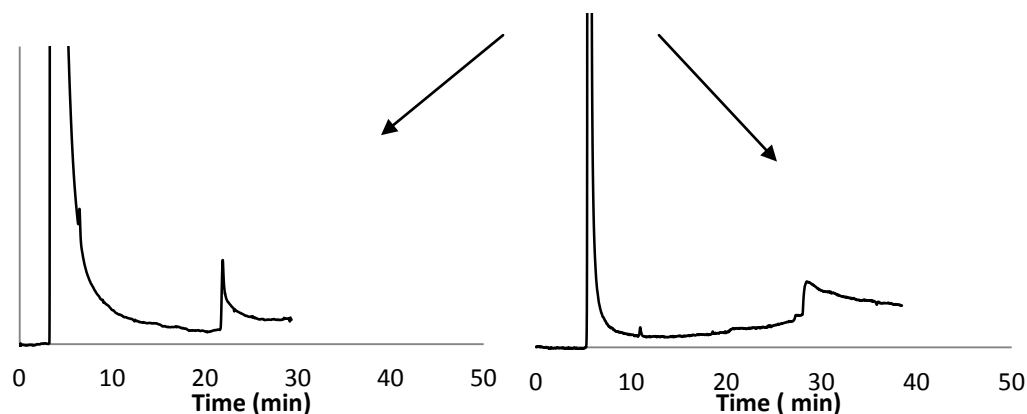


Figure 45: A chromatogram of (A) dicyclohexylamine and (B) heptanoic acid on coated titanium and LTCC tiles (15 m x 100 μ m each). Temperature program: 45 to 200°C at 5°C/min, He flow rate: 0.3 mL/min and 0.25 mL/min for titanium and LTCC tile respectively. Detector temperature: 220°C. Solvent: dichloromethane.

Peak shapes for the analytes illustrated appear sharper and more symmetrical with less tailing on the coated titanium tile compared to that shown on the coated LTCC tile.

For example, tailing was more pronounced for the heptanoic acid peak on the LTCC tile, which could possibly be attributed to a significant amount of active sites present on the LTCC tile compared to the titanium tile. As noted the LTCC tile was also more retentive. Since these separations were encouraging, it was of interest to next explore a titanium tile with a deactivated surface to see if improved peak shapes and separations in general can be achieved in this way for polar analytes.

4.7 Preliminary Trials with Deactivated Titanium Tile

A titanium tile deactivated by Waters with a proprietary process was subsequently obtained and studied with the hope that improved peak shapes can be produced. Figure 46 shows a chromatogram of a Grob's test mixture on this deactivated chip. As seen, surprisingly, peak shapes resulting from the separation were poor for nearly all analytes, contrary to that obtained on the deactivated LTCC tile shown earlier. It was anticipated that the deactivated titanium tile would produce improved separation relative to the undeactivated titanium tile. However, decanal was undetectable while the phenol and aniline peaks co-eluted. The diol was also undetected and generally peak shapes were relatively eroded. This outcome could be attributed to the reagent used in the deactivation process; however, we unfortunately were not privy to its structure. Still, this was only the first attempt at deactivation of titanium and further work needs to be done to clarify its role here. Nonetheless, this clearly indicates that the native titanium surface provides a better separation medium prior to the deactivation used, which is in contrast to that observed for LTCC.

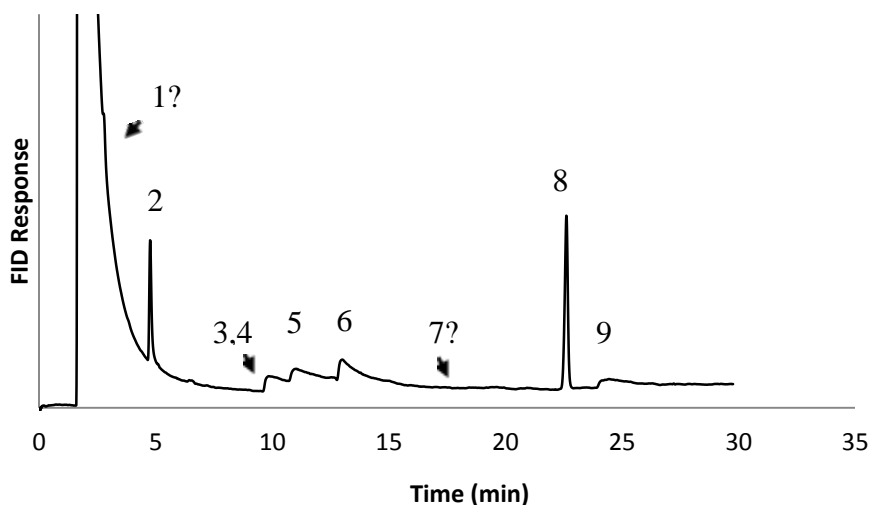
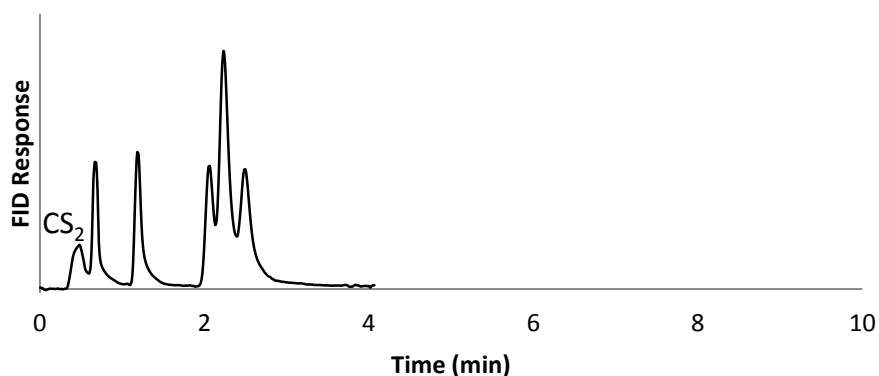


Figure 46: Chromatogram of a mixture of organic compounds of varying functionalities using the deactivated titanium device (15 m x 100 μ m). Temperature program: 45 to 200°C at 10°C/min, He flow rate 0.42 ml/min. Detector temperature: 220°C. Solvent: dichloromethane. Analyte elution order: 1) 1,2-propanediol, 2) butylacetate, 3) phenol, 4) aniline, 5) octanol, 6) heptanoic acid, 7) decanal, 8) tetradecane, and 9) dicyclohexylamine.

4.8 Preliminary Trials with Titanium Packed Columns

In the previous study with an LTCC packed column, it was shown that high pressure GC separations are achievable on short columns. It was also shown that efficiency can be enhanced when the size of the particles used for packing are smaller in diameter. The LTCC tile used was a 10 cm column packed with 5 μ m C18 particles. In this study, a similar 10 cm length of titanium tile was packed with even smaller 1.7 μ m C18 particles and investigated. The only difference was in the particle size, and substrate. These small particles usually provide shorter component paths in the column and less

dispersion resulting in greater efficiency and back pressure. Figure 47 shows preliminary results of BTEX on the packed titanium tile with 1.7 μm C18 particles. As can be seen, the sample components eluted with good to partial resolution, with the exception of ethyl benzene and the Xylene isomers. Elution was also achieved in under four minutes which is fairly rapid for a densely packed column. More importantly, flow restriction was negligible and no adverse effects were noted with this column operated at 60 atm. Therefore, packed titanium tiles may provide good platforms for high pressure GC as well.



Figure

47: Chromatogram of a 1 $\mu\text{g}/\mu\text{L}$ BTEX standard in carbon disulfide using a 10 cm x 300 μm titanium tile packed with 1.7 μm C18 particles. Column temperature: 60°C, CO_2 Pressure: 60 atm. Detector temperature: 220°C. Mass injected on column: 200 ng. Analyte elution order: benzene, toluene, then ethylbenzene, m-, p-, and o-xylene co-elution.

One interesting observation was made when BTEX was separated at room temperature and 60 atm. Peak splitting was observed under these conditions on the packed titanium tile as presented in figure 48. This outcome was not observed using the

packed LTCC tile under the same conditions. Normally, it is possible to create relatively large column pressure drops when working with small particle diameter packed columns. This can result in a significant difference between the inlet column pressure and the outlet column pressure. When this pressure drop occurs in a region where there is a density differential from the column inlet to the column outlet, unusual peak distortion might occur. It is believed that at room temperature, LTCC packed with 5 μ m C18 particles will have much less pressure limitation compared to the 1.7 μ m C18 particles in the titanium tile, which could possibly explain the peak splitting shown below in figure 48. For instance, since 25°C was below the critical temperature of CO₂, this may have led to a two phase (gas and liquid) mobile phase system. However, these features disappeared at 60°C, above the critical temperature of CO₂. This needs to be verified further though.

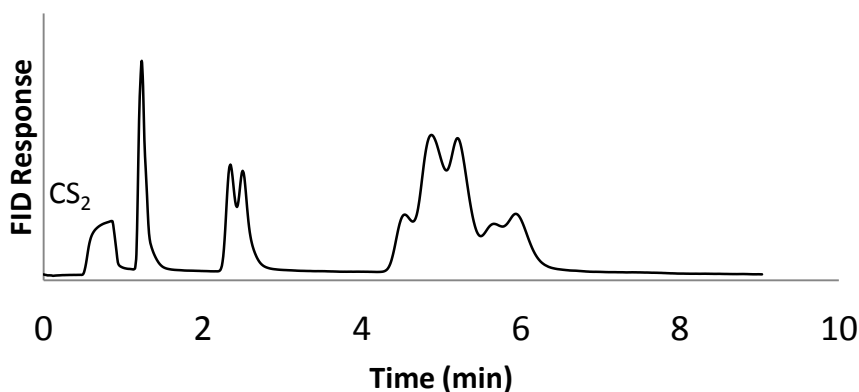


Figure 48: Chromatogram of a 1 μ g/ μ L BTEX standard in carbon disulfide using a 10 cm x 300 μ m titanium tile packed with 1.7 μ m C18 particles. Column temperature: 25°C, CO₂ Pressure: 60 atm. Detector temperature: 220°C. Mass injected on column: 200 ng. Analyte elution order: benzene, toluene, then ethylbenzene, m-, p- and o-xylene co-elution.

4.9 General Comparison of LTCC and Titanium Platforms

Table 4 shows an overview of some separation efficiencies and resolving power calculated for both LTCC and titanium tiles in both the low pressure capillary and high pressure packed modes. Resolution was high for the titanium tile packed with 1.7 μm C18 particles compared to the LTCC tile packed with 5 μm particles. Resolution gives measures how well analytes have been separated and is often enhanced by several factors. For example, on packed columns resolution can be influenced by the particle size. Here, columns packed with smaller particles tend to provide higher resolution than larger particles. The smaller particles generally provide larger surface area which offers greater capacity and longer retention times. Larger particles on the other hand, provide lower surface area which erodes resolution.

On the capillary columns, peaks were more resolved in the LTCC tile than in the titanium tile. Generally, small differences in diameter will affect the analyte velocity through a column. This change in velocity can either impact resolution positively or negatively. However, the two columns here (LTCC and titanium) were identical in diameter but differed in column length as shown in table 4. It was anticipated that the longer column (titanium tile) would have a higher resolution under the same conditions. However, surprisingly it was rather the shorter LTCC tile that gave a higher resolution. This was attributed earlier as possibly due to the relative porosity nature of the LTCC tile which may offer better surface area.

Column efficiency investigated on both packed and capillary forms of these LTCC and titanium tiles are also given in table 4. A calculated value of 8430 plates/m was obtained for the packed titanium tile compared to 2710 plates/m generated on the

packed LTCC tile. This greater efficiency follows for the titanium tile packed with smaller sub-2 micron particles. Conversely, the capillary titanium tile displayed lesser column efficiency throughout the study and capillary LTCC tile overall, demonstrated better resolving power and theoretical plates.

Table 4. Summary of column efficiency measures of the different columns investigated in this work for BTEX sample

	Sample	Capillary		Packed	
		LTCC (7.5m)	Titanium (15m)	LTCC (10cm, 5 μ m)	Titanium (10cm, 1.7)
Resolution	Benzene and Toluene	14.07	8.29	3.62	6.07
Total theoretical plates (N)	Benzene	3890	3074	271	843
Column Efficiency (plates/m)	Benzene	518	204	2710	8430

In spite of these observations, the capillary LTCC tile also proved slightly more difficult and challenging to work with since it is fragile and can break easily when handling or dropped. Unlike the LTCC platforms, titanium platforms are easy to work with due to their unique mechanical strength.

In all, these preliminary studies have shown that the titanium tile has the capability to separate analytes in the absence of a stationary phase (albeit poorly). Nonetheless, the need for a stationary phase was emphasized when broad and unsymmetrical peak shapes were seen on the bare titanium tile. The study showed that coated titanium tiles produced a much improved separation of the individual analytes. However, the efficiency of the coated titanium tile was three fold less compared to the LTCC tiles. A titanium tile whose surface was deactivated was next employed in the study. It is a known fact that deactivated surfaces can help minimize the broadened peak shapes and tailing of some polar analytes. Interestingly, the opposite was rather observed on the deactivated titanium tile, showing very poor separations of the Grob's mixture. This anomaly can possibly be due to the deactivation process on the titanium tile. Despite these challenges, we believe separation on the titanium tile still has the potential to be improved.

Also, separations on titanium tiles packed with sub-2 micron C18 particles were briefly explored. These separations were comparable to those of the packed LTCC tile. In addition, as expected, the titanium column packed with 1.7 C18 particles generated theoretical plates that were higher than those produced on the LTCC packed with 5 μ m

C18 particles. Even though a lot is yet to be done on this column, this work has shown that titanium substrates can also readily support high pressure GC conditions for further exploration.

CHAPTER FIVE

5.0 SUMMARY AND FUTURE WORKS

5.1 Conclusions

Both LTCC and titanium tiles can be an interesting alternative to silicon as base materials for GC columns and microsystems as a whole. These materials have a great potential for product innovations due to their wide range of properties. The use of these materials can minimize the limitations that the other substrates (i.e., silicon, glass and polymer-based material) have on the functionality, durability and overall complexity of microfluidic systems. It has been shown in the study that the LTCC and titanium tiles can effectively be crafted and coated to form channels that can act as GC columns. The LTCC fabricated GC columns provided separations for individual analytes (polar and non-polar) that compared well to commercial capillary columns in terms of efficiency and overall separation capacity. Likewise the titanium tiles compared well with the LTCC tiles. At present, analytes possessing polar functional groups elicited broadened peak shapes with considerable amounts of tailing, especially on undeactivated LTCC tiles. However, these polar analytes showed an improved peak shape when using deactivated LTCC tiles. This situation was somewhat different with deactivated titanium tiles. Relatively poor peak shapes were rather observed on deactivated vs. undeactivated titanium tiles, contrary to what one would expect. In all, the studies showed that the LTCC and titanium tiles can appropriately function as platforms for miniaturized analytical GC. Furthermore, high pressure GC operation modes were briefly studied using both packed LTCC and titanium tiles. The preliminary results were encouraging for

the densely packed columns which had minimal flow restrictions making it viable for high pressure GC separations.

5.2 Future Work

Future work in this area will aim at addressing the broadened peak shapes of polar analytes with different surface deactivation methods. Again, the different chemical composition of the LTCC substrate can be varied at the source before it undergoes fabrication. By so doing, the amount of oxides can be minimised and this may help improve separation efficiency.

Considering the complexity of some sample matrices and analytes, it will be very interesting to investigate in the future the possibility of integrating other multiple GC components such as detectors, injectors and heaters onto these substrates, which will make them more convenient for both lab and field measurements.

REFERENCES

- (1) James, A. T.; Martin, A. J. P. *Analytical Chemistry* **1952**, 24, 1522.
- (2) Evenson, M. A. *Analytical Chemistry* **1977**, 49, R16.
- (3) Blomberg, J.; Schoenmakers, P. J.; Brinkman, U. A. T. *Journal of chromatography A* **2002**, 972, 137.
- (4) Rosie, D. M.; Grob, R. L. *Analytical Chemistry* **1957**, 29, 1263.
- (5) Sandra, P.; David, F. *Journal of Chromatographic Science* **2002**, 40, 248.
- (6) Ettre, L. S. *LC GC Europe* **2003**, 16, 632.
- (7) Perry, J. A. In Dekker, New York: New York, 1981, p 426.
- (8) Poole, C. F., and Schuette, S.A., *Journal of Phamaceutical Sciences* **1984**, 29.
- (9) Supina, W. R. "Packed Columns; Column Selection in Gas Chromatography," in *Modern Practice of Gas Chromatography*; (2nd ed., Grob, R.L., Ed) ed.; Wiley: New York, 1985.
- (10) A.J.P Martin; D. H. Desty *Vapour Phase Chromatography* **1957**, 2.
- (11) Ettre, L. S. *Journal of High Resolution Chromatography & Chromatography Communications* **1987**, 10, 221.
- (12) Bartle, K. D.; Myers, P. *Trac-Trends in Analytical Chemistry* **2002**, 21, 547.
- (13) Ettre, L. S. *Introduction to Open tubular Columns*; Perkin-Elmer Corp.: Narwalk, CT, 1978.
- (14) Jennings, W. J. *Gas Chromatography with Glass Capillary Columns*; Academic: New York, 1980.

- (15) Nawrocki, J. *Chromatographia* **1988**, 25, 404.
- (16) Rutten, G.; Vandeven, A.; Dehaan, J.; Vandeven, L.; Rijks, J. *Journal of High Resolution Chromatography & Chromatography Communications* **1984**, 7, 607.
- (17) Scholten, A. B.; deHaan, J. W.; Janssen, H. G.; vandeVen, L. J. M.; Cramers, C. A. *Hrc-Journal of High Resolution Chromatography* **1997**, 20, 17.
- (18) Schutjes, C. P. M.; Vermeer, E. A.; Cramers, C. A. *Journal of Chromatography* **1983**, 279, 49.
- (19) Markides, K. E.; Tarbet, B. J.; Woolley, C. L.; Schregenberger, C. M.; Bradshaw, J. S.; Lee, M. L.; Bartle, K. D. *Journal of High Resolution Chromatography & Chromatography Communications* **1985**, 8, 378.
- (20) Farrerius, F.; Guiochon, G.; Henniker, J. *Nature* **1962**, 196, 63.
- (21) Shafrin, E. G.; Zisman, W. A. *Journal of Physical Chemistry* **1960**, 64, 519.
- (22) Bartle, K. D.; Novotny, M. *Journal of Chromatography* **1974**, 94, 35.
- (23) Alexandre, G.; Rutten, G. *Journal of Chromatography* **1974**, 99, 81.
- (24) Marshall, J. L.; Parker, D. A. *Journal of Chromatography* **1976**, 122, 425.
- (25) Parker, D. A.; Marshall, J. L. *Chromatographia* **1978**, 11, 526.
- (26) Ogden, M. W.; McNair, H. M. *Journal of Chromatography* **1986**, 354, 7.
- (27) Verzele, M.; Mussche, P.; Sandra, P. *Journal of Chromatography* **1980**, 190, 331.

- (28) Kong, R. C.; Woolley, C. L.; Fields, S. M.; Lee, M. L. *Chromatographia* **1984**, *18*, 362.
- (29) Bouche, J.; Verzele, M. *Journal of Gas Chromatography* **1968**, *6*, 501.
- (30) Redant, G.; Sandra, P.; Verzele, M. *Chromatographia* **1982**, *15*, 13.
- (31) Schomburg, G.; Husmann, H. *Chromatographia* **1975**, *8*, 517.
- (32) Madani, C.; Chambaz, E. M.; Rigaud, M.; Durand, J.; Chebroux, P. *Journal of Chromatography* **1976**, *126*, 161.
- (33) Grob, K.; Grob, G. *Journal of Chromatography* **1981**, *211*, 243.
- (34) Grob, K.; Grob, G. *Journal of Chromatography* **1981**, *213*, 211.
- (35) Wright, B. W.; Peaden, P. A.; Lee, M. L.; Stark, T. J. *Journal of Chromatography* **1982**, *248*, 17.
- (36) Richter, B. E.; Kuei, J. C.; Shelton, J. I.; Castle, L. W.; Bradshaw, J. S.; Lee, M. L. *Journal of Chromatography* **1983**, *279*, 21.
- (37) Richter, B. E.; Kuei, J. C.; Park, N. J.; Crowley, S. J.; Bradshaw, J. S.; Lee, M. L. *Journal of High Resolution Chromatography & Chromatography Communications* **1983**, *6*, 371.
- (38) Schomburg, G.; Husmann, H.; Ruthe, S.; Herraiz, M. *Chromatographia* **1982**, *15*, 599.
- (39) Bertsch, W.; Pretorius, V.; Pearce, M.; Thompson, J. C.; Schnautz, N. G. *Journal of High Resolution Chromatography & Chromatography Communications* **1982**, *5*, 432.

- (40) Hubball, J. A.; Dimauro, P.; Barry, E. F.; Chabot, G. E. *Journal of High Resolution Chromatography & Chromatography Communications* **1983**, 6, 241.
- (41) Lipsky, S. R.; McMurray, W. J. *Journal of Chromatography* **1984**, 289, 129.
- (42) Blum, W. *Journal of High Resolution Chromatography & Chromatography Communications* **1985**, 8, 718.
- (43) Blum, W. *Journal of High Resolution Chromatography & Chromatography Communications* **1986**, 9, 120.
- (44) Schmid, P.; Muller, M. D. *Journal of High Resolution Chromatography & Chromatography Communications* **1987**, 10, 548.
- (45) Welsch, T.; Teichmann, U. *Hrc-Journal of High Resolution Chromatography* **1991**, 14, 153.
- (46) Li, P. Z.; Xu, Z. M.; Yang, X. P.; Bi, W. W.; Xiao, D.; Choi, M. M. F. *Journal of Chromatography A* **2009**, 1216, 3343.
- (47) Cramers, C. A.; Janssen, H. G.; van Deursen, M. M.; Leclercq, P. A. *Journal of Chromatography A* **1999**, 856, 315.
- (48) Cramers, C. A.; Leclercq, P. A. *Journal of Chromatography A* **1999**, 842, 3.
- (49) Berezkin, V. G.; Lapin, A. B. *Journal of Chromatography A* **2005**, 1075, 197.
- (50) D.H. Desty D.H; A. Goldup; and W.T. Swanton in N. Brenner, J. E. C. a. M. D. W. E.; Academic Press: New York, 1962, p 105.

- (51) Guiochon, G. *Analytical Chemistry* **1978**, *50*, 1812.
- (52) Gaspar, G.; Arpino, P.; Guiochon, G. *Journal of Chromatographic Science* **1977**, *15*, 256.
- (53) Gaspar, G.; Olivo, J.; Guiochon, G. *Chromatographia* **1978**, *11*, 321.
- (54) Gaspar, G.; Vidalmadjar, C.; Guiochon, G. *Chromatographia* **1982**, *15*, 125.
- (55) Jonker, R. J.; Poppe, H.; Huber, J. F. K. *Analytical Chemistry* **1982**, *54*, 2447.
- (56) Schutjes, C. P. M.; Vermeer, E. A.; Rijks, J. A.; Cramers, C. A. *Journal of Chromatography* **1982**, *253*, 1.
- (57) Terry, S. C.; Jerman, J. H.; Angell, J. B. *Ieee Transactions on Electron Devices* **1979**, *26*, 1880.
- (58) Stadermann, M.; McBrady, A. D.; Dick, B.; Reid, V. R.; Noy, A.; Synovec, R. E.; Bakajin, O. *Analytical Chemistry* **2006**, *78*, 5639.
- (59) Overton, E. B.; Carney, K. R. *Trac-Trends in Analytical Chemistry* **1994**, *13*, 252.
- (60) Korytar, P.; Janssen, H. G.; Matisova, E.; Brinkman, U. A. T. *Trac-Trends in Analytical Chemistry* **2002**, *21*, 558.
- (61) David, F.; Gere, D. R.; Scanlan, F.; Sandra, P. *Journal of Chromatography A* **1999**, *842*, 309.
- (62) Hada, M.; Takino, M.; Yamagami, T.; Daishima, S.; Yamaguchi, K. *Journal of Chromatography A* **2000**, *874*, 81.

- (63) Vanes, A.; Janssen, J.; Cramers, C.; Rijks, J. *Journal of High Resolution Chromatography & Chromatography Communications* **1988**, *11*, 852.
- (64) Korytar, P.; Matisova, E.; Lefflerova, H.; Slobodnik, J. *Hrc-Journal of High Resolution Chromatography* **2000**, *23*, 149.
- (65) Matisova, E.; Simekova, M.; Hrouzkova, S.; Korytar, P.; Domotorova, M. *Journal of Separation Science* **2002**, *25*, 1325.
- (66) Zrostikova, J.; Hajslova, J.; Godula, M.; Mastovska, K. *Journal of Chromatography A* **2001**, *937*, 73.
- (67) Lee G; Ray C; Siemers R; R., M. *American laboratory* **1985**, *17*, 124.
- (68) Angell, J. B.; Terry, S. C.; Barth, P. W. *Scientific American* **1983**, *248*, 44.
- (69) Dyson, N. *Journal of Chromatography A* **1999**, *842*, 321.
- (70) Sacks, R.; Smith, H.; Nowak, M. *Analytical Chemistry* **1998**, *70*, 29A.
- (71) Wang, J. W.; Peng, H.; Duan, C. F.; Guan, Y. F. *Chin. Journal of Analytical Chemistry* **2011**, *39*, 439.
- (72) Hayward, T. C.; Thurbide, K. B. *Talanta* **2007**, *73*, 583.
- (73) Thurbide, K. B.; Hayward, T. C. *Analytica Chimica Acta* **2004**, *519*, 121.
- (74) Zimmermann, S.; Krippner, P.; Vogel, A.; Muller, J. *Sensors and Actuators B-Chemical* **2002**, *83*, 285.
- (75) Dandeneau, R.; Bente, P.; Rooney, T.; Hiskes, R. *International Laboratory* **1979**, 69.
- (76) Manz, A.; Fettingner, J. C.; Verpoorte, E.; Ludi, H.; Widmer, H. M.; Harrison, D. J. *Trac-Trends in Analytical Chemistry* **1991**, *10*, 144.

- (77) Zeze, D. A.; Cox, D. C.; Weiss, B. L.; Silva, S. R. P. *Applied Physics Letters* **2004**, *84*, 1362.
- (78) Harrison, D. J.; Glavina, P. G.; Manz, A. *Sensors and Actuators B-Chemical* **1993**, *10*, 107.
- (79) Effenhauser, C. S.; Bruin, G. J. M.; Paulus, A. *Electrophoresis* **1997**, *18*, 2203.
- (80) Radadia, A. D.; Masel, R. I.; Shannon, M. A.; Jerrell, J. P.; Cadwallader, K. R. *Analytical Chemistry* **2008**, *80*, 4087.
- (81) Potkay, J. A.; Lambertus, G. R.; Sacks, R. D.; Wise, K. D. *Journal of Microelectromechanical Systems* **2007**, *16*, 1071.
- (82) Reidy, S.; George, D.; Agah, M.; Sacks, R. *Analytical Chemistry* **2007**, *79*, 2911.
- (83) Reston, R. R.; Kolesar, E. S. *Journal of Microelectromechanical Systems* **1994**, *3*, 134.
- (84) Lambertus, G. R.; Fix, C. S.; Reidy, S. M.; Miller, R. A.; Wheeler, D.; Nazarov, E.; Sacks, R. *Analytical Chemistry* **2005**, *77*, 7563.
- (85) Radadia, A. D.; Morgan, R. D.; Masel, R. I.; Shannon, M. A. *Analytical Chemistry* **2009**, *81*, 3471.
- (86) Nishino, M.; Takemori, Y.; Matsuoka, S.; Kanai, M.; Nishimoto, T.; Ueda, M.; Komori, K. *IEEE Transactions on Electrical and Electronic Engineering* **2009**, *4*, 358.
- (87) Bhushan, A.; Yemane, D.; Overton, E. B.; Goetttert, J.; Murphy, M. C. *Journal of Microelectromechanical Systems* **2007**, *16*, 383.

- (88) Dziurdzia, B.; Magonski, Z.; Nowak, S. *Measurement Science & Technology* **2008**, 19.
- (89) Becker, H.; Gartner, C. *Electrophoresis* **2000**, 21, 12.
- (90) Su, Y. C.; Lin, L. W. *Ieee Transactions on Advanced Packaging* **2005**, 28, 635.
- (91) Becker, H.; Rotting, O.; Ropke, W.; Heim, U. In *Micro Total Analysis Systems 2000, Proceedings*; VandenBerg, A., Bergveld, P., Olthuis, W., Eds. 2000, p 151.
- (92) Chen, Y.; Pepin, A. *Electrophoresis* **2001**, 22, 187.
- (93) Malainou, A.; Vlachopoulou, M. E.; Triantafyllopoulou, R.; Tserepi, A.; Chatzandroulis, S. *Journal of Micromechanics and Microengineering* **2008**, 18.
- (94) Ibanez-Garcia, N.; Martinez-Cisneros, C. S.; Valdes, F.; Alonso, J. *Trends in Analytical Chemistry* **2008**, 27, 24.
- (95) Martinez-Cisneros, C. S.; Ibanez-Garcia, N.; Valdes, F.; Alonso, J. *Analytical Chemistry* **2007**, 79, 8376.
- (96) Khanna, P. K.; Hornbostel, B.; Burgard, M.; Schafer, W.; Dorner, J. *Materials Chemistry and Physics* **2005**, 89, 72.
- (97) Yung, W. K. C.; Zhu, J. *Microelectronics International* **2007**, 24, 27.
- (98) Jones, W. K.; Liu, Y. Q.; Larsen, B.; Wang, P.; Zampino, M.; Spie, S. In *2000 International Symposium on Microelectronics 2000*; Vol. 4339, p 669.

- (99) Henry, C. S.; Zhong, M.; Lunte, S. M.; Kim, M.; Bau, H.; Santiago, J. J. *Analytical Communications* **1999**, 36, 305.
- (100) Peterson, K. A.; Patel, K. D.; Ho, C. K.; Rohde, S. B.; Nordquist, C. D.; Walker, C. A.; Wroblewski, B. D.; Okandan, M. *International Journal of Applied Ceramic Technology* **2005**, 2, 345.
- (101) Briscoe C. G; Yu H; Grodzinski P; Huang R. F; Burdon J. W US, 2004; Vol. 6,732,567,B2.
- (102) Martin, C. R.; Aksay, I. A. *Journal of Electroceramics* **2004**, 12, 53.
- (103) Mutlu, M.; Kacar, E.; Akman, E.; Akkan, C. K.; Demir, P.; Demir, A. J. *Laser Micro Nanoeng.* **2009**, 4, 84.
- (104) Gross, G. A.; Thelemann, T.; Schneider, S.; Boskovic, D.; Kohler, J. M. *Chemical Engineering Science* **2008**, 63, 2773.
- (105) He, G.; Liu, H. H.; Tan, Q. B.; Ni, J. H. *Journal of Alloys and Compounds* **2011**, 509, 7324.
- (106) Lambertus, G.; Elstro, A.; Sensenig, K.; Potkay, J.; Agah, M.; Scheuering, S.; Wise, K.; Dorman, F.; Sacks, R. *Analytical Chemistry* **2004**, 76, 2629.
- (107) Neue, U. D.; John Wiley and Sons Ltd: New York, 1997, p 416.
- (108) Giddings, J. C.; Chang, J. P.; Myers, M. N.; Davis, J. M.; Caldwell, K. D. *Journal of Chromatography* **1983**, 255.
- (109) Poppe, H. *Journal of Chromatography A* **2002**, 948, 3.
- (110) Spangler, G. E. *Journal of Microcolumn Separations* **2001**, 13, 285.
- (111) Rozing, G.; van de Goor, T.; Yin, H. F.; Killeen, K.; Glatz, B.; Kraiczek, K.; Lauer, H. H. *Journal of Separation Science* **2004**, 27, 1391.

- (112) Henrich, L. H. *Journal of chromatographic Science* **1988**, 26
- (113) Reid G.L; Armstrong D.W. *Journal of Microcolumn* **1994**, 151.
- (114) Wagner, M.; Roosen, A.; Stiegelschmitt, A.; Schwanke, D.; Bechtold, F.; Imaps, I. In *2002 International Symposium on Microelectronics, Proceedings 2002*; Vol. 4931, p 71.
- (115) Lambertus, G.; Elstro, A.; Sensenig, K.; Potkay, J.; Agah, M.; Scheuering, S.; Wise, K.; Dorman, F.; Sacks, R. *Analytical Chemistry* **2004**, 76, 2629.
- (116) Ishii, D; Asai, K; Hibi, K; Jonokuchi, T; Nagaya, M. *Journal of chromatography* **1977**, 144.
- (117) Ishii, D; Asai, K; Hibi, K; Nagaya, M. *Journal of Chromatography A* **1976**, 152.
- (118) Wu, N.; Medina, J. C.; Lee, M. L. *Journal of Chromatography A* **2000**, 892, 3.
- (119) Zhuravlev, L. T. *Colloids and Surfaces a-Physicochemical and Engineering Aspects* **2000**, 173, 1.
- (120) Budinski, K. G. *Wear* **1991**, 151, 203.
- (121) Zhang, B.; Lei, L. M.; Yang, J.; Guo, X. H.; Zhang, G. P. *Materials Letters* **2012**, 89, 302.